The Thesis Committee for Anderson Kiser Potter
Certifies that this is the approved version of the following thesis:

Statistically Representative Bridge Samples for Seismic Fragility Analysis of Texas Bridges

APPROVED BY
SUPERVISING COMMITTEE:

Supervisor: _____
Patricia Clayton

Co-Supervisor: _____
Eric B. Williamson

Statistically Representative Bridge Samples for Seismic Fragility Analysis of Texas Bridges

by

Anderson Kiser Potter

Thesis

Presented to the Faculty of the Graduate School of

The University of Texas at Austin

in Partial Fulfillment

of the Requirements

for the Degree of

Master of Science in Engineering

The University of Texas at Austin

December 2017

Dedication

I lovingly dedicate this work to my family and many friends who have supported me through the process. Without their guidance and encouragement I would not be the person I am today.

Acknowledgements

I would like to extend a special thanks, and appreciation to the persons below who have played a major role in the successful completion of the thesis:

My Supervisor, Dr. Clayton for her enduring support, guidance, and willingness to answer questions. Her never ending positive attitude was contagious, and inspired me to face every challenge with confidence and determination.

My Assistant Supervisor, Dr. Williamson for his motivation, encouragement, insight, and expertise that was essential in the success of this project.

My fellow teammates, Farid Khosravikia and Slav Prahkov for their hard work, collaboration, and continued support.

Finally, the Texas Department of Transportation for the opportunity to be a part of this project, and I am extremely grateful for the financial support through Grant Number 0-6916.

Abstract

Statistically Representative Bridge Samples for Seismic Fragility Analysis of Texas Bridges

Anderson Kiser Potter, MSE

The University of Texas at Austin, 2017

Supervisor: Patricia Clayton

Co-Supervisor: Eric B. Williamson

Historically, bridges in the State of Texas have not been explicitly designed or detailed for seismic hazards, predominantly due to the negligible seismic activity across much of the state. A recent rise in the number of earthquakes recorded in Texas has raised concerns about the seismic vulnerability of the highway bridge inventory. To investigate the seismic vulnerability of Texas bridges, seismic fragility analysis of the state highway bridge inventory is performed using numerical models of the bridges of concern to generate fragility curves. When assessing such a large number of structures such as the approximately 53,000 bridges in the Texas highway bridge inventory, it is impractical to analyze and develop a fragility curve for each individual structure. Instead, fragility curves are developed for bridge samples that are statistically representative of the entire inventory.

The objective of the work described in this thesis is to develop the representative bridge samples to be used in seismic fragility analysis of the Texas bridge inventory. First, the bridge inventory is separated into various bridge classes based on superstructure type.

Second, statistical distributions of key bridge geometry descriptors (e.g., number of spans, maximum span length, deck width, column height, etc.) are developed from bridge inventory data. Third, typical component details are identified for various types of bridges from various eras of construction. Finally, parameter sampling techniques are used to generate different bridge samples with geometries and construction details that are statistically representative of the entire bridge population. These representative Texas bridge samples can be used in a numerical seismic fragility analysis to develop probabilistic estimations of seismic damage for given earthquake shaking intensities.

Table of Contents

List of Tables

List of Figures

1 INTRODUCTION

1.1 Problem Description

Historically, seismic activity in the State of Texas has not been a source of concern due to the infrequency and low magnitudes of seismic events experienced in the state. Thus, standard bridge details and design practices developed and used by the Texas Department of Transportation (TxDOT) have not explicitly considered seismic hazards. In recent years, however, seismologists have detected a significant increase in the frequency of seismic events occurring across the state (e.g., an average rate of two seismic events per year prior to 2008 has increased to an average of almost twelve events per year in recent years), many of which are thought to be a result of human activity (Frohlich et al., 2016). Figure 1.1 shows the cumulative number of earthquakes greater than a magnitude 3 recorded in the state of Texas since 1847, and depicts the distribution of tectonically induced, possibly human-induced, probably human-induced, and almost certainly human-induced earthquakes across the state during that timeframe.

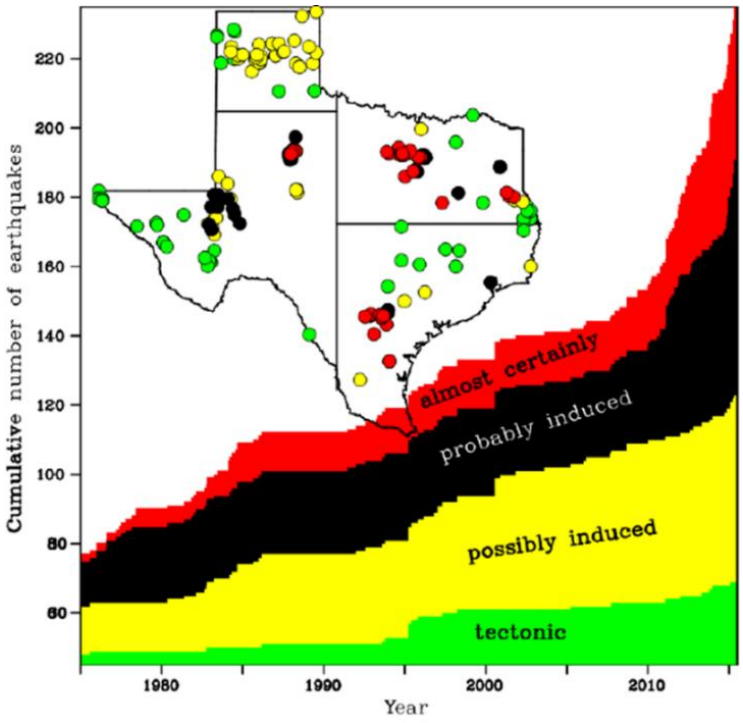

Figure 1.1: Cumulative Texas seismicity (Frohlich et al., 2016).

The largest earthquakes that have been recorded to date in the State of Texas are the 1931 Valentine Earthquake (6.3 moment magnitude) and the 1995 Alpine Earthquake (5.7 moment magnitude), both thought to be from natural causes. The events in Texas that are believed to be human-induced have yet to reach such large magnitudes. For example, the largest human-induced event in Texas is believed to be the 2011 Fashing earthquake, registering a moment magnitude of 4.8; however, the 2011 earthquake in Prague, Oklahoma (moment magnitude 5.7) and the 2016 earthquake in Pawnee, Oklahoma (moment magnitude 5.8) indicate that potentially human-induced earthquakes can reach higher magnitudes.

When considering the lack of seismic detailing for bridges in Texas, the sharp increase in seismicity across the state and the potential for larger magnitude earthquakes (i.e., greater than magnitude 5) has raised significant concern about the seismic

vulnerability of Texas bridges. Bridges are vital links in a highway transportation system, and their functionality following an earthquake event plays a major role in the response and recovery of the affected region. With almost 53,000 bridges in the state of Texas, it is important for TxDOT to evaluate the vulnerability of these critical structures and to develop an effective plan to assess the functionality of the state's transportation network following a seismic event. To this end, the goal of this project is to develop probabilistic tools to predict the seismic performance of different bridges in the Texas inventory for TxDOT officials to evaluate the seismic risk of the state's bridge inventory. To accomplish this goal, seismic fragility curves can be developed, which are used to estimate the conditional probability that a structure will meet or exceed a certain level of damage for a given level of ground shaking. Fragility curves can be developed following three main methodologies (Zong 2015): (i) expert based fragility functions, (ii) empirical fragility functions, and (iii) analytical (or numerical) fragility functions.

Expert-based fragility curves were first developed in the 1980s, when the Applied Technology Council (ATC) put together a panel of 42 experts to develop damage probability matrices for various components of California infrastructure (ATC, 1985). These matrices provided estimations of damage likelihood given a certain ground motion intensity measure (e.g., peak ground acceleration, spectral acceleration, etc.) based on the judgement and experience level of each expert. Expert-based fragility functions rely solely on the experience and the number of experts involved, which brings about a major concern of subjectivity. Due to these concerns, coupled with the collection of post-earthquake damage data and advancements in computational modeling capabilities, this method is rarely used as the sole means to develop seismic fragility functions in the modern day.

Empirical fragility curves are developed from actual earthquake damage data. Following the 1989 Loma Prieta, 1994 Northridge, and the 1995 Kobe earthquakes, the

empirical method became fairly popular due to the increase in observed seismic damage data. Examples of empirical fragility curves can be found in the studies of Basoz and Kiremidjian (1996), Yamazaki et al. (1999), Der Kiureghian (2002), Shinozuka et al. (2003), and Elnashai et al. (2004). Although this method provides a realistic risk assessment of earthquake damage, it does have its limitations, including (i) the potential for statistically insignificant results due to small sample sizes for various types of structures and detailing practices, and (ii) inconsistencies in the post-earthquake assessments of structures due to the subjectivity of inspectors reporting observed levels of damage.

When actual post-earthquake damage and ground motion data are not available, which is the case in the State of Texas, numerical methods must be used to develop fragility curves. Throughout the last decade, researchers have been developing and using such numerical methodologies and procedures to generate what are known as analytical fragility functions (Shinozuka et al., 2000; Mackie and Stojadinović, 2001; Choi, 2002; Karim and Yamazaki, 2003; Choi et al., 2004; Nielson, 2005; Nielson and DesRoches, 2007a; Pan, 2007; De Felice and Giannini, 2010; Ramanathan, 2012; and Zong, 2015). Analytical fragility functions can be generated using seismic response data from elastic-spectral analysis, non-linear static analysis, or non-linear response-history analysis. Despite being one of the most computationally demanding methods, the non-linear response-history analysis is often viewed as one of the more reliable methods available (Shinozuka et al., 2003). Figure 1.2 illustrates the general procedure for generating analytical fragility curves used in this study.

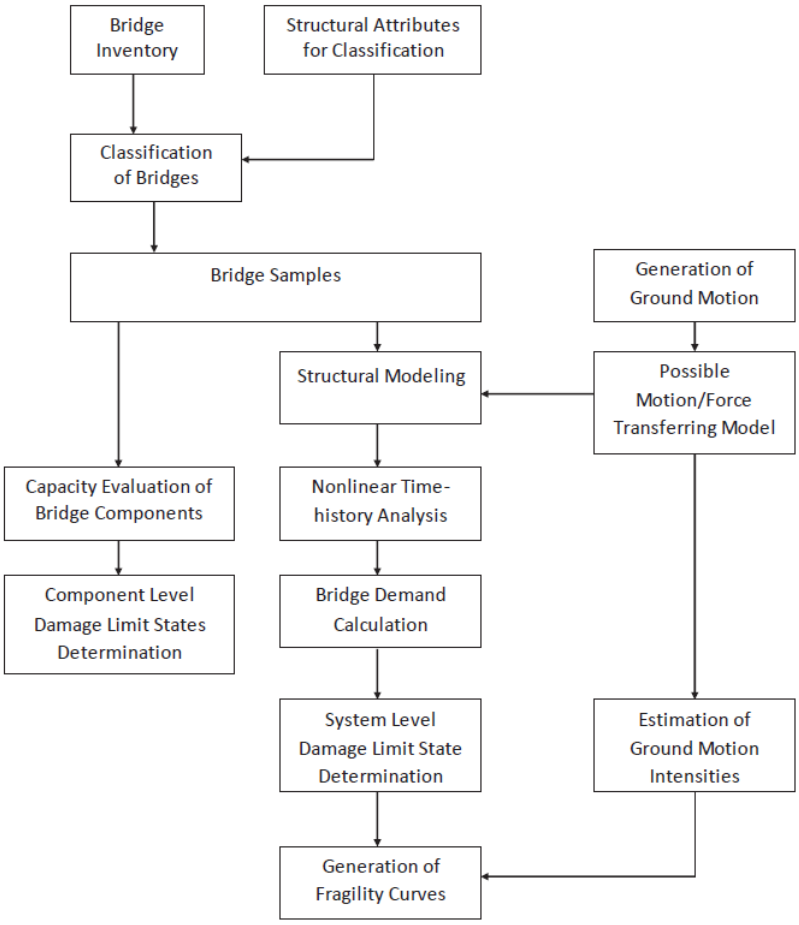

Figure 1.2: Flow chart for the generation of analytical fragility curves (Zong, 2015)

When assessing the seismic vulnerability of an individual bridge, ideally one would generate fragility curves using representative models of the specific bridge in question; however, when assessing the vulnerability of a bridge network for a region or state, as is the case in this study, developing fragility curves for individual bridges is not practical. An alternative approach is to generate fragility curves for typical bridge classes representative of the bridge population in question. Thus, an important part of the fragility assessment is understanding and characterizing the bridge inventory for the area of study. This characterization is typically done by gathering data from the National Bridge

Inventory database, as well as supplementary information from standard or as-built bridge drawings.

The National Bridge Inventory (NBI) is a database compiled by the Federal Highway Administration (FHWA) to track and record bridge inspection data. The NBI was first created in the 1970s following the implementation of the National Bridge Inspection Standards, which required every bridge located on a public road to be inspected at least once every two years (FHWA, 1994). The database does not provide a complete description of each bridge; however, it does provide basic information that can be used to create generalized highway bridge classes and representative bridge models. The NBI contains 116 fields of information including identification information, design types, material types, geometric data, functional descriptions, condition and inspection ratings, etc. The *Recording and Coding Guide for the Structure Inventory and Appraisal of the Nation's Bridges* (NBI Coding Guide, 1995), is used to decode the information in each of the 116 fields.

As depicted in Figure 1.2, another part of the fragility assessment process, is defining component and system level damage states. Table 1.1 shows an example of qualitative damage state definitions, which were developed and used in the FEMA loss assessment package HAZUS-MH (FEMA, 2003) and have been used in several past bridge fragility studies (Tavares, 2013; Padgett, 2007; Nielson, 2005; Choi, 2002). These HAZUS limit states are intended to provide generalized damage descriptions; however, engineering judgment can and should be used in refining these damage states for a particular region of interest, as they can vary greatly depending on the condition, age, and type of the structure (Choi et al., 2004).

Table 1.1: Qualitative damage state descriptions from HAZUS (Taveres, 2013)

Damage State	Description
Slight	Minor cracking and spalling of the abutments, cracks in shear keys at abutments, minor spalling and cracks at hinges, minor spalling of the column (damage requires no more than cosmetic repair), or minor cracking of the deck.
Moderate	Any column experiencing moderate (shear cracks) cracking and spalling (column still sound structurally), moderate movement of the abutment (<2"), extensive cracking and spalling of shear keys, any connection having cracked shear keys or bent bolts, keeper-bar failure without unseating, rocker bearing failure, or moderate approach settlement.
Extensive	Any column degrading without collapse-shear failure (column structurally unsafe), significant residual movement at connections, or major approach settlement, vertical offset of the abutment, differential settlement at connections, shear key failure at abutment.
Complete	Any column collapsing, connection losing all bearing support which may lead to imminent deck collapse, or tilting of substructure caused by foundation failure.

Similar studies investigating the seismic performance of highway bridges have been conducted for various regions across the country. Researchers Choi (2002) and Nielson (2005) conducted seismic vulnerability assessments for typical bridges in the Central and Southeastern United States (CSUS), Pan et al. (2007) investigated the seismic fragility of steel bridges in the State of New York, and Ramanathan (2012) developed seismic fragility curves for bridges in California. While this previous research provides valuable insight to the seismic performance of highway bridges under a variety of seismic hazards, no research has explicitly consider the seismic performance of Texas bridges subjected to the types of earthquakes expected in Texas. The present study aims to fill this gap by providing representative Texas bridge models to be used in a fragility assessment being conducted as part of a larger research project.

1.2 Objective

This research is part of a project being conducted at the University of Texas at Austin and sponsored by Texas Department of Transportation (TxDOT). The goal of the project is to characterize the natural and induced seismic hazards in Texas and to evaluate the seismic vulnerability of the existing Texas highway bridge inventory. The overall project consists of:

- Predicting ground shaking intensity levels and developing a suite of representative ground motions based on geologic conditions and seismic hazards across the State of Texas.
- Creating continuous and simply-supported steel, pre-stressed, and reinforced concrete bridge samples with geometrical and material properties representative of those found in the TxDOT inventory.
- Developing nonlinear bridge component models for those bridge samples based on past experimental, analytical, and numerical research done on bridge components, and assembling these component models into full bridge models for response-history analysis.
- Generating fragility curves for various bridge classes, which describe the probability of a bridge structure reaching a certain level of damage when subjected to different levels of ground motion intensity.
- Recommending a post-event action plan for TxDOT to identify and prioritize the most vulnerable bridges for inspection and repair efforts, given earthquake location and magnitude.

The primary tasks of this thesis concentrate on the development of statistically representative bridge models and capacity models to be used for fragility analysis, particularly:

- Establishing representative bridge classes, and determining the relevant bridge class statistics.

- Developing representative bridge samples through statistical sampling of geometrical parameters and material properties.
- Reviewing as-built drawings and TxDOT standard drawings to determine typical details to be accounted for in the numerical models of the bridge samples.
- Developing bridge capacity limit state statistical models that can be used in fragility analysis.

1.3 Organization

This thesis has been divided into six chapters. Following this introductory chapter, Chapter 2 presents the TxDOT bridge inventory analysis, establishes bridge classes, and presents bridge class statistics. Chapter 3 describes statistical sampling techniques used to develop representative bridge samples. Chapter 4 discusses typical bridge component details that can be found in the TxDOT highway bridge inventory. Chapter 5 discusses the overall procedure of a seismic fragility analysis and describes the development of the capacity limit state statistical models that can be used in the seismic fragility analysis of Texas bridges. Finally, Chapter 6 summarizes the study and provides recommendations for future work.

2 TXDOT BRIDGE INVENTORY ANALYSIS

In this section, information from the TxDOT highway bridge inventory analysis is presented and explained. Utilizing the NBI database and the *Recording and Coding Guide for the Structure Inventory and Appraisal of the Nation's Bridges* (FHWA, 1995), the research team has reorganized and filtered the data to better characterize the TxDOT bridge inventory for seismic fragility assessment. Information of interest in characterizing the bridge inventory includes but is not limited to bridge structural system and material, era of construction, and geometry. It must be noted that the NBI database does not provide a complete description of each bridge; however, it does provide sufficient information to make generalized classifications.

2.1 Bridge Classes

When creating bridge classes for use in a seismic vulnerability assessment, it is important to characterize the bridge classes such that the bridges assigned to them are expected to have similar seismic behavior. In this study bridge classes are represented by superstructure design type, material type, number of spans, and span continuity. Tables 2.1 and 2.2 show possible material and design types as listed in NBI.

Table 2.1: Superstructure Material Types Listed in NBI (adopted from FHWA, 1995)

Description
Concrete (Simply Supported)
Concrete Continuous
Steel (Simply Supported)
Steel Continuous
Pre-stressed Concrete (Simply Supported)
Pre-stressed Concrete Continuous
Wood or Timber
Masonry
Aluminum, Wrought Iron, or Cast Iron
Other

Table 2.2: Superstructure Design Types Listed in NBI (FHWA, 1995)

Description	
Slab	Suspension
Stringer/Multi-beam or Girder	Stayed Girder
Girder and Floorbeam System	Movable - Lift
Tee Beam	Movable - Bascule
Box Beam or Girders - Multiple	Movable - Swing
Box Beam or Girders - Single or Spread	Tunnel
Frame	Culvert
Orthotropic	Mixed Types
Truss - Deck	Segmental Box Girder
Truss - Thru	Channel Beam
Arch - Deck	Other
Arch - Thru	

According to the NBI, there are 52,937 bridges in the state of Texas; however, only 33,586 of them are considered on-system (i.e., maintenance responsibility belongs to TxDOT). For the purposes of this study, only on-system bridges are considered in the analysis. Of the 33,586 on-system bridges, 13,441 are listed in NBI as culverts, which are

assumed out of scope for this project. Table 2.3 shows the remaining 20,145 on-system bridges separated into 11 different bridge classes based on superstructure system and material, along with an abbreviated name for the bridge class and the percentage of bridges that fall into each class.

Table 2.3: Bridge Classes

Bridge Type	Abbreviation	Amount	Percentage (%)
Multi-Span Continuous Reinforced Concrete - Slab	**MC RC - Slab**	**1068**	**5.30%**
Multi-Span Simply Supported Reinforced Concrete - Slab	**MS RC - Slab**	**1566**	**7.77%**
Multi-Span Simply Supported Reinforced Concrete - Girder	**MS RC - Girder**	**3336**	**16.56%**
Multi-Span Simply Supported Reinforced Concrete - Tee Beam	MS RC - Tee	829	4.12%
Single Span Reinforced Concrete - Girder	SS RC - Girder	137	0.68%
Multi-Span Simply Supported Prestessed Concrete - Girder	**MS PC - Girder**	**6808**	**33.79%**
Single Span Prestessed Concrete - Girder	**SS PC - Girder**	**1753**	**8.70%**
Multi-Span Simply Supported Prestressed Concrete - Box Girder	MS PC - Box	849	4.21%
Multi-Span Continuous Steel - Girder	**MC Steel - Girder**	**2075**	**10.30%**
Multi-Span Simply Supported Steel - Girder	**MS Steel - Girder**	**457**	**2.27%**
Single Span Steel - Girder	SS Steel - Girder	141	0.70%
Other		1126	5.59%
Total		20145	100.00%

When examining the results presented in Table 2.3, it is seen that seven out of the twelve bridge classes (those in **bold** in Table 2.3) make up 88.7% of the total on-system bridges in Texas. Based on the research requested by TxDOT in the project problem statement, these seven classes are those considered in this study and will be referenced in later sections of this thesis. The five non-bold face entries in Table 2.3 (i.e., MS RC-Tee, SS RC-Girder, MS PC-Box, and SS Steel – Girder) are considered outside the scope for this study. The SS RC Girder and SS Steel Girder classes consist of a very small percentage (1.38%) of the total on-system inventory. The class listed as "Other" makes up 5.59% of the total bridge inventory, but it consists of a large number of smaller bridge types that by themselves have no real significance towards the total percentage (e.g., bridges of different materials such as wood and masonry, cable-stayed bridges, suspension bridges, etc.). The

MS PC Box and the MS RC Tee bridge types represent a reasonable percentage (4.21% and 4.12%, respectively) of the total; however, neither of these systems were indicated by TxDOT as a superstructure type of initial interest in the research problem statement, and are considered out of scope for the initial phase of this study. Figure 2.1 is a scatter plot showing the locations of all on-system bridges considered in the scope of this study, indicating those with pre-stressed concrete girders (MS PC-Girder and SS PC-Girder), steel girders (MC Steel-Girder and MS Steel-Girder, and those not falling into either of these categories. This figure shows trends in the geographic distribution of Texas bridges. While bridges tend to be concentrated in and around larger cities, this concentration is particularly true for steel girder bridges. Similarly, PC girder bridges tend to be concentrated along major interstate highways in Texas. This concentration of specific bridge classes near highly populated areas and along major interstate thoroughfares could be of interest, as damage to these types of bridges during an earthquake event could have greater impact on the public and state commerce.

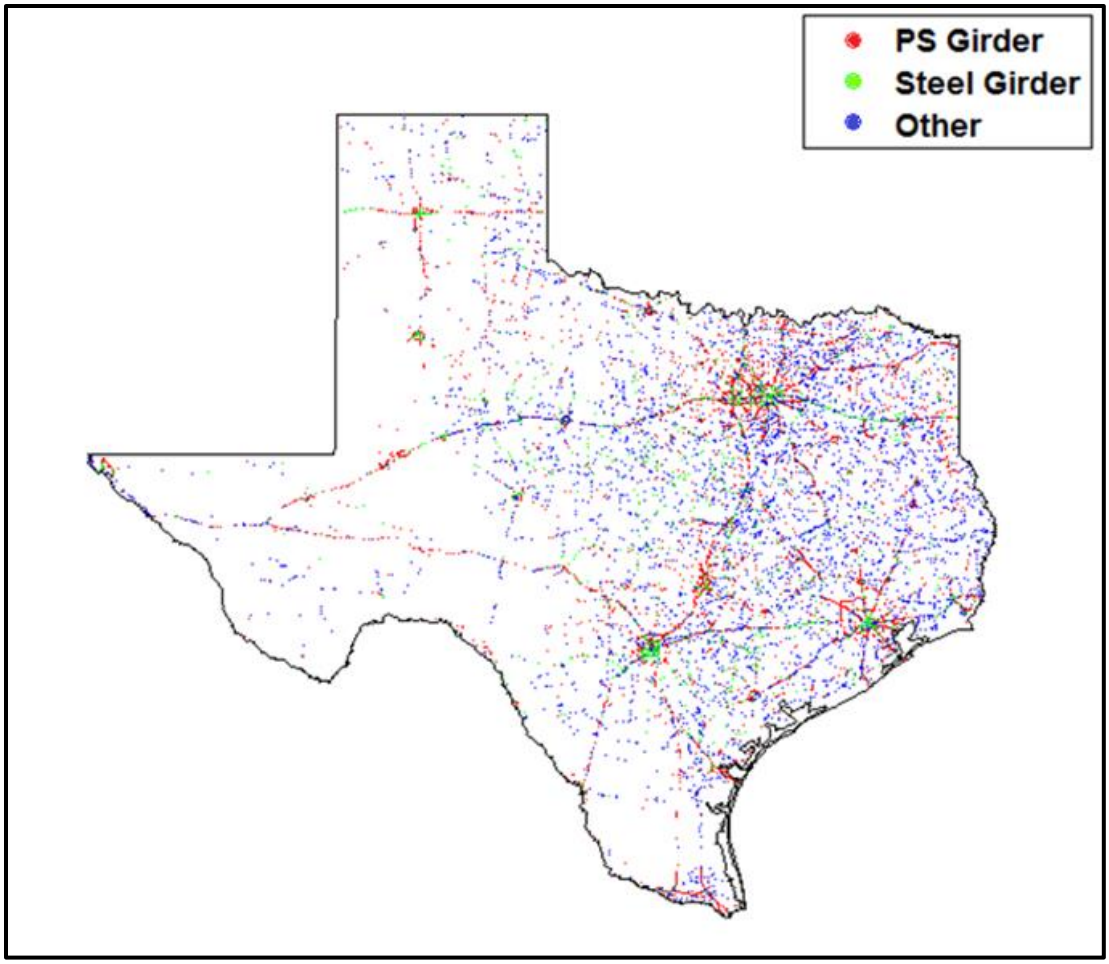

Figure 2.1: TxDOT bridge locations in scope of study

2.2 Bridge Class Statistics

With the general bridge classes defined, the next step is to examine the characteristics of each individual bridge class. The following geometric parameters were retrieved from NBI and the TxDOT bridge database and were analyzed to identify general geometric trends throughout the entire bridge population, as well as within each bridge class:

- Number of spans
- Maximum span length

- Deck width
- Vertical under-clearance
- Skew angle
- Substructure
- Year built

Bridge geometry parameters (e.g., number of spans, span length, deck width, vertical under-clearance) are critical for developing numerical bridge models to simulate seismic behavior, as these parameters greatly affect structural stiffness, mass, and fundamental periods of vibration. Information on year of construction, along with older TxDOT bridge drawings, will be useful in determining component modeling parameters (e.g., bearing details, girder cross-section properties, concrete reinforcement layouts, etc.) that are representative of the actual bridge population. Another parameter of importance when developing numerical bridge models is type of substructure. NBI does not provide information on substructure; however, TxDOT was able to provide their in-house bridge database that does contain substructure information. The following sections will report the findings for each of the parameters above.

2.2.1 NUMBER OF SPANS

The number of spans parameter takes the form of distinct integer values and therefore can be examined through counting the frequency of data at each span number. In this study, probability mass functions (PMFs, denoted mathematically as $F_X(x)$) are generated and used to analyze the number of spans for each bridge class, which are shown in Figures 2.2 and 2.3 for simply supported and continuous span bridges, respectively. PMFs are generated by dividing the number of bridges having a particular span number by the total number of bridges in that class.

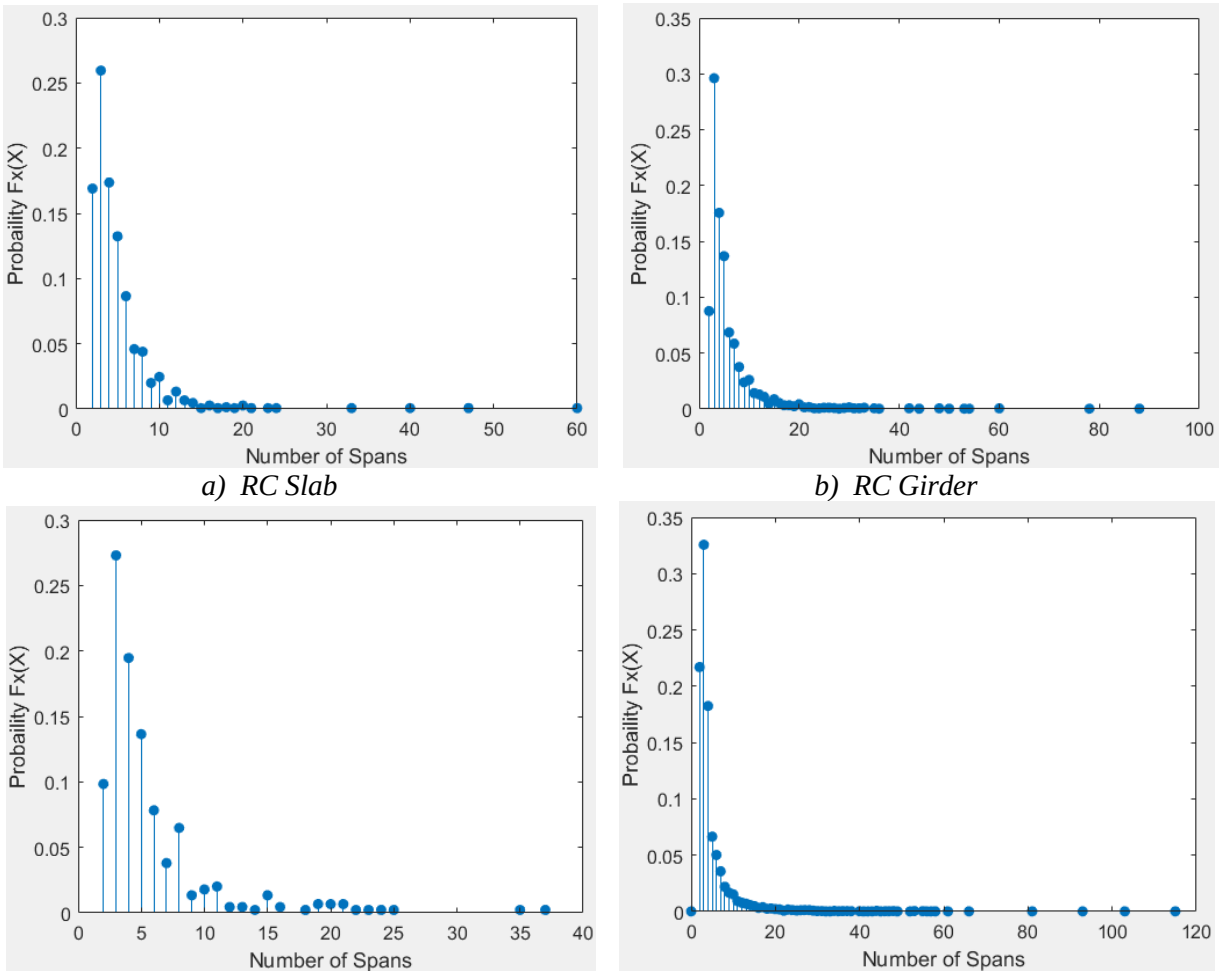

a) RC Slab *b) RC Girder*

c) Steel Girder *d) PC Girder*

Figure 2.2: Number of Spans - PMFs for multi-span simply supported bridge types

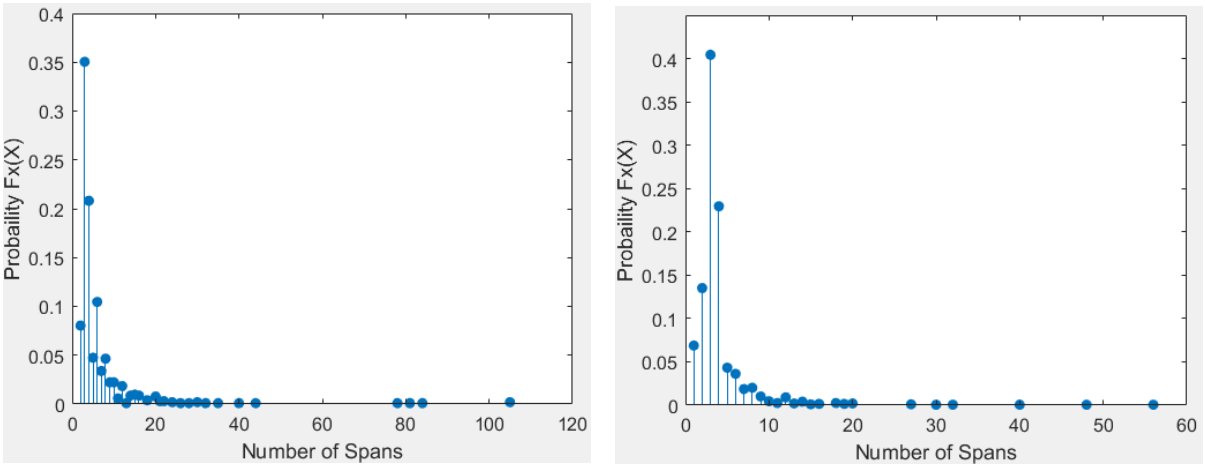

a) RC Slab *b) Steel Girder*

Figure 2.3: Number of Spans - PMFs for multi-span continuously supported bridge types

Table 2.4 shows statistics for the number of spans for each bridge class. The data shows the typical span configuration is between two and six spans, with three spans being the most common. On average, 75% of the simply supported bridges have less than six spans, while 80% of the continous bridges have less than six spans.

Table 2.4: Span number statistics

Class	Mean	Std Dev.	Median	Mode
MS RC-Girder	5.72	6.91	4	3
MS RC-Slab	4.78	3.52	4	3
MS PC-Girders	4.86	5.4	3	3
MS Steel Girders	5.4	4.08	4	3
MC RC-Slab	5.7	7.35	4	3
MC Steel Girders	4.1	3.33	3	3

2.2.2 MAX SPAN LENGTH

Recording the length of every span in every bridge in the NBI would be a daunting task, and therefore considered not feasible. The maximum span length is, however, recorded in NBI and can be used along with some common assumptions to get a generalized representation of the span configuration. The assumptions adopted in this study are: span lengths are symmetrical along the length of the bridge, and approach span lengths are constant among a certain bridge class. For example, a two-span bridge would have two spans with lengths equal to the maximum. A bridge with three or more spans would have interior spans with lengths equal to the maximum, while the end spans would be considered the approach spans with a standard length. Approach span length is not listed in the NBI; however, approach span lengths can be gleaned from specific bridge drawings aquired from TxDOT and can be used to define a standard length per bridge class (see Section 4.1.7). Figure 2.5 shows some statistics to show general trends of maximum span length for each bridge classes, and Figures 2.4, 2.5, and 2.6 show histograms of the actual data.

Table 2.5: Maximum span length statistics

Class	Mean (ft)	Std Dev. (ft)	Median (ft)	Coefficient of Variation
MS RC-Slab	23.52	3.48	24.93	0.15
MS RC-Girder	34.51	5.18	30.84	0.15
MS PC-Girders	86.60	28.20	80.00	0.33
MS Steel Girders	48.20	26.57	40.03	0.55
MC RC-Slab	32.81	11.98	29.86	0.37
MC Steel Girders	102.13	52.82	88.00	0.52
SS PC-Girders	96.30	23.70	98.00	0.25

After examining the data, there are a few trends that should be noted. First, as expected the continuous span bridge types have longer span lengths than their simply supported counterparts. For example, the MC Steel girder bridge class has an average span

length of 103 feet, while the MS Steel girder class only has an average of 48 feet. Second, for the simply supported bridge classes, the PC girder bridge class has the longest spans, exceeding the MS Steel girder class by almost 50%, the RC girder class by 60%, and the RC Slab class by almost 70%. Another thing worth mentioning from Figures 2.4 through 2.6 is most of the bridge classes have one or two prominent span lengths; however, the MS and SS PC girder classes appear to be more evenly distributed between a range of lengths.

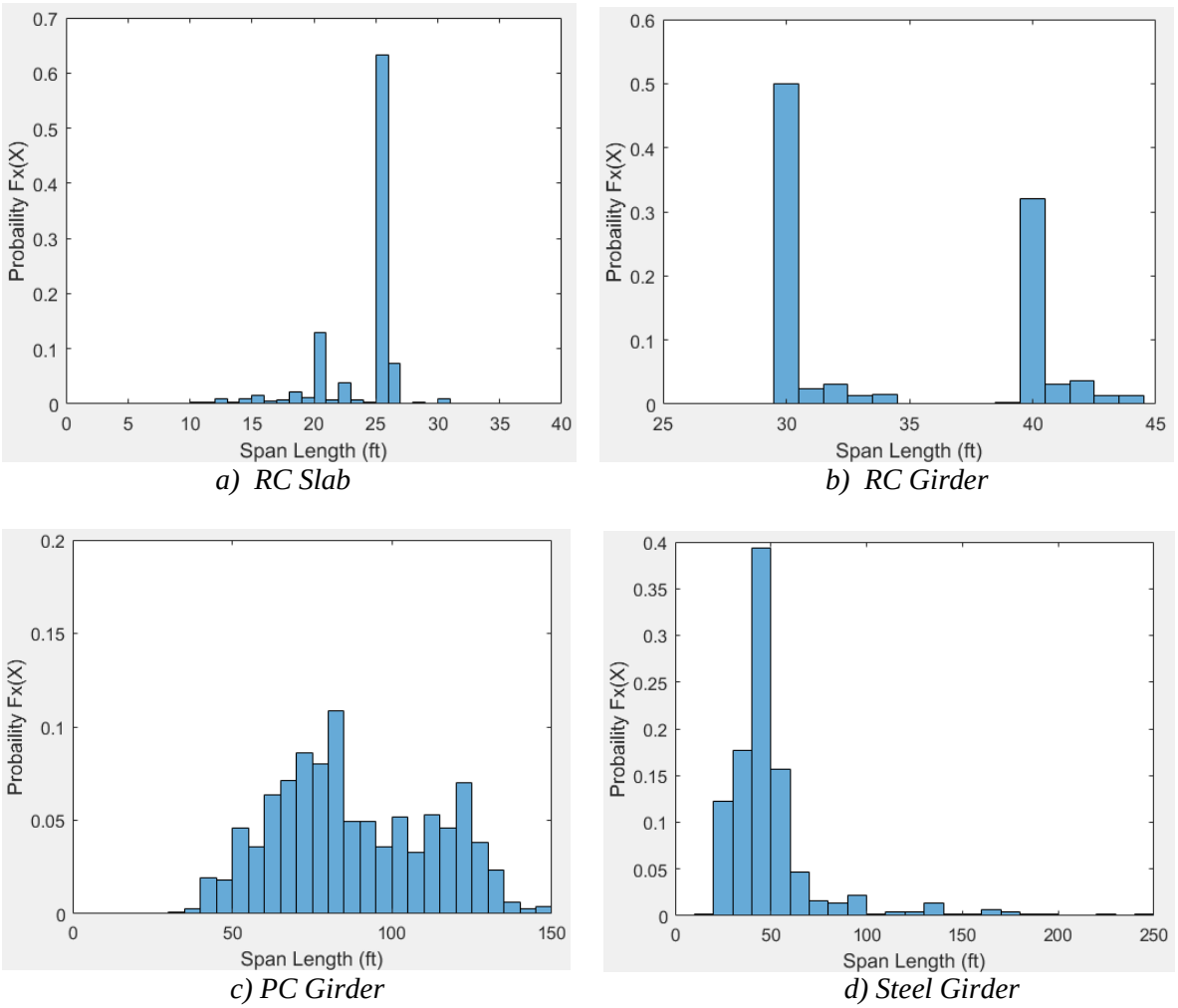

a) RC Slab *b) RC Girder*

c) PC Girder *d) Steel Girder*

Figure 2.4: Maximum Span Length – Histograms for multi-span simply supported bridge types

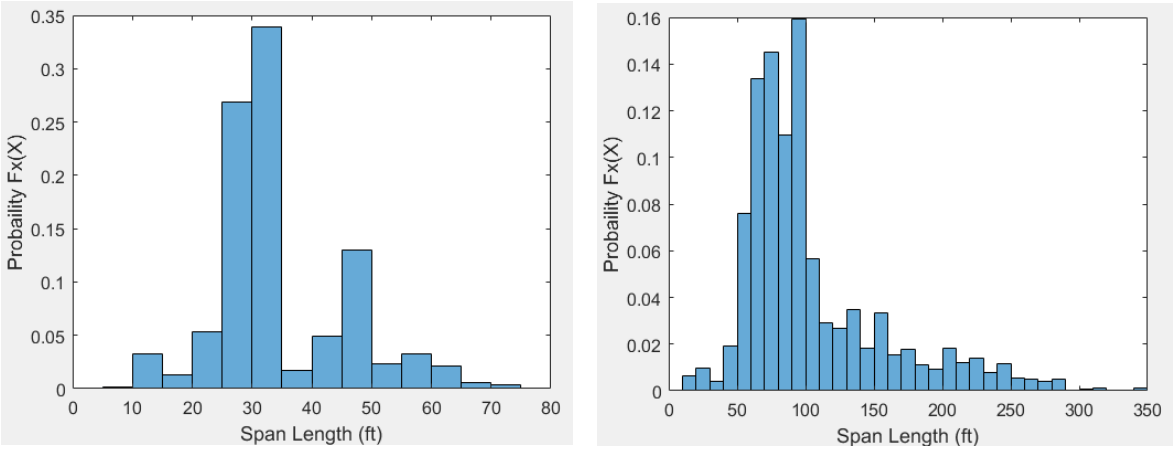

a) RC Slab *b) Steel Girder*

Figure 2.5: Maximum Span Length – Histograms for multi-span continuous bridge types

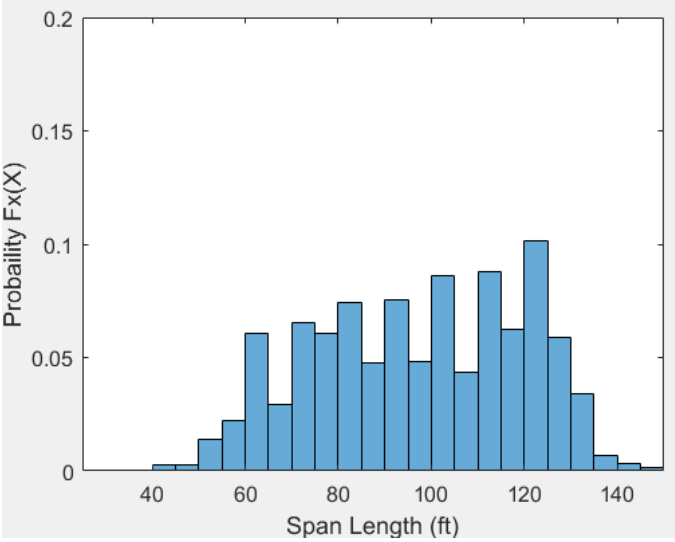

Figure 2.6: Maximum Span Length – Histogram for single span bridge types

2.2.3 DECK WIDTH

Data for both roadway width and deck width can be found in NBI; however, for the purposes of this study, deck width (i.e., outer to outer distance of the bridge deck railings) has be retrieved and analyzed. Table 2.6 reports the basic statistics for this geometric parameter, and Figures 2.7 through 2.9 show the distributions. One trend worth noting is the pre-stressed concrete girder bridges on average have wider decks than the steel and reinforced concrete girder bridges. Both the MS PC girder and SS PC girder classes have an average deck width of about 53 feet, while the steel girder classes have an average in the mid 40 feet range, and the RC classes have an average around 40 feet. However, the median deck width values for the MS PC and SS PC girder classes are lower than the average values and consistent with the other bridge types, indicating there are some larger deck width outliers that area causing the average to be higher. This trend could be due to the fact that PC girder types tend to be from newer construction, which would correspond with higher traffic demands and wider roadways (see Section 2.2.7 for data on year of construction).

Table 2.6: Deck width statistics

Class	Mean (ft)	Std Dev. (ft)	Median (ft)	Coefficient of Variation
MS RC-Slab	35.94	15.62	29.53	0.43
MS RC-Girder	38.59	13.81	37.30	0.36
MS PC-Girders	52.60	25.26	44.30	0.48
MS Steel Girders	45.17	17.88	44.20	0.40
MC RC-Slab	44.98	16.57	42.00	0.37
MC Steel Girders	47.72	22.97	41.67	0.48
SS PC-Girders	53.05	25.43	44.30	0.48

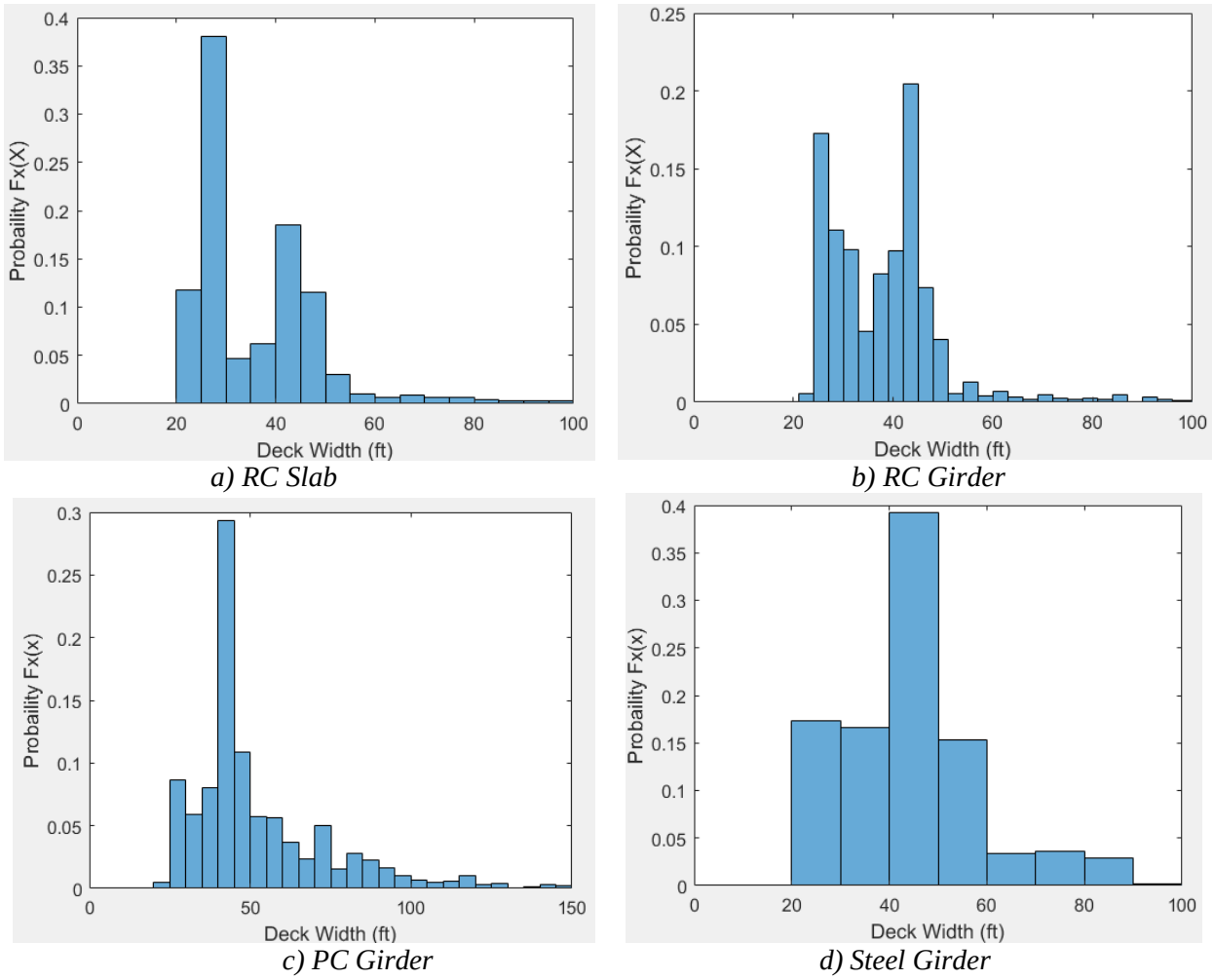

a) RC Slab *b) RC Girder*

c) PC Girder *d) Steel Girder*

Figure 2.7: Deck Width - Histograms for multi-span simply supported bridge types

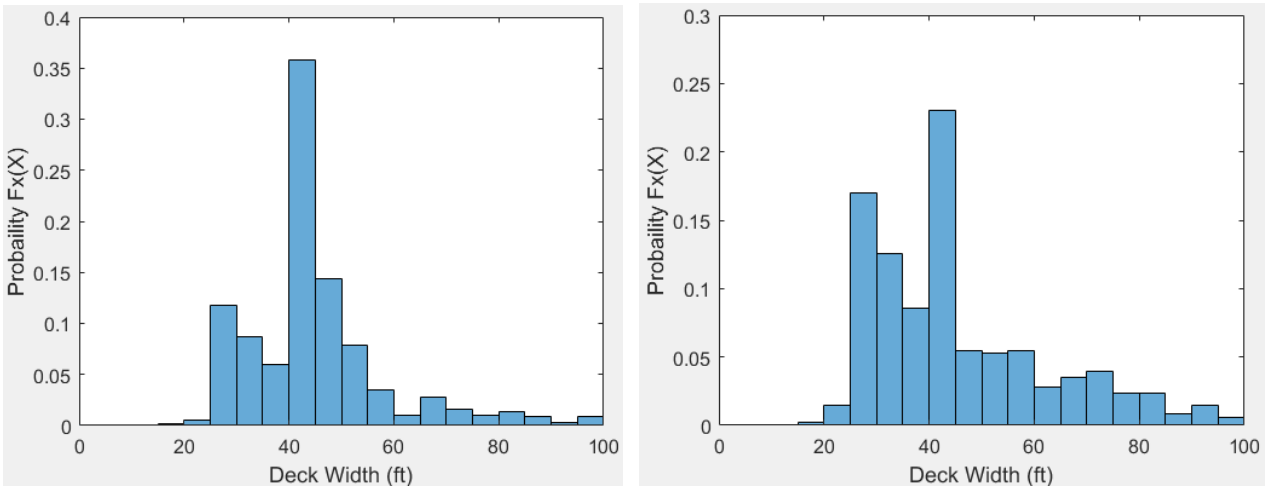

a) RC slab *b) Steel*

Figure 2.8: Deck Width - Histograms for multi-span continuous bridge types

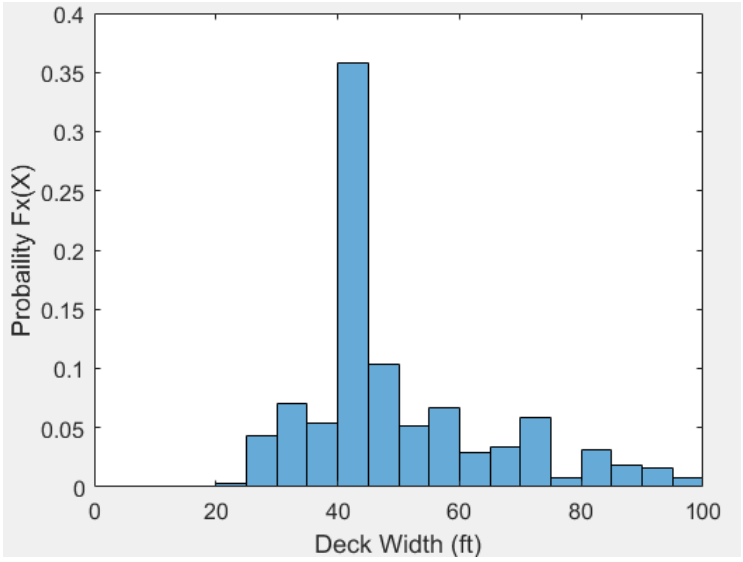

Figure 2.9: Deck Width - Histogram for single span bridge types

2.2.4 VERTICAL UNDER-CLEARANCE

The height of a bridge column or bent plays a major role in the seismic response of a bridge due to its correlation with lateral stiffness and natural periods of vibration. Unfortunately, NBI does not explicitly record column height. NBI does, however, record vertical under-clearance data, which can be used to infer column height. One issue with this approach is that under-clearance data is only listed in NBI for bridges that span over a roadway or railway. Since not all bridges span roadways or railways, the amount of data available to estimate column height is limited and may not be representative of all bridges in the state. In fact, only 43% (about 7,600 bridges) of the in-scope bridges in this study have under-clearance data listed, and some classes have no under-clearance data at all. To gather a large enough dataset to be statistically significant, the under-clearance data for all seven bridge classes was lumped together. It is possible that the available under-clearance data from NBI and TxDOT sources do not capture the actual range of column heights in the bridge population, as it does not account for bridges over water crossings or multi-level flyovers; however, the vertical under-clearance data is the best available source for information on column height.

Vertical under-clearance is measured from the bottom of the superstructure to the top of the roadway or railroad surface below. Figure 2.10 shows the distribution for under-clearance data from NBI. From this figure, the under-clearance parameter appears to take on a bimodal distribution. As shown in Figure 2.10, the most prominent mode is at an under-clearance value of about 17 feet, and the second mode is around 23 feet. The average under-clearance is 17.7 feet with a standard deviation of 3.5 feet. To approximate column height for modeling purposes, the depth of the bent cap and height of the bearings should be subtracted from the under-clearance value.

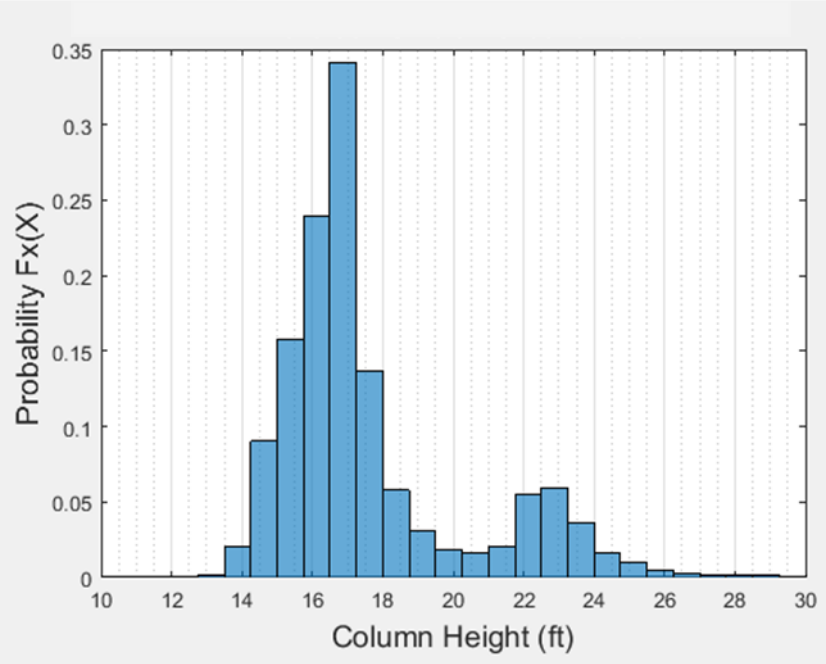

Figure 2.10: Histogram for Vertical Under-Clearance

2.2.5 SKEW ANGLE

Skew angle is another geometric parameter that can greatly impact the seismic response of a bridge (Pottatheere and Renault, 2008; Sullivan and Nielson, 2010). Skew angle is measured as the angle between the centerline of supports and a line perpendicular to the centerline of the roadway (see Figure 2.11). In the NBI, skew angle is recorded based on structural plan drawings or a field measurement; however, for curved bridges or bridges where the skew angle varies, the average skew is recorded in NBI. In certain cases where there is a large variance in skew along the length of the bridge and cannot be accurately represented by an average value, a value of 99 is recorded to identify this variation. For the purposes of this study, bridges with this large variance value (i.e., skew angle values of 99) have been excluded.

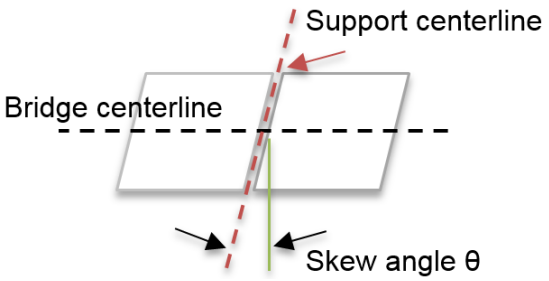

Figure 2.11: Diagram depicting skew angle

Small changes in skew angle do not have a significant effect on seismic response; therefore, instead of looking at the overall distribution of skew, it is more beneficial to look at certain ranges of skew angles (Nielson, 2005; Deepu et al., 2014). The four ranges of interest in this study are skew angle, $\theta = 0°$, 1° - 15°, 15° - 30°, and > 30°. The percentage of bridges that fall into each range, along with some basic statistics for each bridge class can be found in Table 2.7. It is evident the majority of bridges have no or very little skew. On average, a given bridge class has about 75% of bridges with less than fifteen degrees of skew. Sullivan and Nielson (2010) found that a skew angle less than fifteen degrees has little to no effect on seismic vulnerability of a bridge, and therefore can be neglected, as will be done in this study. It should be noted, however, that both PC girder classes, as well as the MC Steel girder class, do have a notable proportion of bridges with skew angles greater than 15 degrees.

Table 2.7: Skew angle statistics

Class	Mean (deg)	Std Dev. (deg)	Median (deg)	Mode	0° (%)	15° (%)	15° - 30° (%)	> 30° (%)
MC RC-Slab	3.96	10.01	0.00	0.00	82.4	5.28	6.23	6.13
MC Steel Girders	15.02	19.05	0.00	0.00	51	9.06	13.85	26.08
MS RC-Slab	9.17	17.02	0.00	0.00	72.4	0.32	3.2	24.07
MS RC-Girder	5.22	12.18	0.00	0.00	81.7	4.89	7.65	5.79
MS PC-Girders	12.23	16.24	0.00	0.00	52.1	10.82	16.17	20.89
MS Steel Girders	6.63	13.72	0.00	0.00	77.49	3.48	2.78	16.24
SS PC-Girders	10.55	14.70	0.00	0.00	53.5	13.56	17.3	15.7

2.2.6 SUBSTRUCTURE

As mentioned earlier, the NBI does not provide substructure information; however, with the help of TxDOT the research team was able to obtain and analyze substructure type from TxDOT's in-house bridge database. The information found in this database is split into three parts, the above ground substructure (i.e., bridge bent or column), the below ground substructure (i.e., foundation), and type of bent cap. Understanding each of these three substructure components is an important part in accurately modeling bridges and simulating seismic behavior.

The above ground substructure can take on one of the following nine configurations: pile bents, single column bents, multiple column bents, concrete column bent with tie beam, concrete column bent wall, concrete pier, masonry pier, trestle (steel, concrete, or timber), or other. Figure 2.12 shows the probability of occurrence of each above ground substructure type for each individual bridge class. This figure shows that the overwhelming majority of PC girder bridges (i.e., MS PC Girder and SS PC Girder), as well as the MC Steel Girder bridges are supported by multiple column bents. The remaining four bridge classes (i.e., MS RC Slab, MS RC Girder, MS Steel Girder, and MC RC Slab) are split between pile bents, and multiple column bents. The MS RC Girder and

MC RC Slab classes are split almost evenly with 49% and 42%, respectively, for pile bents, and 48% and 53%, respectively, for multiple column bents. The MS RC Slab class tends to more commonly employ pile bents with 63%; however, the MS RC Slab class still has a significant percentage with multiple column bents as well, with a probability of 30%. For this reason, multiple column bents will be the above ground substructure considered in this study. See Section 4.2.1 for more details on the multi-column bents used in this study.

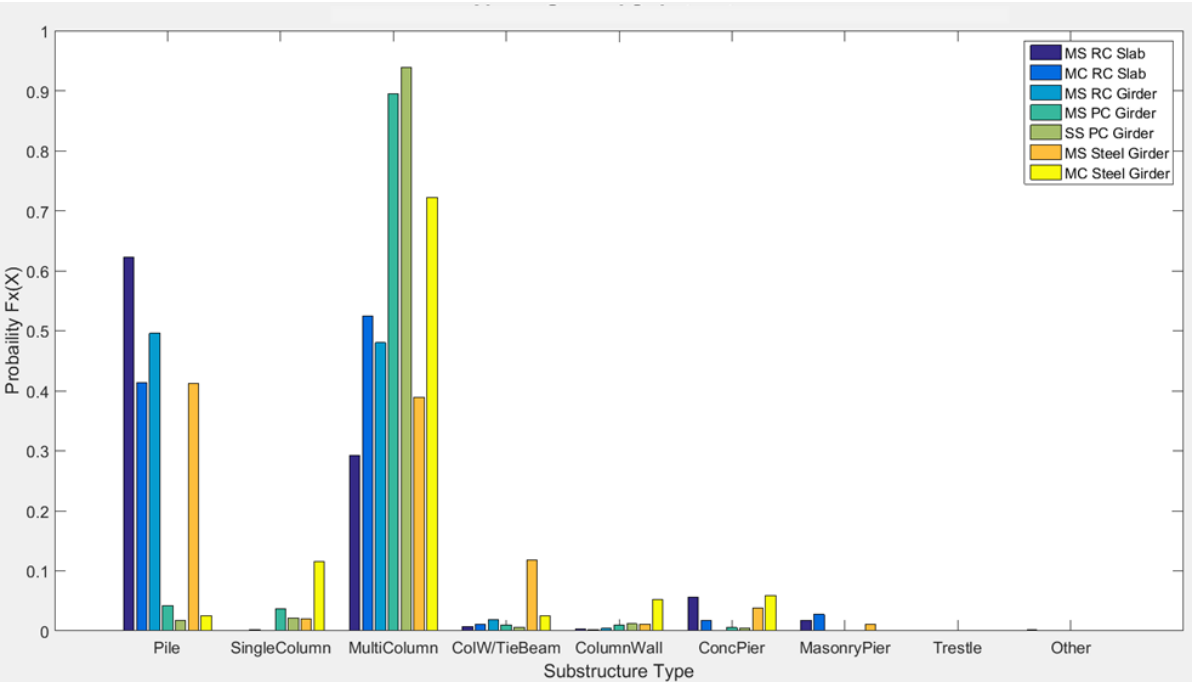

Figure 2.12: Histogram for types of above ground substructure

The below ground substructure, just like its above ground counterpart, is split into nine different types in the TxDOT bridge inventory data. These foundation types are steel piling, concrete piling, timber piling, drilled shafts, spread footings, pile cap on steel piling, pile cap on concrete piling, pile cap on timber piling, and other. Figure 2.13 shows the distribution of foundation types among the seven bridge classes. Below ground

substructure seems to be more varied between different types than the above ground substructure; however, the PC Girder classes (i.e., MS PC-Girder and SS PC-Girder) and the MC Steel Girder class again favor one substructure type with a probability of 83%, 86%, and 73%, respectively, having drilled shaft foundations. The MC RC Slab and MS RC Girder classes favor drilled shafts and concrete pilings, while the MS RC Slab and MS Steel Girder classes are distributed between drilled shafts, concrete piling, spread footings, and steel piling. Due to their relative popularity across various bridge classes, drilled shaft foundations will be of primary interest in this study. Section 4.2.2 provides more information about the drilled shaft foundations used in this study.

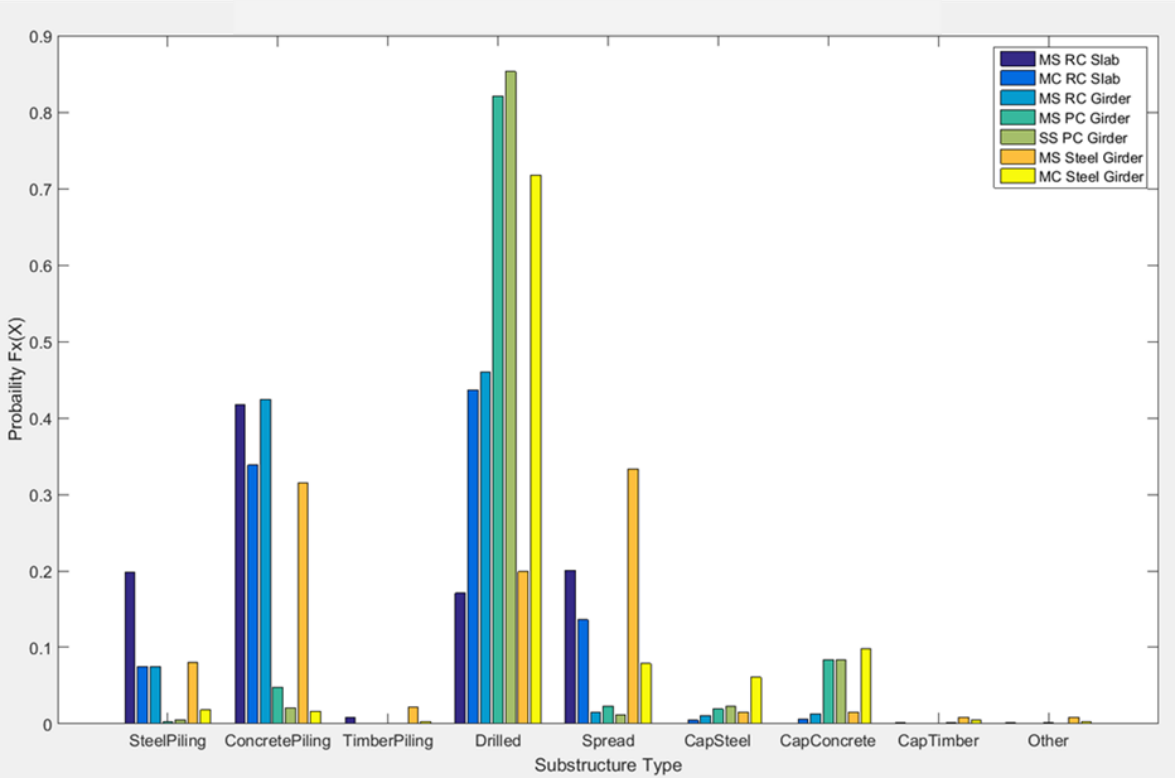

Figure 2.13: Histogram for types of below ground Substructure

TxDOT recognizes four bent cap materials in their inventory database: concrete, steel, timber, and masonry. Figure 2.14 shows the distribution of types of bent caps among

the seven bridge classes. This figure shows that even though TxDOT uses four different bent cap materials, the overwhelming favorite is concrete. For all seven bridge classes the probability of having a concrete bent cap is greater than 90%.

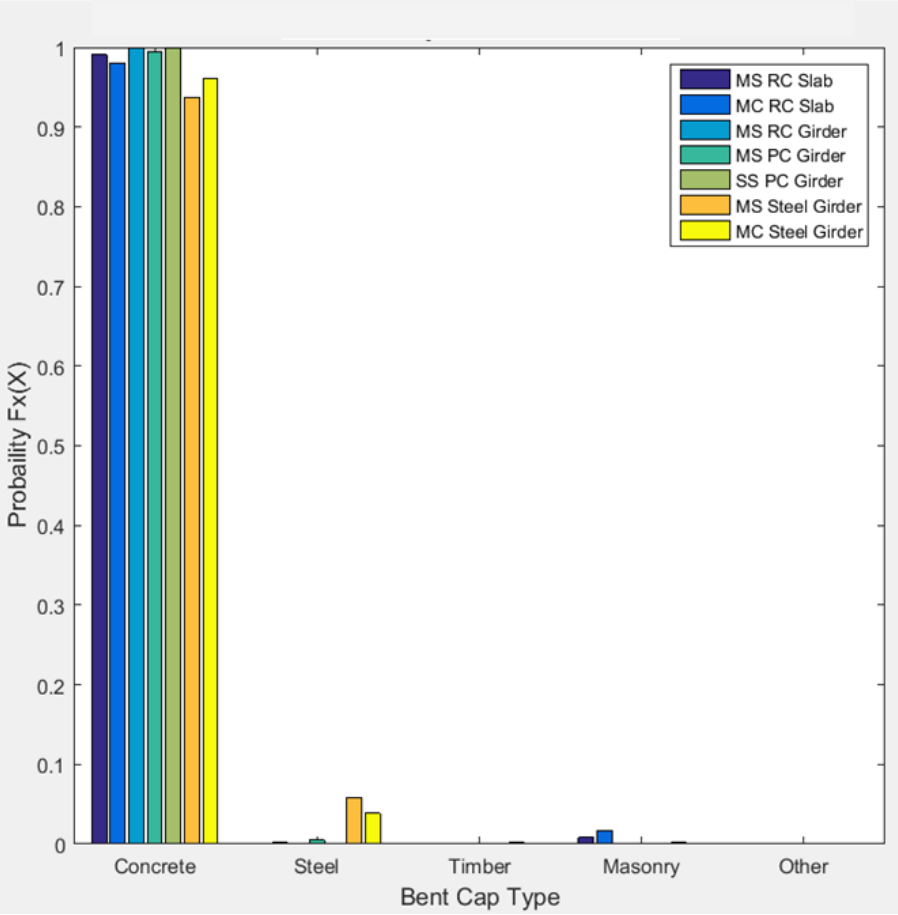

Figure 2.14: Histogram for types of bent caps

2.2.7 YEAR BUILT

Year built is not a geometric parameter, however, it still is a parameter of significance when simulating seismic behavior. Knowing the year a bridge was built can indirectly provide information on typical construction and detailing practices of the time,

including material properties, girder and bent cross-section geometry, bearing details, standard reinforcement and bracing layouts, etc. Table 2.8 shows the median year of construction and average age for each bridge class, and Figures 2.15 through 2.17 show the distributions for year built. This inventory analysis shows that PC girders tend to be the most current design type, as the median year of construction is 1991 for the single span and 1989 for the multi-span types. MS Steel girder bridges tend to be the oldest construction, with a median year of 1940 and a median age of 77 years at the time of writing this thesis.

Table 2.8: Construction year statistics

Class	Median (year)	Median age
MS RC-Slab	1952	65
MS RC-Girder	1966	51
MS PC-Girders	1989	28
MS Steel Girders	1940	77
MC RC-Slab	1958	59
MC Steel Girders	1965	52
SS PC-Girders	1994	23

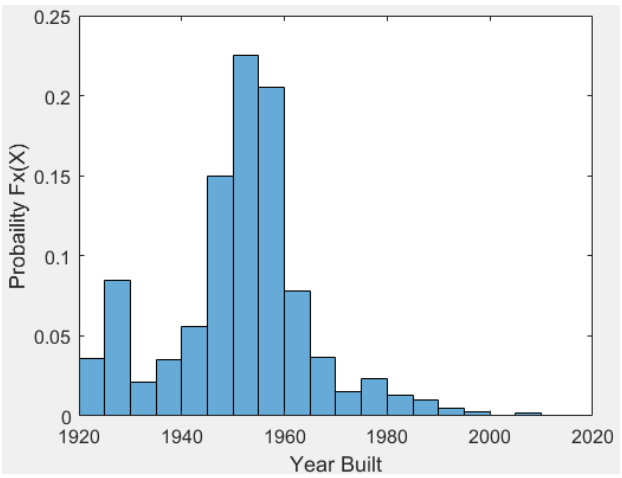

a) RC Slab

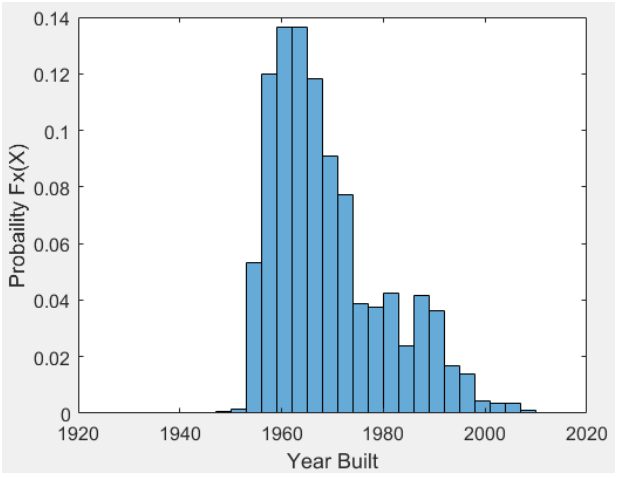

b) RC Girder

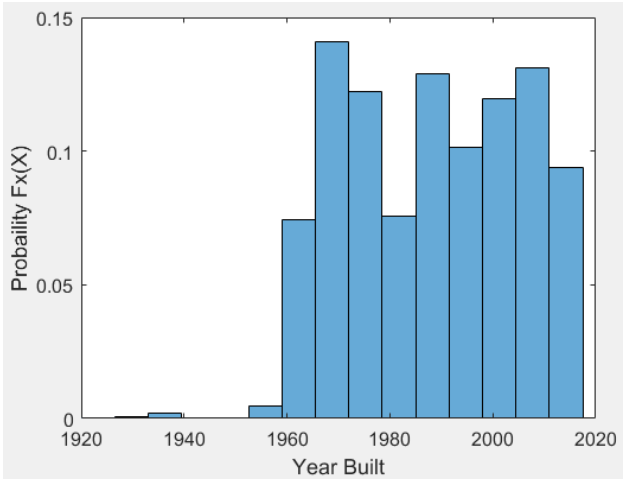

c) PC Girder

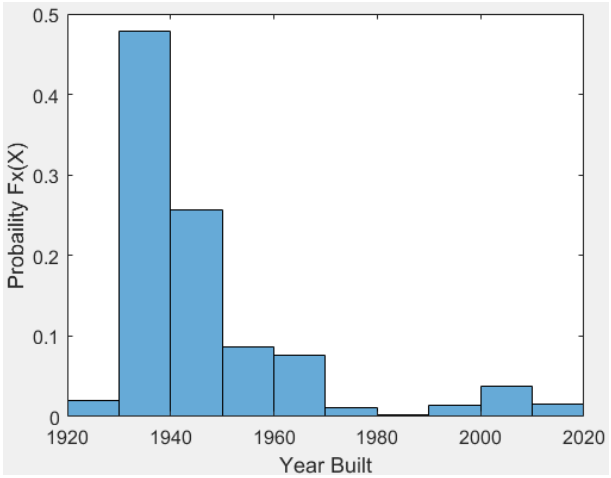

d) Steel Girder

Figure 2.15: Year Built – Histograms for multi-span simply supported bridge types

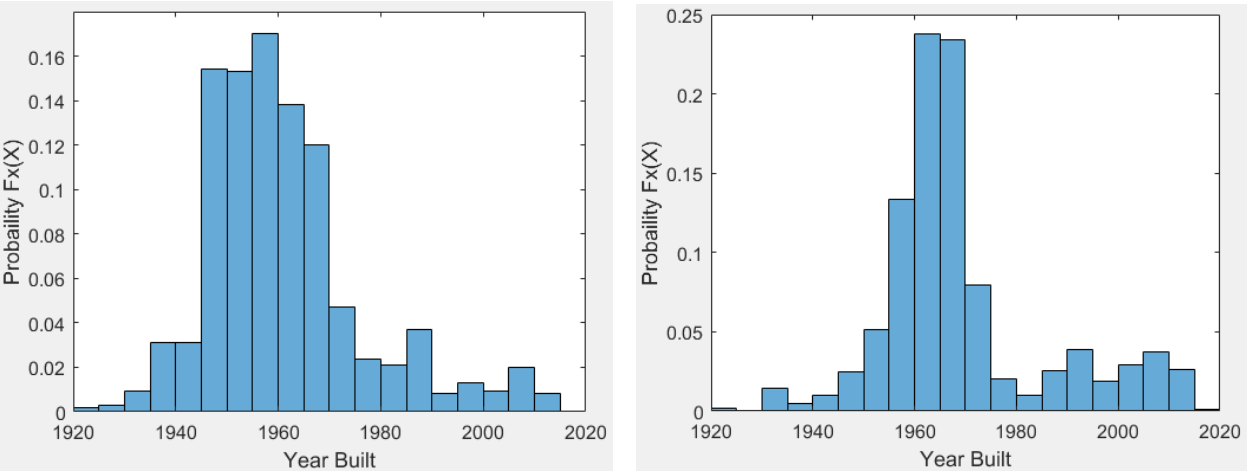

a) RC Slab *b) Steel Girder*

Figure 2.16: Year Built – Histograms for multi-span continuous bridge types

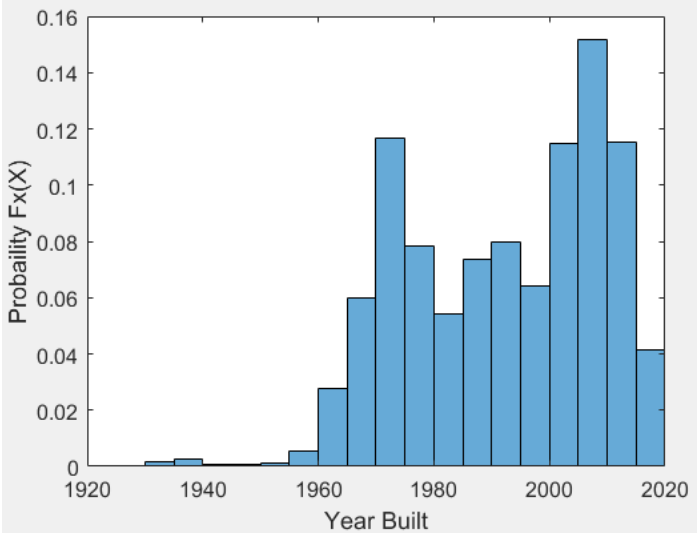

Figure 2.17: Year Built – Histogram for single span bridge types

2.3 Conclusion

The NBI database, along with additional information provided by the in-house TxDOT bridge database, was used to provide statistical information on the TxDOT bridge inventory. Seven bridge classes, representing 84.7% of the on-system bridges in Texas, were identified by TxDOT as being of primary importance in this seismic vulnerability study. These bridge classes are:

- Multi-Span Simply Supported RC – Slab
- Multi-Span Simply Supported RC – Girder
- Multi-Span Simply Supported PC – Girder
- Multi-Span Simply Supported Steel - Girder
- Multi-Span Continuous RC – Slab
- Multi-Span Continuous Steel – Girder
- Single Span PC – Girder

Statistical information on the following parameters were determined using the NBI and TxDOT databases:

- Number of spans
- Maximum span length
- Deck width
- Vertical Under-Clearance
- Skew angle
- Substructure
- Year built

This information will later be used in selection of sample bridges for each bridge class that are representative of those found in the inventory. These sample bridges will later be modeled and analyzed as part of the seismic fragility analysis.

3 ESTABLISH REPRESENTATIVE BRIDGE SAMPLES

When performing fragility analysis on a bridge network for a large region or state, such as Texas, a challenge that arises is determining an accurate way to estimate the seismic vulnerability of the entire bridge inventory without having to assess every individual structure. The first step in addressing this challenge is developing a thorough understanding of the bridge inventory for the area of study, which was addressed in Chapter 2 of this thesis. The second step in this process is using the information from the bridge inventory analysis to create representative bridge samples that are statistically significant yet nominally similar. This section is intended to provide an overview of the sampling methods used to determine the representative bridge samples used in this study.

3.1 Bridge Model Sampling Techniques

Creating a computational bridge model requires a number of different variables to fully and accurately define each bridge. Some of these variables may be geometric parameters such as span length, deck width, number of spans, etc. While other variables are used to model material properties such as concrete strength, steel reinforcing strength, soil stiffness, pile stiffness, bearing stiffness, etc. As seen in past studies (Nielson, 2005; Pan, 2007; Ramanathan, 2012), the number of modeling parameters can be quite large with upwards of 18 to 20 variables per model. To account for uncertainties in geometry and materials, one must sample from a probabilistic distribution for several, if not all of these variables. Thus, it is important to find an accurate yet efficient way to sample each of these parameters.

Over the past several decades, a lot of research and effort has been invested in developing efficient and reliable probabilistic analysis methods used in engineering research (Olsson and Sandberg, 2002). Several different methods have been used (e.g.,

Taylor series expansion and Neumann series expansion methods); however, Monte Carlo simulations, which are a probabilistic based sampling approach, have become the most popular approach in many engineering analysis applications. A concern that often arises when using a Monte Carlo simulation is the computational expense (Hilton and Davis, 2003). Straight Monte Carlo simulations randomly select samples for each uncertain variable in an engineering problem based on their associated probabilistic distributions, which requires a large number of samples in order to accurately represent the entire distribution (e.g., on the order of 1,000 to 10,000 samples, in some cases even more). In certain applications where only a small collection of samples are used, the clustering of samples in the high probability region becomes a concern in that the selected samples are no longer representative of the entire range of the population they are meant to represent.

To reduce the size of the sampling set (and thus reducing computational cost) without affecting the accuracy, other variations of Monte Carlo simulations have been developed. According to Huntington and Lyrintzis (1998), Latin Hypercube Sampling (LHS), which utilizes a stratified random sampling technique, is the best variant of Monte Carlo that utilizes smaller samples. In this approach, the cumulative distribution function for the parameters of interest are divided up into n (i.e., the desired number of samples) equal sections or bins, and then a sample is randomly selected from within each bin (e.g., see Figure 3.1). This approach allows for the full probabilistic distribution to be represented in just a small number of samples. In this study, sixty-four bridge samples are to be modeled for each of the seven bridge classes (i.e., multi-span pre-stressed girders, multi-span steel girders, multi-span reinforced slabs, etc.). Thus, the modeling parameters (which will be discussed in Section 3.2 of this thesis) for each bridge were sampled using a Latin Hypercube technique. More specifically, following the work of Iman and Conover (1982) a ranked Latin Hypercube method was used in order to match the sampled

correlation matrix as closely as possible to the empirical correlation matrix. In other words, the correlation between variables in the sample set should be representative of the correlation between variables in the entire population. The majority of the parameters used in this study show essentially zero correlation, and are thus assumed to have no correlation. It is still recommended, however, to use the ranked sampling method in order to eliminate the introduction of random or accidental correlation. For example, if deck width and column height are uncorrelated in the bridge inventory data, the ranked sampling approach would prevent the deck width and column height from generating a positive correlation during the random sampling process to avoid producing results unrepresentative of the actual population.

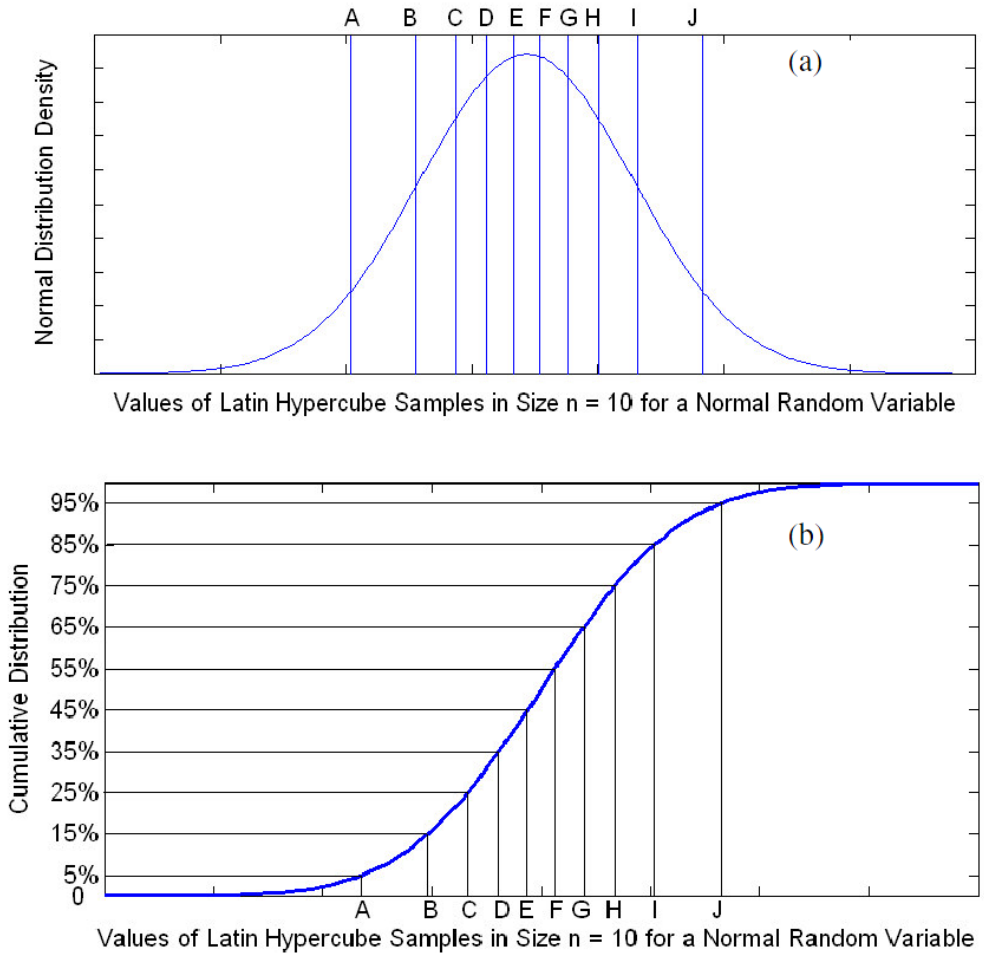

Figure 3.1: Generation of Bridge Parameter Samples by the Latin Hypercube Sampling Approach (Pan, 2007)

3.2 Bridge Samples

A major part of this study is analyzing the seismic vulnerability of the entire TxDOT bridge inventory. As previously mentioned, it is not feasible to analyze each individual structure; therefore, a set of bridge samples representing the variations in the Texas bridge inventory must be used. Based on experience from past studies (Choi, 2002;

Nielson, 2005; Pan, 2007; Ramanathan, 2012) a large number of bridge samples are required to capture the variations in seismic performance. In this project a total of 64 bridge samples are selected for each bridge class of concern (i.e., MS PC girders, MS RC girders, MS RC slabs, MS Steel girders, MC RC Slabs, MC Steel girders, and SS PC girders).

First, eight representative samples per class were selected to represent the variation in bridge geometry. These representative bridges were developed by sampling from the distributions of the five geometric parameters (i.e., number of spans, deck width, span length, year of construction, and under-clearance, which provides an approximate estimation of column height) obtained from the TxDOT bridge inventory using the LHS method as discussed in Section 3.1. To account for material uncertainties and variations in component behavior, the geometrically representative bridge samples are each paired with eight samples of the material properties and component behaviors, creating the 64 bridge samples per bridge class to later be used in the nonlinear response-history analyses. The parameters used to capture variation in material properties and component behaviors include, but are not limited to, steel and concrete strength, steel bearing stiffness, elastomeric bearing shear modulus, coefficient of friction for bearings, deck gap size, abutment stiffness, mass density, and inherent damping ratio.

3.2.1 GEOMETRIC PARAMETERS

The basic geometry, age, and design of a bridge can considerably change the seismic behavior of the structure. Thus, it is important to capture as many geometry and design variations as possible in the fragility analysis. With that being said, it is however, impossible to analyze every possible variation. Therefore, the challenge becomes finding the most common or "typical" structure geometries and designs that exist in the Texas bridge population. With the information found in the National Bridge Inventory (NBI) as

well as the internal bridge inventory database provided by TxDOT, actual probabilistic distributions of the geometric parameters and age of the bridge population were developed and reported in Section 2.2. These distributions along with a few assumptions and modifications were used in the sampling process. The geometric parameters used to create the eight geometrically representative bridges are depicted in Figures 3.2 and 3.3 and listed below:

- Deck width
- Span length
- Number of spans
- Year of construction
- Under-clearance

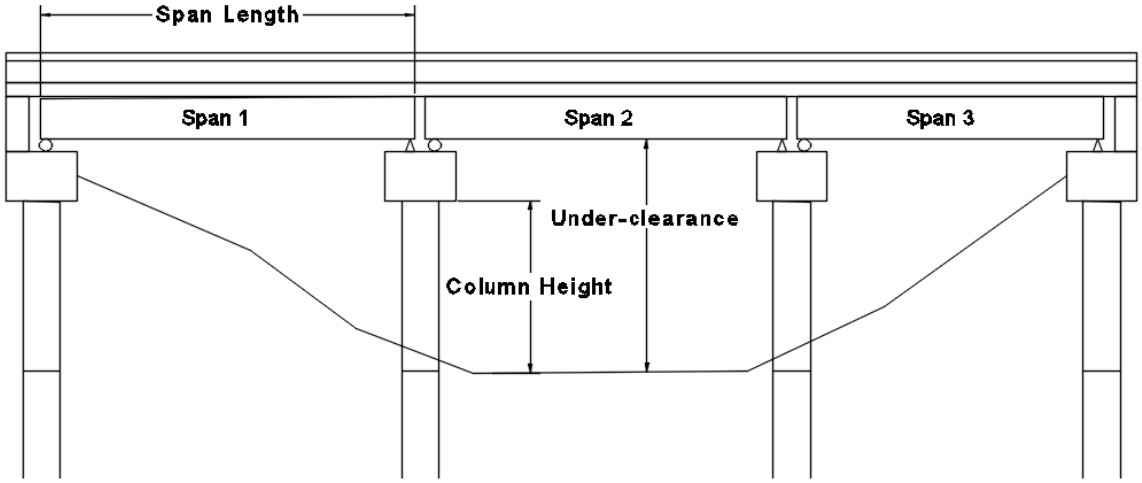

Figure 3.2: Profile of a typical three span bridge

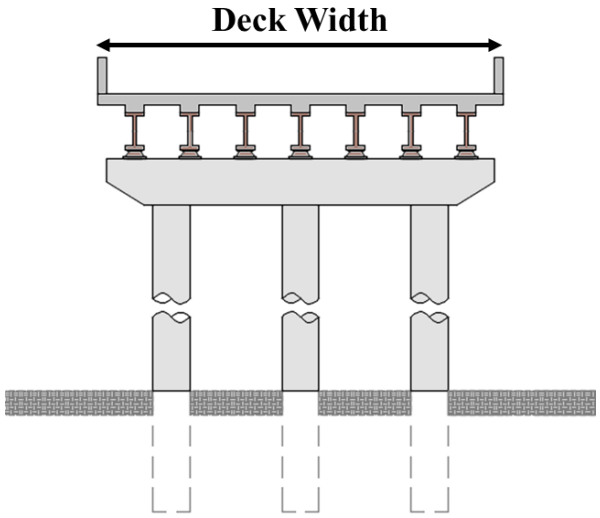

Figure 3.3: Cross section of a typical steel girder bridge

It was found during analysis of the TxDOT bridge inventory that a large majority of Texas bridges have little to no skew (see Section 2.2.5). Thus, skew angle is a geometric parameter that is not considered in this study.

The distributions for two of the geometric parameters, deck width and number of spans, were modified before sampling to reduce unnecessary complexities in the modeling process. For example, for each bridge class, there are some bridges in the population that have a very large number of spans (e.g., 12 or more). Using a Latin Hypercube Sampling approach would result in samples with a similarly large number of spans that would result in a significant increase in computational expense during the nonlinear response-history analyses, while the expected damage is not expected to be significantly different from a bridge with significantly fewer spans (Sullivan and Nielson, 2010).

To ensure that the bridge samples capture the vast majority of the bridge inventory without generating unnecessarily complex and computationally expensive bridge models, the deck width was only sampled from the 10th to the 90th percentile of the entire inventory for each class. For example, the multi-span pre-stressed concrete (MS PC) girder class has

deck widths that range from 10 feet to 223 feet, but were sampled between 31 feet and 86 feet (i.e., the 10th and 90th percentiles, see Figure 3.4). Not only do the very narrow and excessively wide bridges only represent a very small percentage of the population, but the excessive deck width significantly increases the computational expense of the nonlinear analyses without a significant effect on seismic performance.

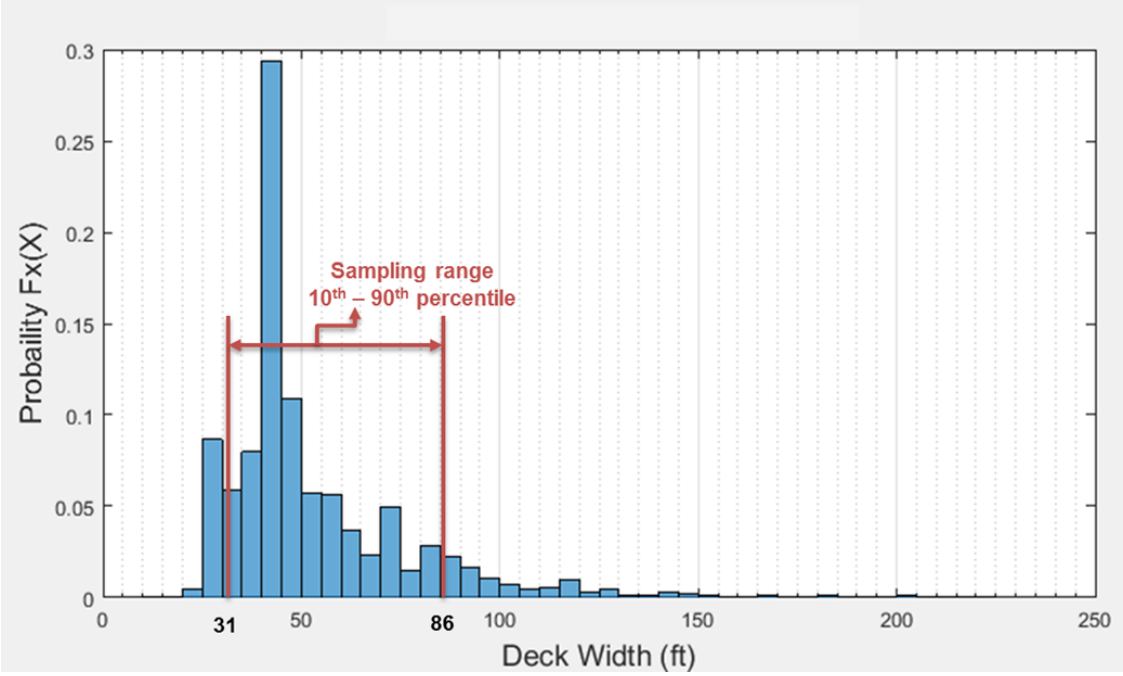

Figure 3.4: Sampling range for MS PC girder deck width

Also in this study, the number of spans considered in the sampling methods are reduced to only two to five span configurations to avoid having models with an excessive number of spans. This range of spans covers over 70% of the population for all bridge classes (see Figure 2.2 and 2.3 for span number distributions), except for the multi-span continuous concrete slab bridges with only 67% of the population having between two to five spans (see Figure 3.5). This modification is done once again to reduce the

computational expense for the large number of nonlinear response-history analyses that will be conducted in the seismic fragility assessment. Following this reasoning and the guidance of HAZUS (FEMA, 2003), most past fragility analysis (Choi, 2002; Nielson, 2005; Pan, 2007; Ramanathan, 2012; Tavares et al., 2013) studies have only considered a constant three-span bridge configuration. In some cases, fragility results from the base three-span configuration can be extrapolated to predict the response of bridges with a larger number of spans (FEMA, 2003; Sullivan and Nielson, 2010); however, the number of spans, ranging from two to five, will be explicitly considered in this study.

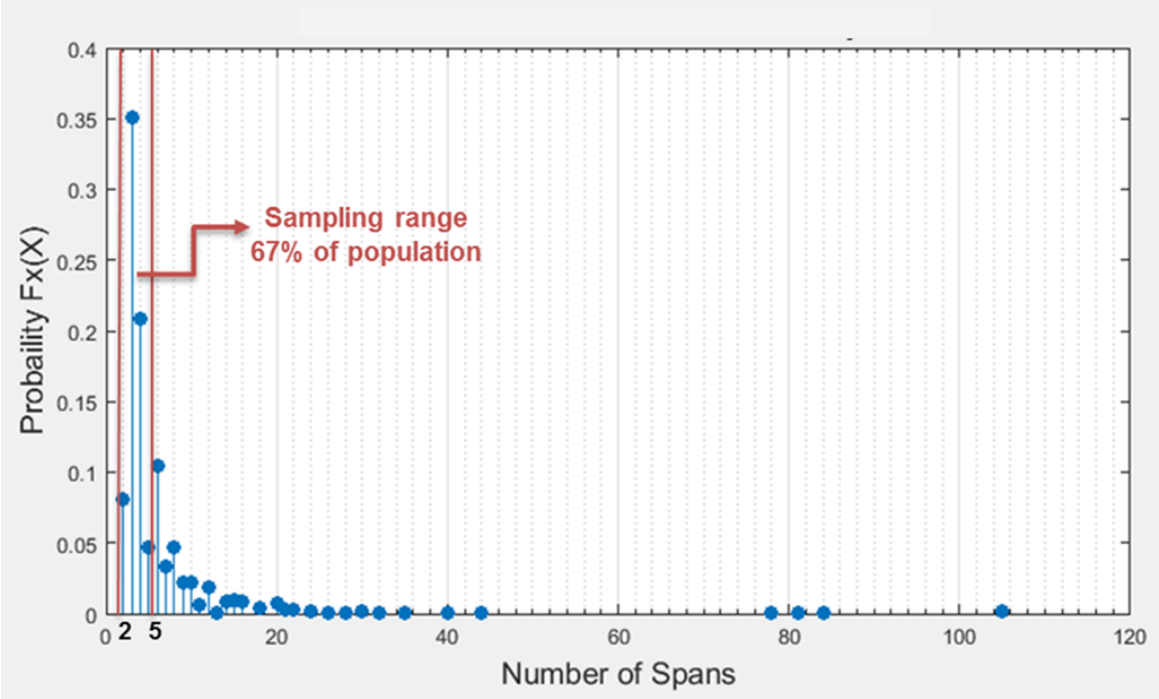

Figure 3.5: Sampling range for number of spans for MC RC Slab bridge class

Year of construction is not a geometric parameter; however, it is an important parameter when developing the bridge samples. Considering the era of construction

represented in the distribution of samples helps ensure that era-specific design details, such as bearing types, are accurately represented (Section 4). Also it was discovered that for certain bridge classes, deck width and span length were correlated with year of construction, particularly span length, which had a strong positive correlation with year of construction for both steel and pre-stressed girders. This observation is consistent with the changes in design procedures, standard details, material properties, and traffic demands through the years. Accounting for year of construction in the sampling process ensures that the era-specific design details are appropriately matched with bridge geometries that are representative of those eras.

Also worth noting is that under-clearance data were only available for approximately 43% of the entire bridge population, as described previously in Section 2.2.4. There were some bridge classes that did not contain a sufficient number of under-clearance data points to be statistically significant. For this reason, the under-clearance height was sampled and selected using the distribution of all the bridge classes combined together. In other words, under-clearance was sampled from the same distribution for all bridge classes, which was based on the distribution for all available under-clearance data in the population.

For modeling purposes the actual column height, not the under-clearance measurement, is needed. Column height is calculated by subtracting the depth of the bent cap from the under-clearance value. So column height was customized to each bridge class by using a typical bent cap depth that is specific to each class (see Section 4.2 for typical bent cap depths).

The geometrically representative bridge samples that will be used for each bridge class in this study can be seen below in Tables 3.1 thorough 3.7.

Table 3.1: Geometric samples of Multi-span reinforced concrete slab (MS RC slab) bridges

Bridge No.	Deck Width (ft)	Span Length (ft)	# of Spans	Year Built	Under Clearance (ft)
1	23.3	22	2	1948	23.08
2	42.2	25	4	1956	14.75
3	41.15	25	3	1952	16.42
4	27.5	25	5	1960	20.83
5	25.3	25	3	1942	15.83
6	25.30	18	4	1928	16.50
7	25.3	25	3	1963	17.00
8	46	25	2	1953	17.42

Table 3.2: Geometric samples of Multi-span reinforced concrete girder (MS RC girder) bridges

Bridge No.	Deck Width (ft)	Span Length (ft)	# of Spans	Year Built	Under Clearance (ft)
1	45.80	41	5	1971	15.50
2	25.70	40	4	1982	23.08
3	32.00	40	3	1963	15.08
4	39.18	30	2	1990	16.33
5	28.30	30	3	1959	16.92
6	42.30	40	3	1961	21.58
7	24.70	30	3	1954	16.50
8	44.20	30	5	1968	17.75

Table 3.3: Geometric samples of Multi-span pre-stressed concrete girder (MS PC girder) bridges

Bridge No.	Deck Width (ft)	Span Length (ft)	# of Spans	Year Built	Under Clearance (ft)
1	45.30	37	5	1938	17.08
2	40.98	107	4	1997	23.58
3	40.00	84	2	1969	18.42
4	36.30	60	3	2006	16.08
5	71.00	72	2	1985	16.67
6	57.20	121	3	1973	15.67
7	62.00	80	3	2015	14.75
8	44.30	100	3	1994	17.50

Table 3.4: Geometric samples of Multi-span steel girder (MS Steel girder) bridges

Bridge No.	Deck Width (ft)	Span Length (ft)	# of Spans	Year Built	Under Clearance (ft)
1	54.00	35	3	1938	23.00
2	29.33	40	4	1955	15.25
3	44.64	77	4	1999	15.00
4	44.00	45	3	1939	16.83
5	46.00	36	2	1946	16.33
6	46.30	40	5	1940	18.83
7	40.00	26	5	1933	17.33
8	35.33	50	3	1935	16.67

Table 3.5: Geometric samples of Multi-span continuous reinforced concrete slab (MC RC slab) bridges

Bridge No.	Deck Width (ft)	Span Length (ft)	# of Spans	Year Built	Under Clearance (ft)
1	54.11	30	3	1947	16.75
2	42.00	55	5	1961	22.67
3	46.00	25	4	1964	21.50
4	40.00	30	4	1969	16.92
5	32.30	25	3	1957	17.33
6	40.00	30	3	1952	16.33
7	46.00	45	2	1986	14.42
8	41.80	32	4	1959	15.67

Table 3.6: Geometric samples of Multi-span continuous steel girder (MC Steel girder) bridges

Bridge No.	Deck Width (ft)	Span Length (ft)	# of Spans	Year Built	Under Clearance (ft)
1	74.98	60	3	1955	22.83
2	27.88	90	4	1962	17.50
3	31.20	87	3	1967	15.58
4	53.70	118	4	1964	14.83
5	41.43	40	3	1970	17.08
6	43.20	145	4	1973	16.25
7	40.00	70	3	1959	16.50
8	35.20	240	2	2004	18.33

Table 3.7: Geometric samples of Single span pre-stressed concrete girder (SS PC girder) bridges

Bridge No.	Deck Width (ft)	Span Length (ft)	Year Built	Under Clearance (ft)
1	42.00	60	1999	17.50
2	60.80	112	2010	16.75
3	82.82	70	1975	16.08
4	35.91	95	1983	17.00
5	46.00	125	1962	15.92
6	40.00	80	1993	21.08
7	44.30	100	2015	23.33
8	46.20	120	2006	15.17

3.2.2 MATERIAL PROPERTIES AND COMPONENT BEHAVIOR

Just like with geometric uncertainties, to accurately account for variation in the current Texas bridge inventory, the uncertainties in material properties as well as component behavior should be considered. The parameters associated with material properties and component behaviors (e.g., steel and concrete strength, steel bearing stiffness, elastomeric bearing shear modulus, coefficient of friction for bearings, deck gap size, abutment stiffness, etc.), however, cannot be found in NBI or any other database, making it difficult to create samples from empirical distributions. Instead, information pertinent to these parameters was gathered from past literature, TxDOT standards, and a large number of as-built drawings of actual Texas bridges (a list of all as-built drawings reviewed and used in this study can be found in Appendix D). The following sections give details regarding the uncertainty models assumed for each of these parameters.

3.2.2.1 Concrete Compressive Strength and Steel Reinforcing Yield Strength

Reinforced concrete is a common material used in bridge construction. Reinforced concrete is frequently used in foundations, bents, bridge decks, and other superstructure

elements. In this study, the uncertainties in concrete compressive strength and steel reinforcement strength are considered explicitly. Bournonville et al. (2004) conducted a study looking at the properties of A615 grade 40 steel bars (f_y = 40ksi, which are commonly used in pre 1990s TxDOT bridge construction) and found that the yield strength, f_y, tends to follow a right skew distribution. So in this study a lognormal distribution was chosen to model uncertainty of reinforcement yield strength. The median value and standard deviation for grade 40 reinforcing bars is 55,000 psi and 4,900 psi, respectively (Bournonville et al., 2004). Concrete compressive strength, f'_c, is assumed to follow a normal distribution following the guidance of Unanwa and Mahan (2014). Concrete bridge construction dating back to the 1950s is expected to have lower bound or nominal compressive strengths between 3,000 psi and 5,000 psi. However, ASCE 41 (2013) suggests that expected strengths are closer to 1.5 times the lower bound. To capture a wide range of compressive strengths in this study, a median value of 4,500 psi is used, and again following guidance from Unanwa and Mahan (2014), a coefficient of variation of 0.19 is used to estimate a standard deviation of 850 psi.

3.2.2.2 Bridge Bearings

Bridge bearings are a very important component of a bridge, as they are the primary mechanism for transferring loads between the superstructure and substructure. Bearings take on many configurations throughout the different bridge classes (e.g., elastomeric bearings, high- and low-type steel bearings, etc.; see Section 4.3 for details); however, there are two main behavior classifications, fixed (i.e., restrained in both the longitudinal and transverse directions) and expansion bearings (i.e., restrained only in the transverse direction). In simply supported spans, you will often find alternating fixed and expansion

constraints. In continuous spans, the fixed type bearing is typically at the interior girder supports while the expansion bearings are at the exterior girder supports.

When it comes to modeling bearing behavior, there are several parameters that are needed: coefficient of friction (COF), stiffness, dowel strength (concrete bridges only), and dowel gap (concrete bridges only). All of these parameters are dependent on the material and configuration of the particular bearing. Older steel girder spans, both continuous and simply supported, typically have a type of steel bearing, which will be used in this study; however, in newer construction steel girders may be supported by elastomeric bearings. Mander et al. (1996) conducted a study looking at the behavior of steel bearings under cyclic lateral loading and determined values for both COF and stiffness, which will serve as the basis for this study. The COF could vary for several reasons; however, Mander et al. (1996) suggests that the COF for low-type sliding bearings could vary from 0.2 to 0.6 depending on the level of corrosion (i.e., ranging from clean to heavily corroded, respectively). For high-type steel rocker bearings, the COF similarly varied from 0.04 to 0.12. To account for uncertainty of corrosion in this study, samples will be selected assuming a uniform probabilistic distribution within the aforementioned COF ranges. Stiffness of fixed bearings is another important parameter that must be considered; however, due to an insufficient amount of data to accurately predict the variation in stiffness, it is suggested to use a uniform distribution with bounds of 50% and 150% of the mean value (Nielson, 2005). Referring again to the Mander et al. (1996) experimental study, a mean initial stiffness value of 765 kip/in will be used in the longitudinal direction for all steel fixed bearings, and a mean stiffness of 114 kip/in will be used in the transverse direction.

For pre-stressed concrete bridges an elastomeric type bearing is used, which consists of a rubber pad and a steel dowel, used to limit the movement of the superstructure.

For elastomeric bearings, a numerical equation can be used to estimate the COF. As seen in Equation 3.1 the COF, μ, is a function of the normal stress, σ_m, on the bearing. To account for uncertainty in the COF, the σ_m and μ will be calculated based on the associated gravity loads acting on each specific bearing, and then the uncertainty will be introduced as a COF multiplication factor. The multiplication factor is assumed to follow a lognormal distribution with a mean of zero and a standard deviation of 0.1 (Dutta, 1999; Ramanathan, 2012).

$$\mu = 0.05 + \frac{0.4}{\sigma_m} \tag{3.1}$$

Initial stiffness of the elastomeric bearing can also be estimated with the following equation:

$$k_o = \frac{GA}{h_r} \tag{3.2}$$

Where, G = shear modulus of the elastomer, A = area of pad, and h_r = thickness of the pad. Past studies have shown variability in G has a strong correlation with the variability in hardness of the elastomer (e.g., the elastomer experiences an increase in hardness with age as it is exposed to external elements) (Mtenga, 2007). AASHTO Design specifications implies that G ranges from 0.66MPa (96 psi) to 2.07MPa (300 psi); however, there is insufficient information on the actual distribution within this range. Thus in this study, G is assumed to have a uniform distribution between the AASHTO-specified limits. The pad area and pad height parameters will be selected deterministically from standard bearing details from the corresponding era of construction.

To accurately capture the full behavior of an elastomeric bearing, the dowel strength and the gap between the dowel and the slotted hole in the bottom of the girder must also be considered. During a seismic event it is possible that the dowel could

experience significant inelastic deformations. Following the guidance of Choi (2002), it is assumed that the ultimate strength of the dowel is directly related to the ultimate strength of the steel. Attempting to better understand the behavior of dowels in an earthquake event, Choi developed a finite element model of a typical dowel (i.e., a 1 inch diameter dowel that projected 3 inches into the bottom of the girder). Choi found that the ultimate lateral strength of this typical dowel was approximately 58kN (13 kips). However, if a different size dowel is used the strength is assumed to be quadratically proportional (i.e., the strength gets scaled according to the cross-sectional area ratio between the two dowels). In Texas, it is common to use a 1.25 inch diameter dowel (as opposed to the 1 inch diameter dowels in the Choi (2002) study); therefore, in this study it is assumed that the average ultimate lateral strength is 20 kips. To account for variation, the dowel strength is assumed to follow a lognormal distribution with a mean value of 20 kips and a coefficient of variation (COV) of 0.08. Accounting for the fact that the dowel is not sitting perfectly in the middle of the slotted holes in the girders (i.e., slotted holes only at expansion bearings), it is important to capture the variations in the dowel gap in the model. Thus, in this study it is assumed that dowel gap varies uniformly between 0 and 2.75 inches (based on the maximum length of slot in the bottom of the girder minus the dowel diameter, i.e. a 4 inch slot and 1.25 inch dowel).

Reinforced concrete girder and slab type bridges have multiple bearing design options. Nielson (2005) determined that these type of bridges in the CSUS utilize elastomeric bearings; however, in Texas it is common to use an alternative type of concrete bearing. This alternative bearing design does not use elastomeric pads. Instead alternative materials (e.g., a combination of powdered graphite, oil, roofing felt, asphalt board, etc.) are used to lubricate the interface of the concrete superstructure and concrete bridge seat at expansion bearing locations, and at fixed bearing locations the concrete superstructure sits

directly on the concrete bridge seat and is restrained by 0.75 inch steel dowels. Section 4.3.3 provides more details pertaining to this alternative concrete bearing. For modeling purposes the behavior of the alternative concrete bearing is governed by the COF for concrete on concrete as well as the strength of the dowel. Following the guidance of the ACI 318 building code (ACI, 2014) the median value of COF for a hardened concrete on concrete surface is assumed to be 0.6. To consider uncertainty in the COF, a multiplication factor will be selected and used in the same fashion as discussed previously for the elastomeric bearing. Similarly, the ultimate strength of the 0.75 inch dowel can be calculated following the same procedure (i.e., the dowel strength can be scaled by the cross-sectional area ratio) as for dowels used in the elastomeric bearing. Thus, a median ultimate dowel strength of 7 kips and COV of 0.08 will be used in this study.

3.2.2.3 Superstructure Mass

Mass of the superstructure is a variable that can have significant effects on the seismic response of a structure. Variations in mass can be linked to varying geometric parameters (i.e., span length, deck width, etc.), as well as from incidental sources such as material densities, varying slab thickness, parapets and barrier rails, riding surface overlay, etc. In this study, variations in mass due to geometric parameters are considered explicitly by parameter sampling; however, the uncertainty due to incidental sources will be considered with a mass scaling factor. Following the guidance of Ramanathan (2012), this mass factor is assumed to follow a uniform distribution with bounds of 110% to 140% of superstructure mass calculated from given geometries and material densities. Specific values for these bounds are not presented in this section since superstructure mass changes with every bridge sample.

3.2.2.4 Damping Ratio

Damping ratios for bridges typically range from 0.02 to 0.07 of critical damping, which represents the 2nd and 98th percentiles according to Bavirisetty et al. (2000). Fang et al. (1999) found that damping in tall buildings follow a normal distribution, which can be extended to bridges (Nielson, 2005; Ramanathan, 2012). Therefore, in this study uncertainty in damping ratio will be represented by a normal distribution with a mean of 0.045 and standard deviation of 0.0125.

3.2.2.5 Loading Direction

Torbol and Shinozuka (2012) conducted a study looking at the effect of the angle of incidence (i.e., the angle of "attack" of the ground motion) on bridge fragility curves. Their results indicated that the angle of seismic incidence could lead to significant variation in the fragility of a bridge, and ultimately could lead to the underestimation of the vulnerability of the structure. Determining the angle of incidence of a seismic event on a particular structure is not easy; however, with enough site specific information and knowledge of seismic fault activity one could argue that a particular angle of incidence could be generated with reasonable error. In the current study, an entire network of bridges with very different site information and orientations are being assessed. Thus, it is unreasonable to determine bridge specific loading directions for unknown earthquake sources. Following the guidance of Torbol and Shinozuka (2012), in this study the angle of seismic incidence is considered a random variable sampled from 0 to 360 degrees.

3.2.2.6 Deck Gaps

Deck gaps are used in bridge design to allow for expansion and contraction of the superstructure. These gaps can be found at designated expansion joints at both the abutments and interior bents. Temperature variations as well as construction imperfections

can create large uncertainties in the expansion gaps, thus it is important to account for this in the modeling process. Expansion joint details vary between the bridge classes and are typically selected based on the expected thermal movement and any anticipated shortening. Common types of joints include poured sealant and neoprene compression sealant, which are common in RC slab and RC girder construction, and armor joint and sealed expansion joints, which are common in PC girder and steel girder construction. Following the study by Ramanathan (2012), the gaps at both the abutments and interior bents are assumed to follow a uniform distribution, with two sampling ranges (i.e., smaller and larger gaps). Looking through the TxDOT standards and as-built drawings, it was observed that the poured sealant, neoprene sealant, and the armored expansion joints have a much smaller movement range (e.g., 0 to 2 in) than their sealed expansion joint counterpart (e.g., 0 to 6 in). Thus in this study, the deck gaps for the RC slab and RC girder classes will be sampled from 0 to 2 inch, while the steel and PC girder classes will be sampled from 0 to 6 inch.

3.2.2.7 Foundation Stiffness

Foundation stiffness depends on many variables (e.g., soil characteristics, pile characteristics and layout, foundation type, etc.). Gathering information from the TxDOT bridge database, it was determined that the predominate type of foundations found in Texas (i.e., ~83% of on-system bridges) are deep foundations comprising of a system of drilled shafts or pile groups. This substructure system consists of an integral column and shaft/pile foundation, or a pile group foundation connected to the columns through a pile cap (details and schematics of typical foundations can be found in Section 4.2.2).

Due to the nature of this study (i.e., a large number of generic bridge samples representing varying soil profiles from across the state) and the lack of relevant foundation testing data, a simplified foundation model was selected to represent foundation behavior.

This foundation model assumes a rotationally fixed condition with translational springs in the longitudinal and transverse directions (Prakhov, 2016). Following the works of Choi (2002) and Nielson (2005), the translational foundation stiffness is assumed to be linearly related to the stiffness of the shafts and/or piles. Following the guidance of the Caltrans Seismic Design Criteria (Caltrans, 2007) the initial stiffness of 40 kip/inch per pile is assumed as the median value for translational pile stiffness. Due to the lack of available data, Caltrans recommends a constant stiffness for all types of piles, regardless of pile material or geometry. Although this assumption does not account for changes in stiffness associate with different pile size or depths, it represents the current state of practice regarding abutment modeling. To account for uncertainty, the initial pile stiffness used in this study was sampled from a uniform distribution with bounds of 20 kip/inch to 75 kip/inch per pile. After a thorough review of TxDOT design standards and as-built drawings, it was determined that a typical pile group foundation (e.g., pile footing) can be represented by four piles per column (see Section 4.2.2 for foundation details). Resulting in a translational foundation stiffness for a pile foundation ranging between 80 kip/inch and 300 kip/inch in both the transverse and longitudinal direction.

Ramanathan (2012) performed an analysis on a variety of integral column and drilled shaft/pile systems and soil profiles using the software called LPILE, which is a program used for the analysis and design of piles and drilled shafts under lateral loads. From this analysis, it was determined that the translational stiffness of an integral column and shaft/pile is linearly related to the diameter of the shaft/pile (see Table 3.8, and Figure 3.6). Following the linear relationship shown in Figure 3.6 (i.e., stiffness=10.75(diameter)-149.43) and using a typical shaft diameter found in Texas (e.g., 30 inch dia. for the MS PC girder bridge class), a median translational stiffness for an integral column and shaft/pile was found to be 173 kip/inch. Comparing this stiffness to a four pile group foundation

with a median pile stiffness of 40 kip/inch per pile (i.e., 160 kip/inch translational foundation stiffness for the four-pile group), it is evident that the pile group foundation and the integral column/shaft foundation have similar stiffnesses. For the case of simplicity, in this study the translational foundation stiffness for drilled shaft foundations is determined by the sampled value of initial pile stiffness (i.e. 20 kip/inch/pile to 75 kip/inch/pile) multiplied by a relevant coefficient that is determined based on shaft diameter. For example, a 24 inch shaft is equivalent to the stiffness of 3 piles (median of 120 kip/inch), 30 inch diameter shaft is equivalent to the stiffness of 4 piles (median of 160 kip/inch), 36 inch shaft is equivalent the stiffness of to 6 piles (median of 240 kip/inch), and a 42 inch shaft is equivalent to the stiffness of 8 piles (median of 320 kip/inch).

Table 3.8: Translation foundation stiffness (Ramanathan, 2012)

Foundation Type	**Translational stiffness (kip/in)**
16 in intergral pile column	30
6 ft dia. Drilled shaft	600
8 ft dia. Drilled shaft	900

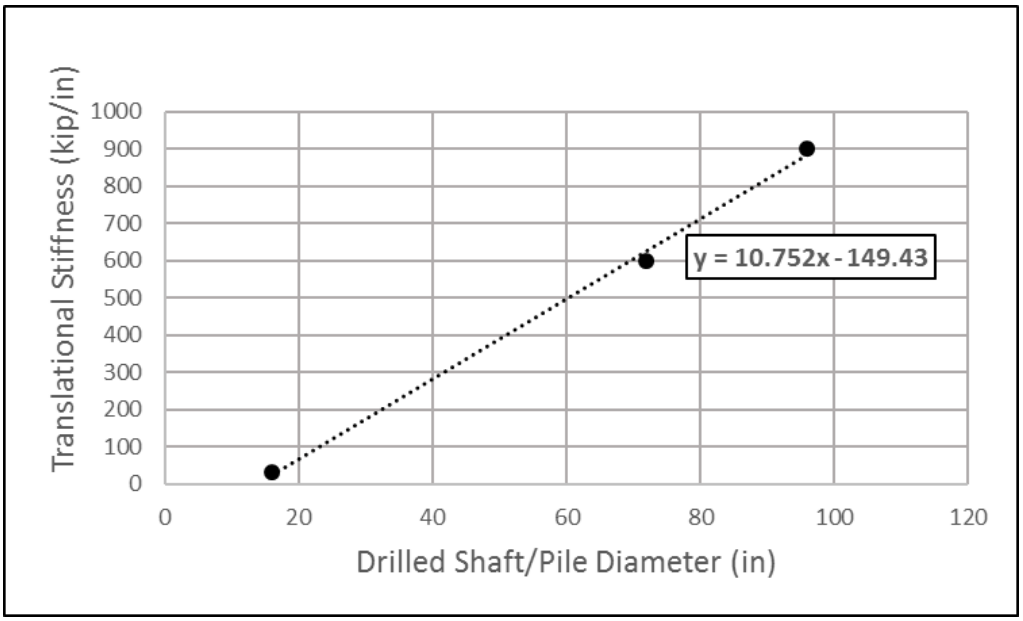

Figure 3.6: Translational foundation stiffness vs. shaft/pile diameter

A thorough review of TxDOT design standards and as-built drawings indicates that pile groups and drilled shafts were the most common below ground substructure type (see Section 2.2.6). Where pile foundations are used, it was assumed that four piles were used per column, and where drilled shafts are used, the shaft diameter was correlated to an equivalent stiffness of a pile group as mentioned above. More information on the foundation type assumed for each bridge class can be found in Section 4.2.2.

3.2.2.8 Abutment Stiffness

In addition to vertical gravity loads, abutments also experience horizontal loads during a seismic event. Two types of horizontal resistance are present during loading in the longitudinal direction as shown in Figure 3.7. The first is a passive resistance, which is developed as the abutment backwall is pressed into the soil backfill. In this case, the resistance is provided by the soil and the shafts/piles. The other type is active resistance, which is developed from the shafts/piles when the abutment pulls away from the backfill.

The resistance in the transverse direction is provided by the shafts/piles and wing walls (Nielson, 2005). Following the work of Borzorgzadeh et al. (2007) the initial stiffness per unit length of a 5.5 feet tall abutment, k_i, in the passive direction is suggested to be 20 kip/inch per foot of abutment length; however, the abutment stiffness, k_{abut}, can be adjusted proportionally to the backwall height as follows:

$$k_{abut} = k_i (= 20.0 \ \frac{\text{kip/in}}{\text{ft}}) \times b \times \left(\frac{h_{abut}}{5.5} \right) \tag{3.3}$$

Where, b is the width of the backwall and h_{abut} is the height of the abutment. This particular study also found that the initial passive stiffness is dependent on several other variables (i.e., soil properties, vertical wall movement, and area of structural backfill), thus should be sampled to account for uncertainty. Due to insufficient data on the distribution of initial stiffness, this parameter is assumed to follow a uniform distribution between 20 kip/inch per foot of abutment length and 50 kip/inch per foot of abutment length based on recommendation from Caltrans (1999).

Active resistance, as well as transverse resistance, is provided by the shafts/piles. As discussed in Section 4.2.3 abutment foundations are typically the same type as those used in the interior supports. Due to this characteristic and the nature of active abutment behavior (i.e., resistance provided solely by the shaft/piles), it is assumed in this study that the active abutment behavior is the same as the foundation as described in Section 3.2.2.7 (e.g., active abutment stiffness is equal to the translational foundation stiffness).

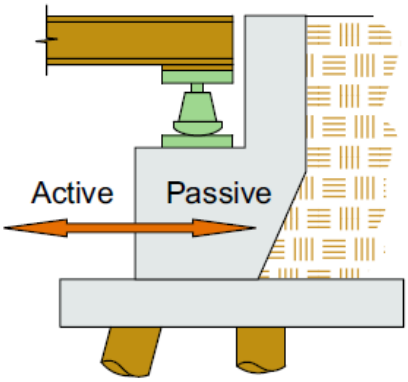

Figure 3.7: Horizontal Abutment Behavior (Nielson, 2005)

3.2.2.9 Parameter Samples

A summary of all the material properties and component behaviors, and their respective distribution characteristics can be seen in Table 3.9. As an example, Tables 3.10 through 3.17 show the parameter samples for the MS PC girder bridge class that are to be matched with the geometric representative bridge samples from Section 3.2.1. The parameter samples for the rest of the bridge classes (i.e., MS RC girder, MS RC slab, MS Steel girder, MC RC Slab, MC Steel girder, and SS PC girder) are presented in Appendix C.

Table 3.9: Summary of parameters and distribution characteristics

Parameter Description	Abbreviation	Distribution Type	Median	Std. Deviation	Upper	Lower	Units
Material Properties							
Concrete strength	Conc Str	Normal	4500	850	--	--	psi
Reinforcing strength	Reinforcing Str	Lognormal	55,000	4900	--	--	psi
Bearing Stiffness							
Steel fixed - Longitudinal	Steel Fix - Long	Uniform	765	--	1147	352	kip/in
Steel fixed - Transverse	Steel Fix - Trans	Uniform	114	--	171	57	kip/in
Elastomeric shear modulus	Elasto shear mod	Uniform	--	--	96	300	psi
Bearing Coeff. Friction (COF)							
Steel Rocker	Steel Rocker	Uniform	--	--	0.12	0.04	--
Steel Sliding	Steel Sliding	Uniform	--	--	0.6	0.2	--
COF Multiplication factor	COF MF	Lognormal	0	0.1	--	--	--
Steel Dowel Properties							
Dowel Stength - Elastomeric	Dowel Str	Lognormal	20	1.6	--	--	kip
Dowel Stength - Alternative	Dowel Str	Lognormal	7	0.56	--	--	kip
Dowel Gap	Dowel Gap	Uniform	--	--	2.75	0	in
Abutment and Foundation Stiffness							
Passive Stiffness	Abr-Pas Stf	Uniform	--	--	50	20	kip/in per foot
Pile Stiffness	Pile Stf	Uniform	--	--	75	20	kip/in per pile
Other Structural Attributes							
Superstructure mass	Mass	Uniform	--	--	140	110	%
Damping ratio	Damp Ratio	Normal	0.045	0.0125	--	--	--
Deck Gaps - Large	Large Gap	Uniform	--	--	6	0	in
Deck Gaps - Small	Small Gap	Uniform	--	--	2	0	in
Loading direction	Load Dir	Uniform	--	--	360	0	degrees

Table 3.10: MS PC Girder parameters for geometric sample 1

	Bridge Sample 1							
	1	**2**	**3**	**4**	**5**	**6**	**7**	**8**
Conc Str	4303	4703	5437	5558	3669	4783	3932	3165
Reinf Str	53867	53215	48248	56264	58834	50585	58016	63368
Elasto Shear Mod	294	103	206	140	241	272	197	153
Elasto MF	1.19	0.97	0.84	0.91	1.03	1.08	0.96	1.04
Dowel Str	18.91	22.12	21.12	18.13	19.61	20.28	20.65	18.29
Dowel Gap	1.748	0.132	1.687	1.159	0.965	2.483	2.109	0.573
Abt-Pas Stf	29.5	42.6	49.3	40.4	21.4	27.4	32.6	35.6
Pile Stf	22.3	56.2	70.7	30.5	38.5	50.0	43.6	63.6
Mass	131	121	111	134	123	127	116	137
Damp Ratio	0.077	0.044	0.029	0.055	0.049	0.048	0.041	0.032
Large Gap	4.34	5.99	5.02	2.04	0.31	2.70	3.61	1.21
Load Dir	336	42	249	271	194	96	158	77

Table 3.11: MS PC Girder parameter for geometric sample 2

	Bridge Sample 2							
	1	**2**	**3**	**4**	**5**	**6**	**7**	**8**
Conc Str	5186	4920	4761	3461	4208	5718	4438	3878
Reinf Str	55543	59314	56588	43373	53625	51135	52159	61557
Elasto Shear Mod	160	123	212	258	237	107	299	178
Elasto MF	1.03	1.05	1.00	1.08	0.92	0.96	0.75	1.14
Dowel Str	17.58	18.34	20.08	21.81	19.86	20.89	23.15	19.35
Dowel Gap	0.220	2.020	0.819	1.253	1.594	2.726	0.389	2.249
Abt-Pas Stf	42.5	20.3	38.7	31.1	24.8	48.0	44.3	33.1
Pile Stf	39.7	43.1	63.0	48.8	25.0	72.0	31.0	57.1
Mass	119	122	125	129	111	139	114	135
Damp Ratio	0.035	0.016	0.040	0.064	0.048	0.044	0.051	0.059
Large Gap	1.32	2.08	5.26	2.29	4.02	0.37	3.48	4.67
Load Dir	8	300	141	258	190	63	359	103

Table 3.12: MS PC Girder parameter for geometric sample 3

	Bridge Sample 3							
	1	**2**	**3**	**4**	**5**	**6**	**7**	**8**
Conc Str	3419	4152	3904	5322	6624	4743	5050	4256
Reinf Str	52631	55994	51354	57827	53348	49364	61097	59225
Elasto Shear Mod	247	273	220	130	116	294	172	179
Elasto MF	1.16	0.93	1.04	0.80	1.02	0.95	1.00	1.10
Dowel Str	21.74	22.87	18.15	19.15	20.07	19.85	18.62	20.98
Dowel Gap	1.576	2.496	0.381	1.366	0.984	1.917	0.081	2.226
Abt-Pas Stf	24.0	29.9	23.5	31.4	47.6	40.9	44.0	37.4
Pile Stf	69.2	42.2	67.3	53.7	36.1	24.3	33.0	57.0
Mass	122	121	126	130	137	114	113	136
Damp Ratio	0.050	0.060	0.029	0.049	0.057	0.043	0.039	0.031
Large Gap	3.76	3.01	4.58	0.19	5.50	0.95	1.92	2.70
Load Dir	21	110	227	213	303	346	65	163

Table 3.13: MS PC Girder parameter for geometric sample 4

	Bridge Sample 4							
	1	**2**	**3**	**4**	**5**	**6**	**7**	**8**
Conc Str	6293	3988	3839	4764	5242	2458	4836	4392
Reinf Str	50209	52627	56148	56967	59285	67869	47694	54304
Elasto Shear Mod	246	208	144	119	161	293	250	185
Elasto MF	1.13	0.83	1.03	0.96	0.93	1.12	1.07	0.99
Dowel Str	18.48	17.71	21.17	23.57	18.91	20.02	19.77	20.66
Dowel Gap	0.980	0.229	2.216	2.561	0.632	2.022	1.582	1.089
Abt-Pas Stf	35.5	44.6	29.8	40.3	33.9	23.4	26.1	49.2
Pile Stf	21.8	53.4	33.3	43.8	56.1	69.3	35.7	62.0
Mass	136	126	121	123	117	113	132	134
Damp Ratio	0.039	0.033	0.051	0.082	0.049	0.043	0.054	0.025
Large Gap	4.62	5.60	4.34	1.10	0.12	2.84	3.21	1.60
Load Dir	140	190	229	134	317	312	77	23

Table 3.14: MS PC Girder parameter for geometric sample 5

	Bridge Sample 5							
	1	**2**	**3**	**4**	**5**	**6**	**7**	**8**
Conc Str	5522	3251	4653	5463	4363	3939	3831	4844
Reinf Str	55396	47291	54070	57045	50139	63356	52291	59464
Elasto Shear Mod	271	293	236	126	103	185	201	148
Elasto MF	1.14	0.90	1.09	0.97	0.89	0.95	1.07	1.03
Dowel Str	19.14	19.57	21.79	22.55	20.33	17.85	20.70	18.40
Dowel Gap	1.412	2.549	0.709	2.194	1.289	0.309	0.500	1.910
Abt-Pas Stf	36.6	43.4	34.3	21.9	41.1	23.8	46.5	27.9
Pile Stf	39.3	73.6	64.5	33.2	59.6	43.1	26.1	50.2
Mass	133	132	140	126	125	114	111	118
Damp Ratio	0.025	0.034	0.079	0.045	0.058	0.048	0.038	0.051
Large Gap	2.86	5.67	1.13	4.60	1.71	0.28	3.68	4.42
Load Dir	86	304	198	337	4	150	113	241

Table 3.15: MS PC Girder parameter for geometric sample 6

	Bridge Sample 6							
	1	2	3	4	5	6	7	8
Conc Str	4443	6231	3686	5014	3459	5309	4660	4204
Reinf Str	57262	53086	45119	55641	50264	61685	59832	53879
Elasto Shear Mod	150	235	118	250	177	298	140	213
Elasto MF	1.07	0.93	0.93	0.83	1.16	1.00	1.01	1.04
Dowel Str	21.81	20.89	18.29	17.69	19.93	20.21	18.99	22.00
Dowel Gap	0.690	0.210	1.091	1.735	0.380	2.117	2.515	1.660
Abt-Pas Stf	30.6	33.9	43.0	24.2	40.7	21.5	47.3	38.2
Pile Stf	43.5	24.7	56.6	31.0	39.1	52.7	65.5	74.8
Mass	118	115	123	136	128	133	132	110
Damp Ratio	0.057	0.047	0.038	0.062	0.029	0.050	0.032	0.043
Large Gap	2.86	1.53	5.60	4.56	0.27	1.38	3.71	4.49
Load Dir	1	125	311	344	147	63	205	229

Table 3.16: MS PC Girder parameter for geometric sample 7

	Bridge Sample 7							
	1	2	3	4	5	6	7	8
Conc Str	4815	4439	3255	5308	3665	3945	6135	4566
Reinf Str	54529	55672	63954	57096	49895	59551	47218	51657
Elasto Shear Mod	204	195	248	289	271	122	149	98
Elasto MF	1.08	0.80	0.93	1.25	0.94	0.99	1.04	1.00
Dowel Str	20.37	20.45	17.71	19.15	21.60	19.50	23.82	18.33
Dowel Gap	1.329	0.673	1.925	2.201	0.028	0.930	2.563	1.450
Abt-Pas Stf	47.0	40.0	44.2	24.9	35.2	28.9	20.7	34.3
Pile Stf	22.5	32.0	37.7	60.1	48.3	65.8	73.6	42.0
Mass	120	125	110	135	122	114	129	140
Damp Ratio	0.028	0.049	0.062	0.035	0.042	0.053	0.056	0.041
Large Gap	2.09	0.84	5.21	2.39	4.48	0.44	5.55	3.60
Load Dir	168	334	70	116	268	33	214	283

Table 3.17: MS PC Girder parameter for geometric sample 8

	Bridge Sample 8							
	1	2	3	4	5	6	7	8
Conc Str	4717	4064	3039	5663	4406	5088	3842	4842
Reinf Str	55711	50887	59420	54204	49258	52551	62232	57574
Elasto Shear Mod	181	132	264	297	101	217	160	228
Elasto MF	1.10	1.02	1.04	1.13	0.94	0.84	0.98	0.90
Dowel Str	18.43	17.94	22.23	21.51	20.17	19.32	20.50	19.75
Dowel Gap	1.198	0.554	0.007	1.962	0.828	1.522	2.195	2.557
Abt-Pas Stf	37.9	34.0	29.7	20.0	39.1	47.9	25.3	46.0
Pile Stf	65.2	43.0	71.0	56.1	22.5	30.3	47.9	36.5
Mass	136	122	140	131	128	114	118	111
Damp Ratio	0.052	0.047	0.030	0.060	0.058	0.035	0.042	0.038
Large Gap	3.98	2.83	4.52	0.77	5.78	0.50	1.50	3.16
Load Dir	147	256	18	55	220	289	96	329

3.3 Conclusion

When conducting a fragility analysis for a large transportation network, an important step is developing samples that accurately represent the entire network. The Texas bridge inventory consists of bridges of many different types, materials, sizes, and construction eras. The focus of this section was creating representative bridge samples that are statistically significant yet nominally similar. First, geometric parameters (i.e., deck width, span length, number of spans, year of construction, and under-clearance) were sampled to create eight geometrically representative bridge samples for each bridge class. Second, material properties and component behaviors (i.e., concrete strength, steel strength, bearing stiffness and coefficient of friction, mass, damping ratio, loading direction, deck gaps, and abutment and foundation stiffness) were sampled eight times and assigned to each of the geometric samples, creating a total of 64 bridge samples. These representative bridge samples will be paired with ground motions to conduct non-linear response-history analyses as part of the fragility assessment.

4 TXDOT BRIDGE COMPONENTS AND TYPICAL DETAILS

Having discussed bridge class statistics and sampling techniques in the previous chapters, the next step in developing representative bridge models is understanding the specific components and structural details for each bridge class. Bridge design and construction techniques not only vary among the different bridge classes, they also may vary based on era of construction. The bridge design standards and specifications are constantly evolving as new research and technologies become available. Thus, it is important to incorporate typical details from construction eras that are representative of each specific bridge class. The following sections will discuss bridge components and typical details specific to Texas, evaluating how these construction details have evolved over time and, in some cases, how they compare to details employed in other regions around the country. The details provided here are based on an extensive review of TxDOT bridge plans (as-built drawings, see Appendix D for more details) and standards pertinent to the bridge classes of concern in this study.

4.1 Superstructure

A highway bridge can be separated into three main components: the superstructure, the substructure, and the bearings as illustrated in Figure 4.1. The superstructure consists of the roadway surface, the railings, and some type of structural system (e.g., steel or concrete girders). As shown in Chapter 2, bridge superstructures can be made of a variety of different construction materials and various types of structural systems. This study specifically focuses on four different types of superstructure (e.g., steel girders, pre-stressed concrete girders, reinforced concrete girders, and reinforced concrete slabs) as shown in Figure 4.1.

When conducting a dynamic seismic analysis, the superstructure is the main contribution of mass for the bridge system, which must be accounted for in the model. Previous bridge fragility studies (Ramananthan, 2012) indicate that the superstructure is expected to remain elastic during a seismic event; thus, the superstructure is commonly assumed to behave elastically to reduce the complexity of the analysis or model. This assumption can be verified by simply monitoring the flexural demands in the superstructure during the seismic analysis. There are a variety of different ways to apply this assumption in the development of the superstructure model. For example, the stiffness and mass of the bridge superstructure could be lumped into a single beam-column element, two beam-column elements, or multiple beam-column elements. As the number of elements in a model increases, the computational demands also increases; however, the added complexity more accurately simulates the distribution of mass along the width of the bridge. For this particular study, multiple beam-column elements were distributed within the deck width to simulate the horizontal distribution of mass and stiffness of the superstructure, and additional mass nodes were vertically offset from the beam-column elements to simulate the vertical distribution of mass associated with the deck and rails. Specific details dealing with modeling techniques can be found in Prakhov (2016).

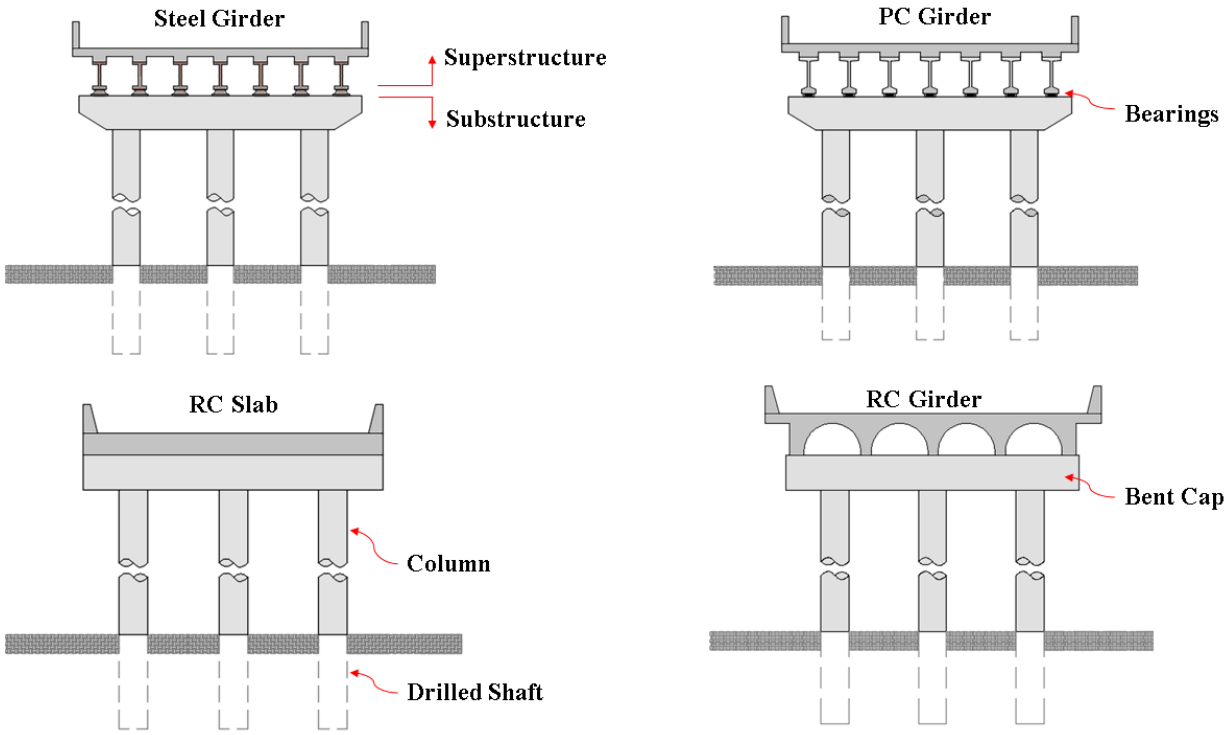

Figure 4.1: Bridge component classification for different bridge classes

4.1.1 STEEL GIRDERS

Structural characteristics of the different superstructure types are necessary to accurately assign the stiffness and mass to the superstructure elements. Steel girders, for example, will have different girders sections based on span length, girder spacing, and span continuity. Shorter steel spans (i.e., spans less than approximately 100 feet) are typically supported by standard rolled wide-flange, or W–shape, sections. Table 4.1 shows examples of steel beam sections allowed per the TxDOT standard drawings (TxDOT, 2006) based on span length and roadway width. From this table it is evident that there are a several different girders with varying section properties and weights that can be used for a given bridge geometry. Thus, it is important to employ a sampling technique to select beam sizes

and section properties that are representative of those that could be used for steel girders in the Texas bridge population. Information about the sampling technique and the beam sizes used can be found in Appendix A.

Table 4.1: Table of required beam sizes (TxDOT, 2015)

	30 - 50ft Span	60ft Span	70ft Span	80ft Span	90ft Span
24ft Roadway	W18 x 130	W21 x 166	W24 x 207	W27 x 235	W30 X 261
	W21 x 122	W24 x 146	W27 x 178	W30 X 211	W33 X 221
	W24 x 104	W27 x 146	W30 X 173	W33 X 169	W36 X 231
	W27 x 146	W30 X 173	W33 X 130	W36 X 150	W40 X 199
	W30 X 173	W33 X 118	W36 X 135	W40 X 149	
	W33 X 118	W36 X 135	W40 X 149		
	W36 X 135	W40 X 149			
	W40 X 149				
28ft Roadway	W18 x 130	W21 x 166	W24 x 207	W27 x 235	W30 X 261
	W21 x 132	W24 x 131	W27 x 178	W30 X 191	W33 X 241
	W24 x 117	W27 x 146	W30 X 173	W33 X 201	W36 X 231
	W27 x 146	W30 X 173	W33 X 141	W36 X 170	W40 X 199
	W30 X 173	W33 X 118	W36 X 135	W40 X 167	
	W33 X 118	W36 X 135	W40 X 149		
	W36 X 135	W40 X 149			
	W40 X 149				
30ft Roadway	W18 x 130	W21 x 132	W24 x 162	W24 x 229	W27 x 258
	W21 x 111	W24 x 117	W27 x 146	W27 x 194	W30 X 211
	W24 x 104	W27 x 146	W30 X 173	W30 X 173	W33 X 201
	W27 x 146	W30 X 173	W33 X 118	W33 X 152	W36 X 231
	W30 X 173	W33 X 118	W36 X 135	W36 X 150	W40 X 199
	W33 X 118	W36 X 135	W40 X 149	W40 X 149	
	W36 X 135	W40 X 149			
	W40 X 149				

Longer steel spans (i.e., greater than 100 feet, which are typically continuous spans) require girder depths larger than any of the available standard rolled shapes, necessitating the use of built-up plate girders. When built-up plate girders are designed, time and care is typically taken to determine an efficient plate girder design for each specific bridge to minimize the cost of material and fabrication. Consequently, TxDOT does not have a set

of standard drawings for continuous steel girders, making it more challenging to determine representative section properties for the bridge samples in the MC Steel girder class. One approach to obtaining properties for continuous steel girders is to conduct a full superstructure design following the TxDOT design manual for each bridge sample in this class. This approach, however, would be very time consuming, and may not reflect design practices representative of the era when much of the MC Steel girder bridges were constructed. Alternatively, as-built drawings of structures from the TxDOT database with geometries and construction eras similar to the MC Steel bridge samples can inform selection of section properties. In this study, continuous girder section properties were selected based on a combination of data from as-built drawings from representative MC Steel girder bridges and from typical "rules of thumb" used in girder design. More information about the selection guidelines and section properties used can be found in Appendix A.

4.1.2 PRE-STRESSED CONCRETE GIRDERS

Determining the section properties and mass of pre-stressed concrete girder spans (MS PC bridge class) tends to be a much simpler process. Historically the American Association of State Highway and Transportation Officials (AASHTO) has provided standard pre-stressed sections to be used in highway bridge design. Most state departments of transportation have adopted and used the AASHTO standard sections; however, TxDOT is one of the few states that has developed and used their own standard sections. The overall shape of the two designs are similar; however, there are minor differences in the dimensions resulting in slightly different section properties. Figure 4.2 shows the generic shape and the dimensions of both the AASHTO girders (i.e., Type II, III, and IV) and the TxDOT girders (i.e., Type B, C, 54, and 72). It also should be noted that in 2008 TxDOT

revised their pre-stressed girder sections to bulb-T sections (see Figure 4.2), which are used in new highway bridge construction.

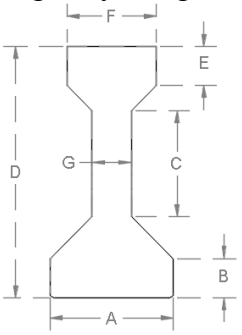

TxDOT and AASHTO prior 2008

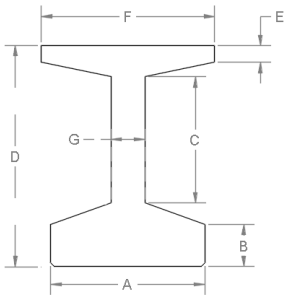

TxDOT Bulb – T girders

TxDOT I-Girders

Beam Type	A (in)	B (in)	C (in)	D (in)	E (in)	F (in)	G (in)
B	18	6	14	34	4	12	6.5
C	22	7	16	40	6	14	7
54	16	8	32	54	4	16	6
72	22	11	40.5	72	5.5	22	7

AASHTO I-Girders

Beam Type	A (in)	B (in)	C (in)	D (in)	E (in)	F (in)	G (in)
II	18	6	15	36	6	12	6
III	22	7	19	45	7	16	7
IV	26	8	23	54	8	20	8

Tx Girders (TxDOT Bulb-T)

Beam Type	A (in)	B (in)	C (in)	D (in)	E (in)	F (in)	G (in)
Tx 28	32	6.75	9	28	3.5	36	7
Tx 34	32	6.75	12	34	3.5	36	7
Tx 40	32	6.75	18	40	3.5	36	7
Tx 46	32	8.75	22	46	3.5	36	7
Tx 54	32	8.75	30	54	3.5	36	7
Tx 62	32	8.75	37.5	62	3.5	42	7
Tx 70	32	8.75	45.5	70	3.5	42	7

Figure 4.2: PC girder sections

In this study, the section properties and mass of the PC girder bridge samples (see Section 3.2.1 for PC girder samples) were selected from the old TxDOT sections if the construction year of the sample was prior to 2008 and from the new Tx girder sections for samples constructed after 2008. More specifically, after reviewing as-built drawings and standards for bridges constructed before 2008, it was determined that Type B girders are typically used for spans less than 70 feet, Type C girders for spans between 70 feet and 90 feet, and Type 72 girders for spans greater than 90 feet. Following TxDOT's recommendations for the new Tx girders, Tx 40 girders were used for samples with spans less than or equal to 90 feet, and Tx 62 girders for spans larger than 90 feet.

4.1.3 REINFORCED CONCRETE GIRDERS

Reinforced concrete girders (i.e., the MS RC girder class), also known as pan formed girders, are a style of cast-in-place concrete superstructure that was most commonly employed in the 1960s and 1970s. Figure 4.3a shows a standard RC girder cross-section typically used in Texas. In this figure the superstructure depth is shown as 24 inches; however, TxDOT does have a 33-inch RC girder section as well. Again, following the guidance of the as-built and standard drawings, the 24-inch section depth is used for span lengths less than 40 feet, while the 33-inch depth is used for spans of 40 feet and longer.

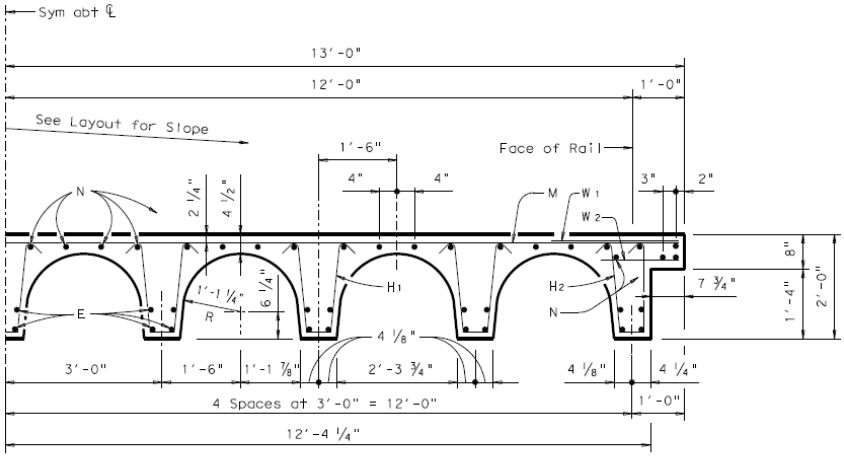

TYPICAL HALF TRANSVERSE SECTION

(a)

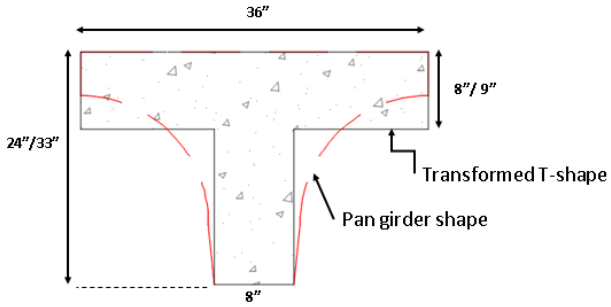

(b)

Figure 4.3: (a)RC Girder standard section (TxDOT, 2005), (b)Transformed T-section

To simplify calculations of the RC pan girder section, the section was transformed into a T-section with equal cross-sectional area and similar moments of inertia to ensure an accurate representation of the RC girder mass and stiffness. Figure 4.3b shows an example of the transformed section used to calculate section properties.

4.1.4 REINFORCED CONCRETE SLABS

The last superstructure bridge class is the RC slab class, in which the structural system is made up of either a cast-in-place reinforced concrete slab or pre-cast reinforced concrete slab panels. In Texas, the RC slab superstructure was most popular in the early to mid-1900s (e.g., 1930s-1970s, see Section 2.2.7 for year of construction statistics). This slab superstructure type can be constructed as either simply supported or continuous spans and is typically used in structures requiring much shorter span lengths (e.g., simply supported spans of approximately 25 feet, continuous spans of approximately 35 to 40 feet). Current TxDOT standard drawings and standards from the 1980s and 1990s indicate that in modern construction, MS RC slabs are specified to have a 16-inch thick slab, whereas MC RC slabs have 14-inch thick slabs for span lengths less than 30 feet and 16-inch thick slabs for spans greater than or equal to 30 feet. However, as-built drawings from RC slab girder bridges constructed prior to the 1980s indicate that MS RC slabs from this era were typically built with 12-inch slabs, and MC RC slabs were typically built with either a 12-inch or 14-inch slab. Based on the typical age of RC slab bridges in the Texas bridge population, in this study the MS RC slab bridges were assumed to have a 12-inch slab, and the MC RC slabs were assumed to have a 12-inch slab for spans less than 30 feet and a 14-inch slab for spans greater than or equal to 30 feet.

4.1.5 GIRDER SPACING

Knowing the size and type of girder is an important part in determining the mass and stiffness of the superstructure; however, the number and spacing of girders are also important parameters that need to be determined. Review of TxDOT standard and as-built drawings for pre-stressed and steel girder bridges showed that depending on the deck width, girder spacing is typically specified in 4 inch intervals with a lower and upper bound of 5 feet and 9 feet, respectively. To improve economy in the superstructure design, a design engineer commonly chooses to minimize the number of girders, while maintaining a reasonable girder spacing and a reasonable amount of overhang (e.g., the distance from the center line of exterior girder to the outside of the bridge deck, see Figure 4.4). This design process can lead to a variety of different girder spacings. For example, a bridge with a 26 feet deck width, as shown in Figure 4.4, can have four girders spaced at 7.33 feet and an overhang of 2 feet, four girders spaced at 7 feet with an overhang of 2.5 feet, three girders spaced at 9 feet with an overhang of 4 feet, and a variety of other combinations. After further investigation of standard and as-built drawings it was found that overhang distance ranges from 2 to 5 feet; however, it is evident that an overhang or approximately 2 to 3 feet is preferred. In this study, girder spacing is selected from a range of 6 to 9 feet, at intervals of 4 inch, based on which spacing value produces an overhang closest to 2 feet.

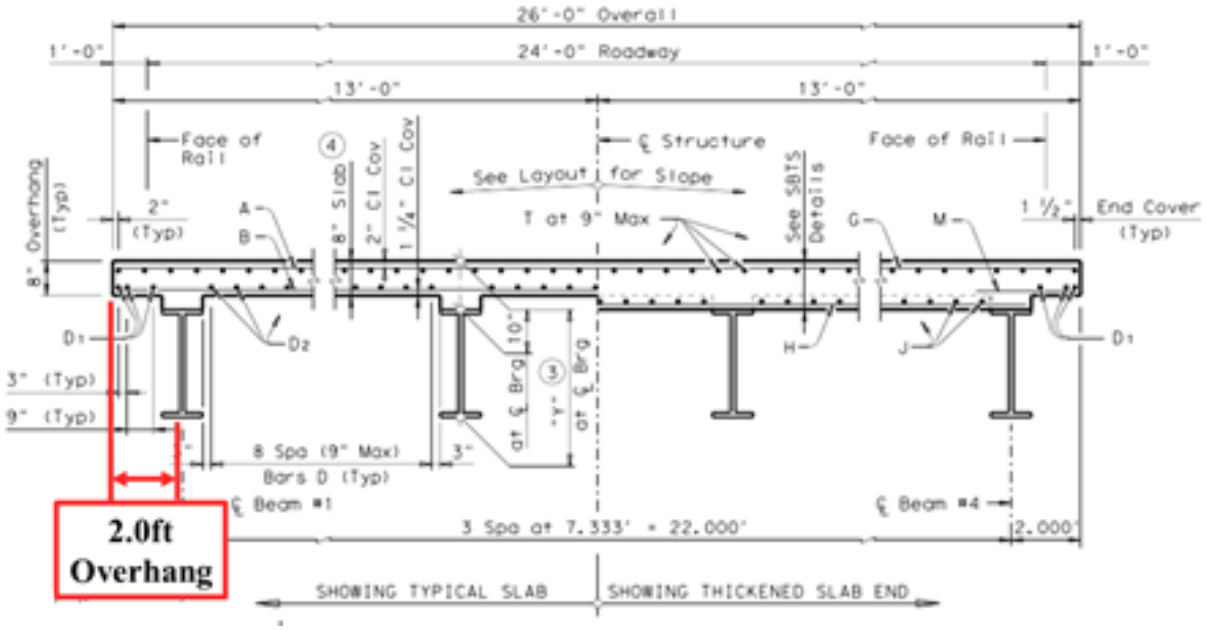

Figure 4.4: Typical transvers superstructure cross-section (TxDOT, 2004)

Reinforced concrete girder bridges are built using standard sections (e.g., Figure 4.3a) which are designed with a standard girder spacing of 3 feet and a 1 foot overhang. In this study, girder spacings for the RC girder bridge samples are assumed to be 3 feet, and the number of girders is selected resulting in an overhang as close to 1 foot as possible. The number of girders and girder spacing for each bridge sample are presented in Appendix A.

4.1.6 Bridge Deck and Railings

In addition to the girders themselves, the concrete bridge deck and railings also contribute significantly to the superstructure mass and stiffness. In steel girder construction, it is common to have composite slabs (i.e., shear studs connecting the girders and concrete slab), in which part of the slab contributes to the flexural stiffness of the superstructure. Past fragility studies have considered composite construction for the MS and MC Steel girder classes (Nielson, 2005; Pan et al., 2007); however, TxDOT did not

adopt composite construction until the mid to late 1980s, while the majority of the steel bridges in Texas were built between the 1940s and 1970s. Therefore, this study does not consider any contribution from the bridge deck in determination of the girder flexural stiffness. In terms of superstructure mass, however, the bridge deck does have a big contribution. The current TxDOT standards for the MS Steel bridge class requires an 8 inch bridge deck; however, a 7.25-inch deck was commonly found in the as-built drawings from bridges built in the 1930s to1950s. The MS PC girder class has similar variation in deck thickness as the current standard specifies an 8.5-inch deck, while the as-built drawings indicate that a 7.25 to 8-inch deck is typical for bridges built in the 1960s to 1990s. Due to these variations in deck thickness observed in as-built drawings and limited information regarding deck detailing for the entire bridge population, the bridge deck for both the MS Steel and MS PC girder class were assumed to be 8 inches thick. The typical deck thickness for the MC Steel bridge class was assumed to be 6.5 inches based on as-built drawings from the 1940s to 1970s, which will be used in this study. For the RC girder and slab bridge classes the bridge deck is part of the structural system, thus no additional mass or stiffness from the bridge deck is considered in the model.

Bridge railings (i.e., traffic barriers placed along the edge of the bridge deck) certainly contribute to superstructure mass; however, the weight of the barrier is a relatively small percentage (i.e., approximately 4 to 5%) of the total weight of the superstructure. TxDOT has a variety of different sizes and shapes of railings in their standard drawings. Determining a typical size and shape for railings of a specific bridge class is difficult, as railings are specified by roadway type and traffic demands. Due to the uncertainty in railing type and design, the railing mass was not explicitly considered in this study; however, the increased superstructure mass due to railings will be considered through a

mass factor applied to the entire superstructure mass, as discussed in Section 3.2.2.3. The railings are assumed to have no effect on the superstructure stiffness.

4.1.7 APPROACH SPAN LENGTH

Highway bridges with three or more spans typically consist of a combination of main spans and approach spans. Main spans are typically the longer spans at the middle of the structure, while the approach spans are designated as the shorter spans used on either end of the bridge. To develop representative bridge models, it important to understand and utilize appropriate approach span lengths for each bridge class. As previously mentioned in Section 2.2.2, approach span lengths are not listed in the NBI database and are, therefore, commonly determined through review of relevant bridge plans (Nielson, 2005; Ramanathan, 2012). Through this review process (i.e., review of Texas as-built drawings) it was determined that span lengths are typically symmetrical along the length of the bridge, and approach span lengths follow noticeable trends among each bridge class. Some of these trends and the approach span lengths selected for each bridge class in this study are presented below.

The multi-span, simply supported pre-stressed and steel girder bridge classes (i.e., MS PC and MS Steel) have some variability in approach span lengths (e.g., ranging from 40 feet to 65 feet); however, an approach span length of 40 feet was found to be the most common, and is used in this study for both of these bridge classes. For the continuous span steel girder bridge class (MC Steel), it was determined that the approach span lengths had more variability and were directly correlated to the main span length. After a thorough investigation of as-built drawings (see Appendix D for list of relevant as-built drawings), it was concluded that approach span lengths for the MC Steel girder bridge class range between 60 to 80 percent of the main span length. To capture this variability, the approach

span lengths for each of the MC Steel girder bridge samples used in this study were randomly selected assuming a uniform distribution in this range.

The reinforced concrete bridge classes (i.e., MS RC Girder, MS RC Slab, and MC RC Slab) tend to have very different trends when it comes to approach span lengths. For example, the MS RC Girder and Slab type bridges do not typically have shorter approach spans; instead, the main span length is utilized for all spans throughout the length of the structure. This is predominantly due to the heavily standardized design and construction processes used for these particular bridge types. Whether pre-cast or cast-in place construction is used, standardized forms and span lengths are often utilized for ease of design and construction. This is evident when looking at the main span length distributions for each of these bridge classes (see Section 2.2.2), which show that the majority of the MS RC Girder and Slab bridges in the Texas inventory utilize one or two prominent span lengths (e.g., 30 or 40 feet span lengths, and 25 feet span lengths respectively). The continuous reinforced concrete slab bridge class (i.e., MC RC Slab) varies from its simply supported counterpart, utilizing approach spans that are typically shorter than the main spans. Review of relevant bridge plans showed that an approach span length of 25 feet is the most commonly used value for the MC RC Slab bridge class; thus, is used for all the MC RC Slab bridge samples in this study.

4.2 Substructure

The substructure (i.e., the columns, foundation, and abutments) supports the superstructure as shown in Figure 4.1. Unlike the superstructure, the substructure is expected to see highly nonlinear behavior during a seismic event, requiring a more complex computational model to accurately capture these behaviors and potential failure modes. Computational modeling techniques and specific details regarding modeling can be found

in Prahkov (2016), while the following sections will focus on TxDOT typical details used to develop the substructure models used in this study.

4.2.1 BRIDGE BENTS

The above ground substructure, which are typically the intermediate supports along the length of a bridge, are often referred to as bridge bents or piers. Piers are usually comprised of a single support (e.g., single column or pier wall), while bents are typically comprised of multiple supports (e.g., multiple columns or piles). Based on the substructure information gathered from TxDOT's bridge database, it was determined that the majority of bridges in Texas have either multi-column or pile bents (see Section 2.2.6 for substructure statistics). Multi-column bents are predominantly built with cylindrical reinforced concrete columns, while pile bents can be built using either steel H-pile or concrete piles (either reinforced or pre-stress concrete). Bridge bents with either concrete columns or piles are constructed with a reinforced concrete bent cap, while steel pile bents have either reinforced concrete or steel caps. Reinforced concrete bent caps are, however, by far the most prominent in the Texas bridge inventory (see Figure 2.14).

To model the behavior of a bridge bent, it is important to know typical member sizes and details for both the columns and bent caps. Bent caps are typically much stiffer than the columns below them and are often assumed to remain elastic for seismic analysis (Prahkov, 2016). Thus, the basic geometry (i.e., depth and width) of a typical bent cap is all that is needed to calculate section properties and mass for the modeling process. Concrete bent caps used in Texas typically have a square or rectangular cross-section (Figure 4.5); however, the dimensions may vary between the different bridge classes and are typically governed by span length and column diameter. The bent cap dimensions for each bridge class used in this study are listed in Table 4.2 below and are based on a

combination of as-built drawings from the 1930s to 1990s, TxDOT standard drawings from the 1980s to 1990s, as well as current TxDOT standard drawings.

Table 4.2: Bent cap dimensions per bridge class

Bridge Class	Bent Cap Dimensions
MS Steel Girder	Width: 2.5 ft
	Depth: 3 ft
MC Steel Girder	Width: 2.5 ft
	Depth: 2.5 ft
MS PC Girder (circa 2008)	Width: 2.75 ft
	Depth: 2.75 ft
MS PC Girder (2009 – present)	Width: 3.5 ft (4 ft - spans > 100ft)
	Depth: 3.5 ft (4 ft - spans > 100ft)
MS RC Girder	Width: 2 ft
	Depth: 2.5 ft
MS RC Slab	Width: 2 ft
	Depth: 2.5 ft
MC RC Slab	Width: 2 ft
	Depth: 2.5 ft

Columns are typically one of the more vulnerable components of a bridge during a seismic event and are expected to experience highly nonlinear behavior when subjected to large seismic demands. To capture this nonlinear behavior in the modeling process it is important to simulate the flexural and shear strength of the reinforced concrete column section, as well as potential longitudinal reinforcement development length and splicing failure modes (Prahkov, 2016). The flexural and shear strength of a cylindrical concrete column is directly related to the cross-sectional dimensions and the reinforcing layout. Investigation of TxDOT standard drawings and as-built bridge drawings from the 1930s to 2000s indicated that TxDOT multi-column bents have historically utilized one of two prominent column sizes (i.e., 30-inch diameter and 24-inch diameter). However, recently

(since approximately 2008) TxDOT has started specifying 36 and 42-inch columns for the new PC girder bridges (TxDOT, 2017). Among the two main column sizes (i.e., 30-inch diameter and 24-inch diameter) there are minor differences in the reinforcing details; however, they do follow some general trends. For example, it is standard for all columns to have a #3 spiral reinforcing cage with a 6 inch pitch along the entire length of the column. Another typical detail is longitudinal bars extending straight into bent caps and foundations without any 90 degree hooks. Figure 4.6 shows typical reinforcing details for both a 30 and 24-inch diameter column, while specific column sizes and details used for each bridge class can be found in Appendix B. It should be noted that Texas bridges, in general, have different column sizes and reinforcing details than bridges considered in previous CSUS studies. Past seismic vulnerability studies focusing on the CSUS (Nielson, 2005; Choi, 2002) use 30 and 36-inch diameter columns with transverse reinforcement at 12 inch spacing. Like the current study, these past studies assume similar details for the column-to-bent cap and column-to-foundation joints, where longitudinal bars extend straight through the joint. This type of joint reinforcement detailing without any 90 degree hooks is consistent with detailing used in low seismic hazard regions such as Texas and the CSUS, whereas 90 degree hooks are more commonly employed in moderate and high seismic regions.

The number and spacing of columns also has a big influence on overall bent behavior under lateral loads. Determining a standard column number and spacing for all bridge classes and samples is not a trivial task, as these parameters vary with deck width and design details (e.g., slab overhang or column inset from end of bent cap). By studying standard and as-built drawings; however, one can identify common trends (e.g., max spacing, minimum spacing, spacing intervals, etc.) that can be used to develop a standard procedure for determining number of columns and column spacing for a generic multi-

column bridge bent in this study. For example, in this study it was determined that column-to-column spacing is typically between 7 feet and 16.5 feet, typically specified at 6 inch intervals. The next step is to find a relationship between deck width, length of the bent cap, and distance from edge of cap to the first column. Again typical standard and as-built drawings indicated that for some bridge classes the length of the bent cap is the same as the deck width (i.e. RC Slab, and RC girder classes), while other classes have some variability in cap length; however, on average the bent cap was found to be 2 feet shorter than the width of the superstructure. Typically, in multi-column bents there is a certain amount of column inset (i.e., the bent cap extends beyond the outside columns as shown in Figure 4.5). An estimation of this typical column inset is necessary to determine the number of columns and overall multi-column bent layout. In as-built and standard drawings, this column inset dimension (i.e., the distance from edge of bent cap to center of outside column) varies significantly, as this distance is typically varied in order to optimize column spacing. However, knowing the upper and lower limits as well as a typical value for column inset will inform the bent layout for sample bridges. Based on bent dimensions found in drawings, in this study a lower limit of 2 feet, an upper limit of 6 feet, and a typical value of 4 feet will be assumed for the column inset dimension used to determine the column spacing and layout within the bent.

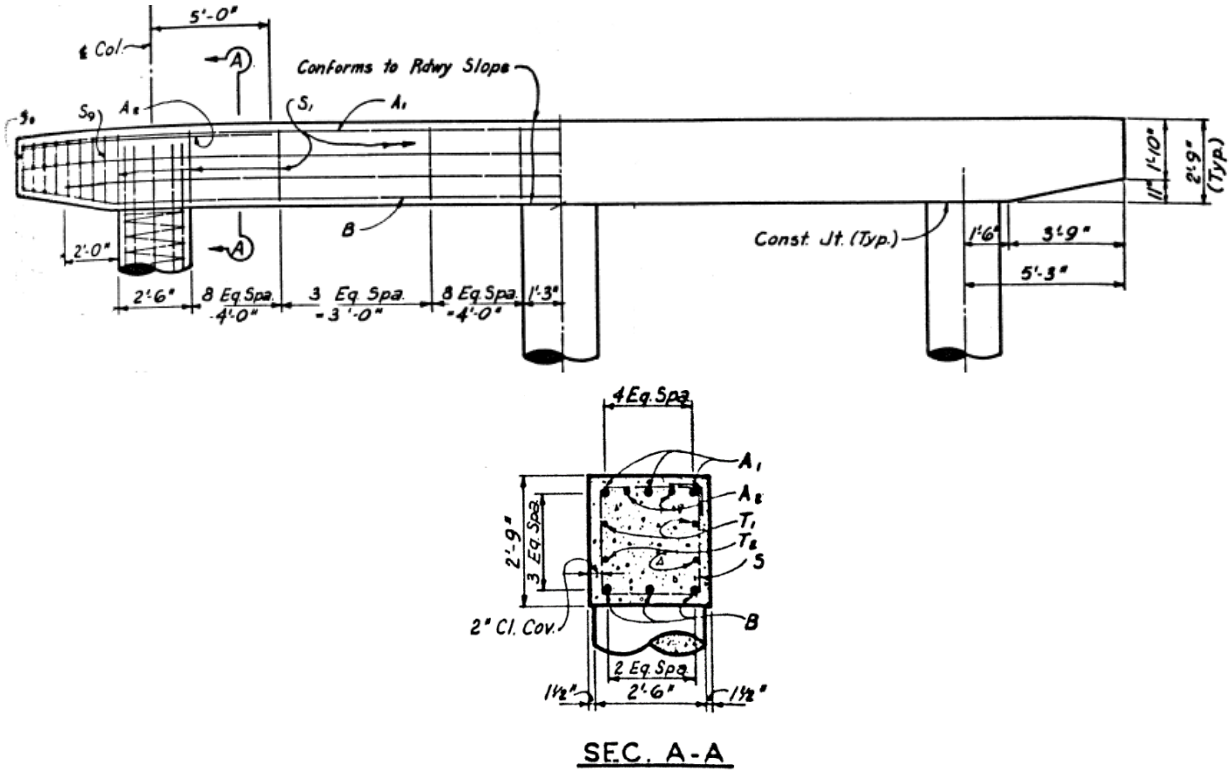

Figure 4.5: Typical bridge bent, and bent cap detail (TxDOT, 1962)

The process of determining the number of columns and column spacing in a multi-column bent relies on the aforementioned dimensions: the deck width, the width of the bent cap, and the typical column inset. The process is iterative and is as follows: Subtract 10 feet from the sampled deck width to get the center-to-center distance between outside columns (i.e., subtract 2 feet to get width of cap, and 8 feet to account for column inset on either side of cap). Then divide this value in half (which initially assumes three columns per bent) to get an initial column spacing estimate. If the initial spacing is larger than 16.5 feet, columns are added until the spacing is adequate (i.e., less than 16.5 feet). The final step is to round the column spacing to the nearest 6-inch interval (e.g., a 12.23 foot spacing would be rounded to 12 feet, and a 12.36 foot spacing would be rounded to 12.5 feet). The

number of columns and column spacing for each of the bridge samples used in this study can be found in Appendix B.

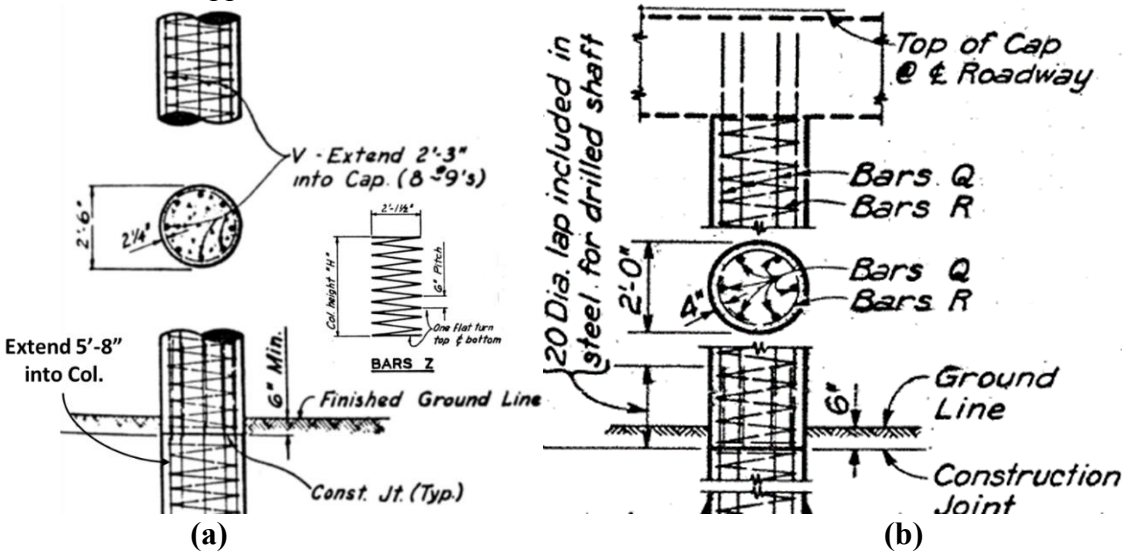

Figure 4.6: Typical column cross-section and details (TxDOT, 1962) for (a) 30-inch diameter and (b) 24-inch diameter (TxDOT, 1970) columns

4.2.2 FOUNDATIONS

Foundations are considered as the below ground portion of the substructure, which transfers the structural loads to the surrounding soil or rock. Foundations can take on a variety of different configurations depending on the loading demands, soil type, and other site-specific constraints (e.g., superstructure type, overhead clearances, existing utilities, etc.). Typical foundation systems found in Texas are spread footings, integrated pile/column (i.e., drilled shafts or pile), or pile footings. Figure 4.7 shows examples of these foundations systems.

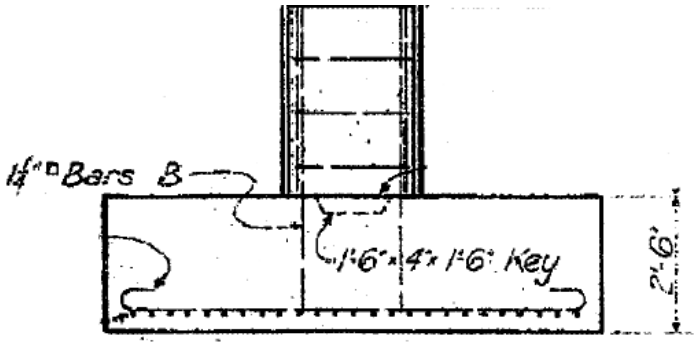

(a) Spread footing (TxDOT, 1939)

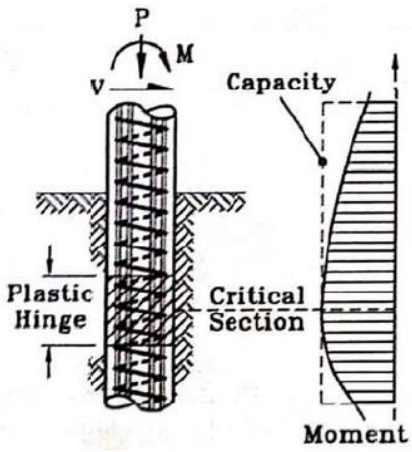

(b) Integral pile/column (Ramanathan, 2012)

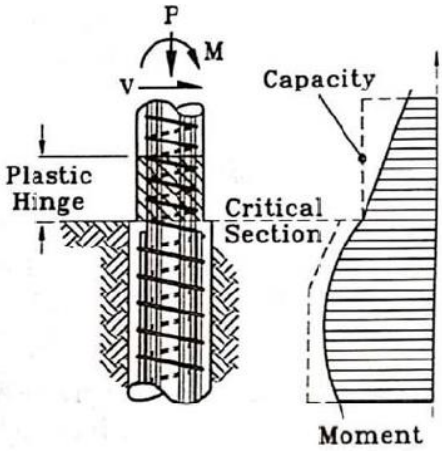

(c) Integral pile/column (oversized pile) (Ramanathan, 2012)

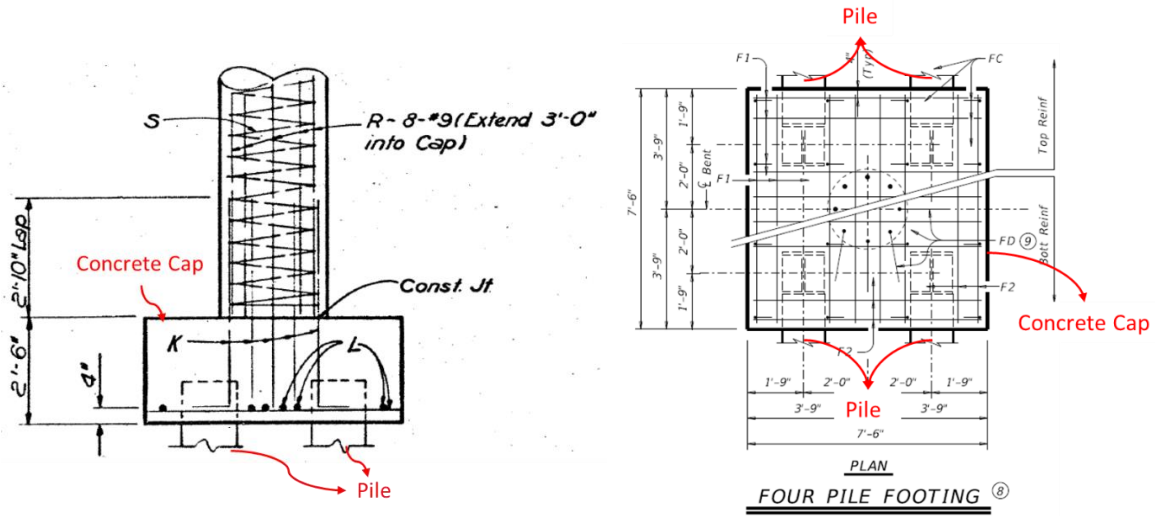

(d) Pile footing, as adopted from TxDOT (1962 and 2015, respectively)

Figure 4.7: Typical foundation systems

Spread footings (Figure 4.7a) are considered shallow foundations and are typically used in locations where firm soil or rocky conditions are found at relatively shallow depths. Integrated column/pile, also referred to as an integral column/shaft, and pile footings (Figures 4.7b through 4.7d) are typically considered deep foundations. According to the TxDOT Geotechnical Design Manual (TxDOT, 2012), drilled shafts are the most economical in competent soil or rock, while the pile foundations are best suited for the softer soils. Based on the bridge database provided by TxDOT engineers, the distribution of foundation types among Texas bridges (see Figure 2.13) indicate that the integral shaft or integral pile foundations are the most common and are considered as the prominent foundation types in this study. As shown in Figure 4.7b, when subjected to lateral loading the critical section or plastic hinge region of an integral shaft foundation consisting of the same diameter column is below the ground line. The plastic hinge typically forms at a depth of about twice the pile diameter below the surface (Priestley, 1996), which makes it difficult to identify during a post-earthquake inspection. The integral shaft foundations with an oversized shaft (Figure 4.7c) have an increase in stiffness at the shaft-column joint, forcing the plastic hinge to form at the base of the column (typically at or above the ground line). This case of damage above the soil surface is much easier to identify during a visual inspection. Both of these drilled shaft types are used in Texas.

Pile supported foundations typically consist of either driven steel H-pile, precast (reinforced or pre-stressed) concrete pile, or cast in drilled holes (CIDH) connected with a concrete pile cap. In certain cases the pile cap can be continuous along all columns in a bent (e.g., a strip footing), but more commonly each column has an individual pile footing (Figure 4.7d). Regardless of the pile type it is important to have a positive connection

between the pile and pile cap (i.e., adequate embedment into the pile cap) to insure the proper force transfer.

Generally, bridge foundations have performed well in past earthquake events, which have typically occurred in regions of high seismicity, but there is not as much evidence of foundation performance in earthquakes in areas of low seismicity. The foundation damage that has been reported is typically preceded by extensive damage in the columns (Ramanathan, 2012). To model foundation behavior it is important to know the drilled shaft diameter or the pile size and pile layout. Based on the substructure distribution for Texas bridges (Figure 2.13) it was determined for this study to use pile foundations for the MS RC girder and MS Steel girder bridge classes, while drilled shaft foundations are used for the remaining bridge classes (e.g., MS PC girder, SS PC girder, MS RC Slab, MC RC Slab, MC Steel girder). For drilled shaft foundations, TxDOT standard drawings show details for drilled shafts with diameters from 18 inches up to 48 inches. Due to insufficient data regarding actual shaft diameters, this study assumes the shaft diameters of sample bridges are the same size as the columns specified above. Section 3.2.2.7 provides details on how to correlate shaft diameter to foundation stiffness for modeling purposes. For pile foundations (e.g., integral pile/columns or pile footings), concrete piles have been the material of choice for most of Texas bridges (e.g., approximately 80% of bridges with pile foundations utilize concrete piles). Concrete piles can be either plain reinforced or pre-stressed square piles ranging in size from 16 inches up to 24 inches. When steel piles are used, TxDOT standards typically specify the use of HP14, 16, or 18. However, as stated in Section 3.2.2.7 it is common to assume a constant initial stiffness for a pile regardless of the size or material based on modeling recommendations from state departments of transportation (e.g., Caltrans 1999). If pile stiffness is constant, the last parameter needed to model pile foundations is pile layout (i.e., number of piles per footing). Based on review

of TxDOT standards, typical footings consist of three to five piles per column. For the purpose of this study, a footing supported by four piles per column (Figure 4.7d) was chosen as the basis for modeling.

4.2.3 ABUTMENTS

Abutments are a component of the substructure that can have multiple functions. First, abutments are the end bridge bents that provide the vertical and horizontal support for the superstructure. Abutments can also provide soil retention at grade separations. Lastly, abutments provide the link between the superstructure and the roadway approach. There are a variety of different types and designs of abutments; however, they can be broken down into two main categories, seat type and integral abutments. Seat type abutments act like a bent cap where the superstructure rests on the bridge seat allowing movement independent from the abutment (Figure 4.8), while integral abutments are built monolithically with the superstructure as shown in Figure 4.9. Integral abutments tend to provide a much stiffer structure and help prevent unseating of the superstructure during a seismic event (Ramanathan, 2012). Following an in-depth review of TxDOT standard and as-built drawings, it was concluded that seat type abutments, and more specifically pile-bent-type abutments (Figure 4.8d), are the most common among Texas bridges.

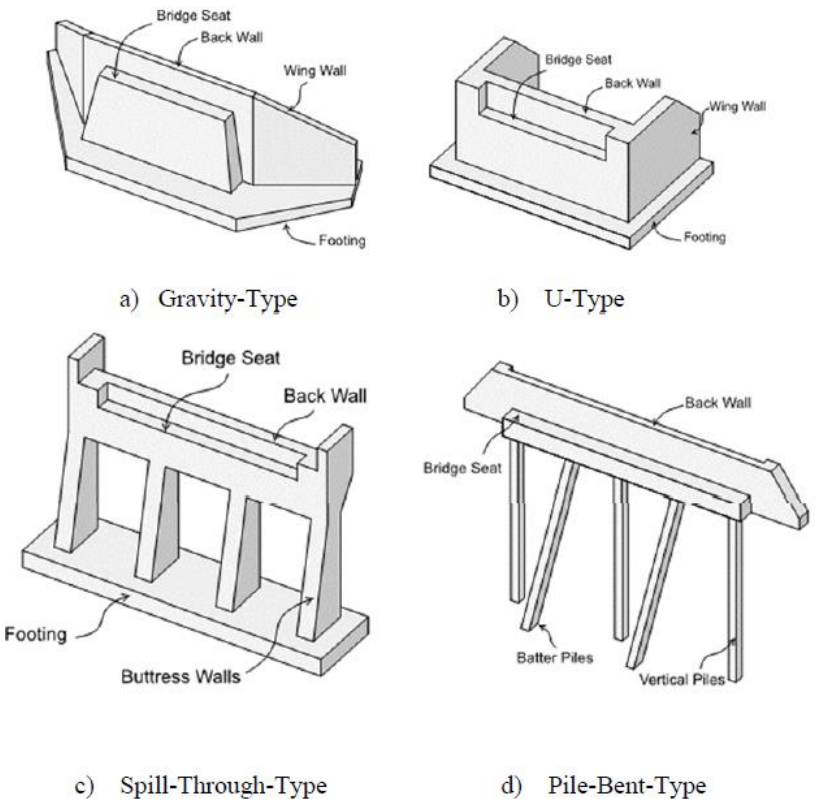

Figure 4.8: Common seat type abutments (Nielson, 2005)

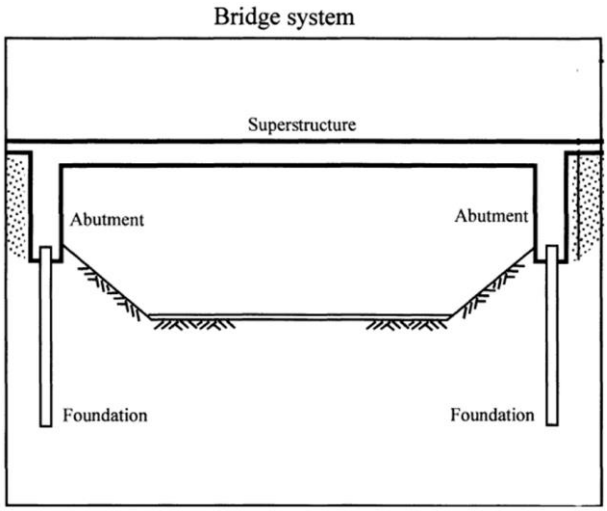

Figure 4.9: Integral type abutment (Arsoy, 1999)

During a seismic event, abutments provide horizontal stiffness to the superstructure. This lateral resistance is provided by either passive or active action of the abutment (see Section 3.2.2.8 for abutment stiffness). The active stiffness is directly related to the number of piles (or shafts) in the abutment, which can act in either the longitudinal or transverse directions, while the passive stiffness is provided by both the soil behind the abutment and the piles. The passive stiffness thus depends on both the number of piles and the size of the abutment (i.e., abutment height and width). The abutment width is considered to be the width of the bridge deck, while the height is considered as the depth of the bent cap (see Table 4.2) plus the height of the backwall. Backwalls are intended to support the approach slab and retain soil, so they typically extend from the top of the bent cap to the bottom of the approach slab. Therefore, the backwall height for pre-stressed concrete and steel girder bridges can be determined by the depth of the girder plus the height of the bearing (e.g., 11-inches for steel bearings, 4-inches for elastomeric bearings). For the reinforced concrete girder bridge class, the slab is actually part of the girder depth; therefore, the backwall height is 8-10 inches less than the total superstructure depth. Reinforced concrete slab bridges don't actually have a backwall as the approach slab typically rests directly on the bent cap.

Pile bent abutments can be constructed with either driven piles or drilled shafts. For ease of design and construction, abutment foundations typically utilize the same foundation type and layout as the interior bents. Therefore, the active abutment behavior for a specific bridge class is assumed the same as the foundation types discussed above (Section 4.2.2). For example, a bridge sample in the MS PC girder class is modeled with an active abutment stiffness based on the diameter of the drilled shafts. A bridge sample in the MS Steel girder class is modeled with an active abutment stiffness based on the stiffness of four piles per column location. Section 3.2.2.8 provides more details on active abutment stiffness.

4.3 Bearings

The final component needed to develop a bridge model are the bearings. The main responsibility of the bearings is to transfer loads from the superstructure to the substructure (i.e., vertical live and dead loads, longitudinal and transverse loads, and material thermal expansion loading). During a seismic event, bridge bearings typically experience very different demands than they are designed for (i.e., significant longitudinal and transverse loadings), which can introduce structural vulnerability. Thus, it is important to accurately represent and capture bearing behavior in the modeling process. There are two main types of bearings used in this study: steel bearings and elastomeric bearings.

4.3.1 STEEL BEARINGS

Prior to the 1990s, steel bearings were the prominent bearing type used in steel girder bridge construction. There are two types of steel bearings – fixed bearings and expansion bearings. Fixed bearings are intended to transfer vertical and horizontal loading to the foundation while accommodating superstructure rotations relative to the substructure. Expansion bearings are intended to relieve material expansion forces by accommodating large relative longitudinal displacements, while also maintaining their vertical load carrying capacities (Mander et al., 1996). Figure 4.10 shows examples of fixed and expansion steel bearings.

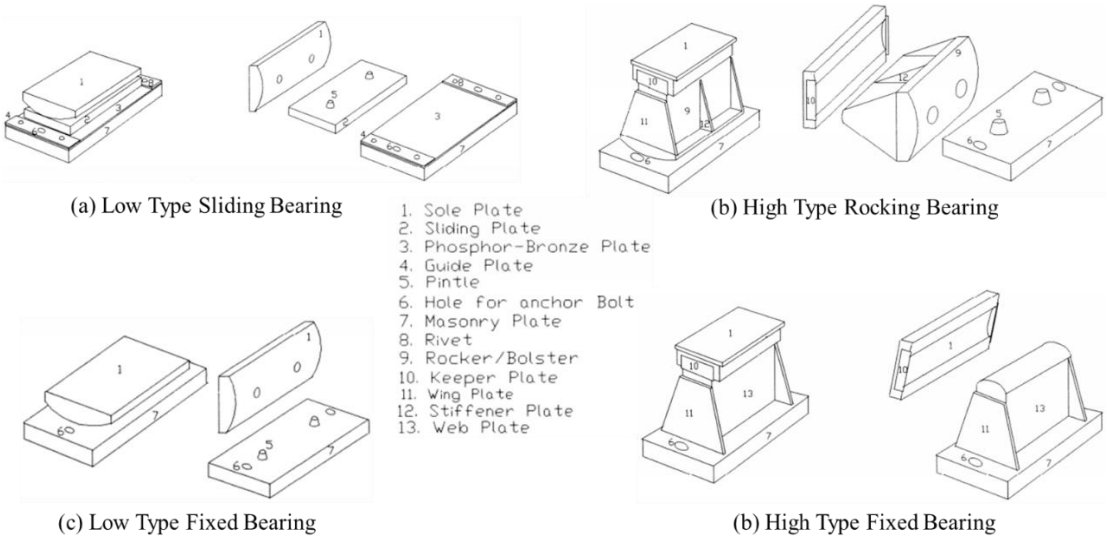

Figure 4.10: Typical steel bearings (Mander et al., 1996)

Steel bearing designs may vary in different areas of the country; however, most steel bearings have the same general geometry and main components (i.e., sole plates, masonry plates, web plates, stiffener plates, pintles, anchor bolts, etc.). Figure 4.11 shows a typical high type rocker bearing used in Texas, which shows an example of these design variations when compared with the bearings in Figure 4.10. Due to the lack of experimental data and the similarities in the overall bearing designs, however, the Texas specific bearings in this study will be assumed to follow the behavior of the steel bearings presented in the Mander et al. (1996) study and shown in Figure 4.10.

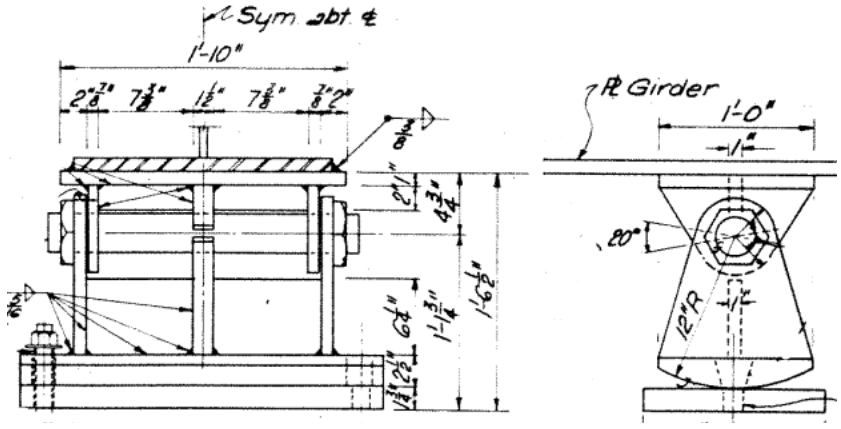

Figure 4.11: Typical steel rocker bearing used in Texas

From the current TxDOT standards for new steel girder construction, steel bearings have been replaced with an elastomeric type bearings for steel girder bridges. However, studying the bridge class statistics (Section 2.2.7) it is evident that the majority (e.g., 83%) of steel girder bridges (i.e., both the MS and MC steel girder bridge classes) were built between the 1930s and the 1970s. So in order to accurately capture the vulnerability of the steel girder bridge population, steel bearings will be used to model the behavior of the MS and MC steel girder bridge classes. One thing that should be noted is that this study only considers the high type steel bearings. Due to lack of data on the bearings used in the entire Texas bridge population, it is not possible to determine which bridge samples should use high type versus low type bearings. A thorough review of as-built drawings of Texas bridges from the 1930s to the 1970s, did, however, indicate that high type bearings were commonly employed in both steel bridge classes.

4.3.2 ELASTOMERIC BEARING

Elastomeric bearings are a very common bearing type used for pre-stressed concrete girder bridges. These type of bearings consist of an elastomeric rubber pad, with or without steel dowels anchored into the bent cap extending through the pad into the

bottom of the girder. The elastomeric pad transfers horizontal loads through a frictional force at the interface with the concrete bent cap, while the dowels transfer load through beam type dowel action (Nielson, 2005). As with steel bearings, elastomeric bearings also have both a fixed type bearing and an expansion bearing. To relieve material expansion forces through longitudinal movement, elastomeric expansion bearings are equipped with slotted holes in the rubber pad and in the bottom of the concrete girder such that bearings accommodate translation in the longitudinal direction without engaging the dowel. Figure 4.12 shows the typical configuration for an elastomeric bearing.

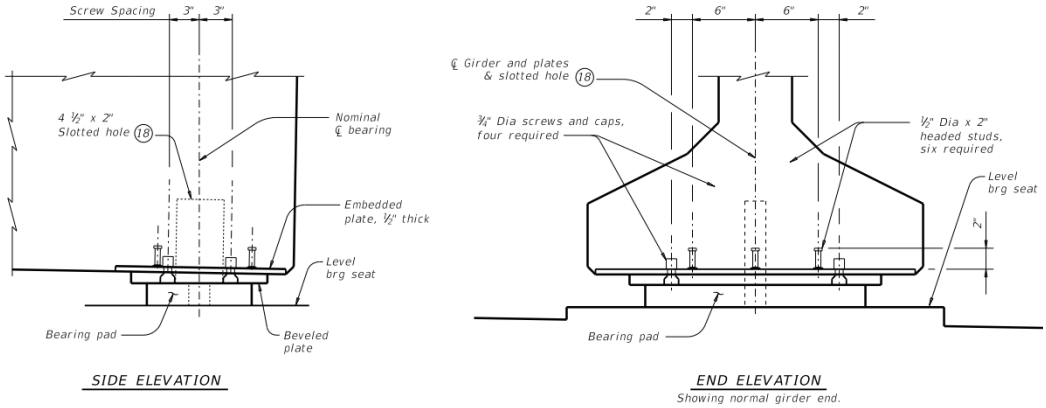

Figure 4.12: Typical elastomeric bearing (TxDOT, 2017)

During an earthquake event it is possible for an elastomeric bearing to undergo deformation in the rubber pad, displacement due to sliding, deformation in the steel dowel, or a combination of all three. To model these behaviors, it is important to understand the bearing material and geometry. For example, deformation in the elastomeric pad is directly related to the stiffness of the elastomer, as well as the surface area and the thickness of the pad (see Section 3.2.2.2). Stiffness of the elastomer is typically governed by construction and design specifications (e.g., AASHTO design specifications states that the elastomeric

shear modulus ranges from 96 psi to 300 psi), while surface area and thickness vary with girder dimensions and span length. Current TxDOT standards specify elastomeric pad dimensions as 8 inch by 21 inch for Tx28 through Tx54 girders, and a 9 inch by 21 inch pad for Tx62 and Tx70 girders with a minimum thickness of approximately 2.75-inches. Review of as-built drawings revealed that bearing pads for old style PC girders (i.e., Type A, B, C, 54, and 72) have a standard width of 6-inches, a length that is 2-3 inches shorter than the flange width, and a minimum thickness of 0.75-inch for bridges with spans up to 60 feet then increasing by 1/8 inch for every additional 10 feet in span length. Displacement due to sliding also depends on the surface area of the bearing pad; however, it also is dependent on the coefficient of friction, the weight of the superstructure, and the gap between the dowel and the hole in the pad. Deformation in the steel dowel is directly related to the size of the dowel and the strength of the dowel. All of these parameters are discussed in detail in Section 3.2.2.2 One additional note that should be mentioned is the TxDOT current standards for elastomeric bearing pads utilize thin layers of steel shims embedded within the elastomeric pad to increase the vertical stiffness and durability of the pad. Based on observations during review of as-built drawings and the age of sample bridges, this type of bearing was not selected as representative of Texas highway bearings and, therefore, is not used in this study.

4.3.3 ALTERNATIVE CONCRETE BEARING

In certain regions of the country, elastomeric bearings are the bearing of choice for any concrete superstructure (i.e., PC I-girders, PC box-girders, RC slabs, and RC girders); In Texas, however, the RC girder and slab bridge classes do not typically utilize elastomeric bearings, predominantly due to the cast in place construction used for these superstructure types. TxDOT does have some precast slab and beam type bridges in their

system that utilize elastomeric bearings; however, this type of superstructure and bearing configuration is more typical of modern construction and was not found to be representative of the RC superstructures considered in this study, which were typically built between the 1920s and 1990s (see Section 2.2.7). Careful review of standard and as-built drawings was necessary to determine typical bearing details for RC girder and RC slab superstructure types. Figure 4.13 shows an example of the alternative concrete bearings used for RC girder and slab construction in Texas.

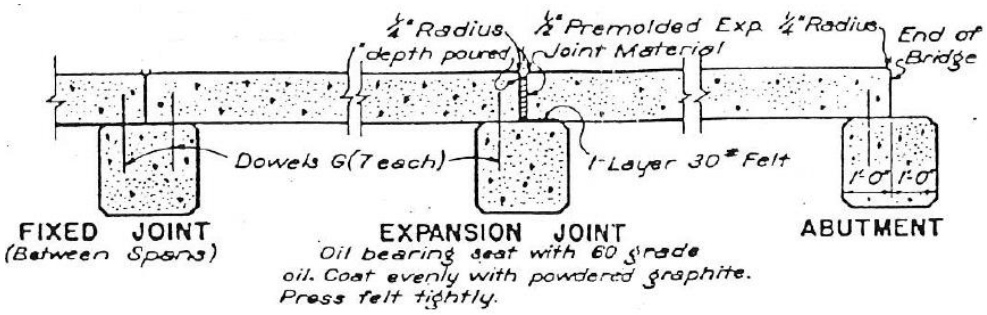

(a) RC slab (TxDOT, 1955)

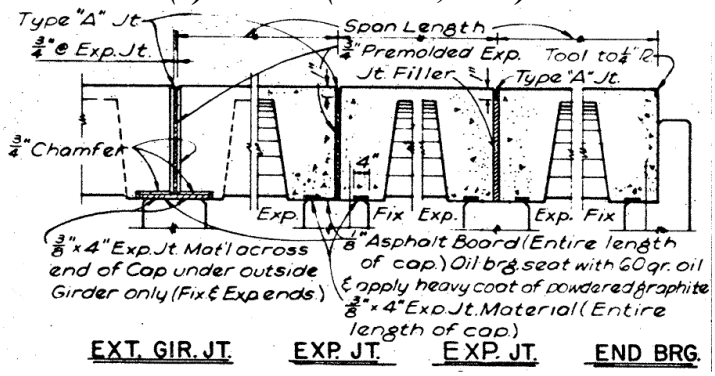

(b) RC girder (TxDOT, 1966)

Figure 4.13: RC girder and slab bearing details

As with both the steel and elastomeric bearings, Figure 4.13 shows both fixed and expansion type bearings for RC girder and slab superstructures. For the expansion type bearings, it is common to coat the bridge seat with some kind of lubricant (e.g., 60 grade

oil or powdered graphite), and then utilize a thin material barrier (e.g., roofing felt or asphalt board) between the concrete superstructure and concrete bridge seat. Figure 4.13 also shows the elimination of retention dowels at the expansion bearing locations. Fixed bearing locations vary slightly among the two details shown in Figure 4.13. For RC slab bridges it is typical for the concrete slab to sit directly on the concrete bridge seat with #6 (i.e., ¾-inch diameter) dowels, spaced at 2 foot intervals along the length of the bridge seat. For the RC girder bridge class, a thin piece of expansion joint material is placed along the face of the bridge seat and #6 dowels are placed at each girder location. The expansion joint material helps protect the edge of the bridge seat due to small deflections and rotations in the superstructure. These materials are, however, very thin and narrow (e.g., 3/8 inch thick and 4 inches wide) and may degrade over decades of exposure to the elements; thus it is reasonable to assume that the concrete girder is likely in direct contact with the concrete cap.

Modeling the behavior of these alternative concrete bearings is similar to the elastomeric bearing model previously discussed, which includes resistance from elastomeric pad, sliding friction, and dowels, with some modifications. The first, most significant modification is the elimination of the elastomeric pad from the elastomeric bearing model. The material used in the bearings shown in Figure 4.13 are significantly thinner than the elastomeric pads and are assumed to contribute very little to no stiffness or deformation to the bearing model. The second modification is the coefficient of friction (COF). For the fixed bearing locations, the concrete superstructure is assumed to rest directly on the concrete bridge seat; therefore, a COF for concrete on concrete will be used as discussed in Section 3.2.2.2. For expansion bearing locations, the COF for concrete on concrete will also be used. This assumption is again based on the thin nature of the bearing material used in these alternative expansion joint details, as well as the age of the RC girder

and RC slab bridge classes (i.e., bridges from these classes have been exposed to weathering for a median age of 50 years and 64 years, respectively, leading to deterioration of the bearing material and lubricant). The dowels found in these alternative type bearings are considered to behave in the same fashion as in the elastomeric bearing, with a slight reduction in stiffness due to the reduction in cross sectional area (see Section 3.2.2.2 for details on relating dowel cross sectional area and dowel stiffness).

4.4 Conclusion

Developing representative bridge models is a major part of the fragility assessment process. To accurately develop these bridge models, it is important to understand the specific components and structural details commonly used in the region of interest. This section presented bridge component details specific to Texas and the construction eras in which most of the bridges in Texas were built, which provided guidance in developing the representative bridge models used in this study. Information was given on typical superstructure, substructure, and bearing details that were gleaned from extensive review of TxDOT standard and as-built bridge drawings. The next step in the fragility assessment is performing the actual fragility analysis, which includes development of component limit states, development of Probabilistic Seismic Demand Models, and finally developing fragility curves. The following section will provide details on fragility analysis.

5 FRAGILITY ANALAYSIS

Fragility analysis provides a means to probabilistically assess the performance of a structural system or its components (Erberik, 2015). More specifically, seismic fragility, which is the focus of this study, can be defined as a conditional probability that the demand (D) of a structure (e.g., a bridge) or its components (e.g., bearings, columns, abutments, etc.) will exceed the capacity (C), for a given ground motion intensity measure (e.g., peak ground acceleration (PGA), peak ground velocity (PGV), spectral acceleration (S_a), etc.). This probability statement is given in Eq. 5.1, where P_f is the probability of meeting or exceeding a given level of damage for a given ground motion intensity measure.

$$P_f = P\left[\frac{D}{C} \geq 1\right] \tag{5.1}$$

The continuous form of this probabilistic function can then be used to generate a fragility curve, which can be used to predict the likelihood of a structure achieving a certain level of performance during an earthquake event. Seismic fragility analysis can be separated in to three main steps: developing probabilistic seismic demand models (PSDMs), determining capacity limit state models to be compared to those demands, and finally developing the fragility curves. The following sections will discuss in detail each of these three steps.

5.1 Probabilistic Seismic Demand Models

In this study analytical, or numerical, fragility curves are developed using nonlinear three-dimensional computational models of representative Texas bridges subjected to a suite of ground motions representative of the seismic hazards in Texas. When developing analytical fragility functions using nonlinear response-history analyses, it is common to use PSDMs to model the variability associated with the structural response (Nielson and

DesRoches, 2007). PSDMs are developed by recording peak component demands (e.g., column rotational ductility, bearing displacement, abutment displacement, etc.) from each ground motion-bridge model pair, and by plotting the demand versus the ground motion intensity measure (*IM*) values for that ground motion. Cornell et al. (2002) recommend PSDMs be represented by a power function (Eq. 5.2), where S_d is the median seismic demand, and both *a* and *b* are coefficients estimated through a regression analysis.

$$S_d = a(IM)^b \tag{5.2}$$

The actual regression used to estimate the coefficients *a* and *b* is most commonly performed in a lognormal transformed space, which is done by taking the natural logarithm of each side of Equation 5.2. This transformation results in a linear form shown in Eq. 5.3.

$$ln(S_d) = ln(a) + (b)ln(IM) \tag{5.3}$$

Figure 5.1 shows a schematic of a typical PSDM, showing the linear regression of Eq. 5.3 through the peak demand data obtained from nonlinear response-history analyses. Cornell et al. (2002) observed that the structural demand parameters typically follow a lognormal distribution; therefore, in the transformed space the variation of data about the mean should follow a normal distribution. This variation or dispersion about the mean is depicted in Figure 5.1 as σ, which is an estimate of the conditional lognormal standard deviation of the demand, *d*, at a given intensity measure, *IM* ($\beta_{d|IM}$). The development of a PSDM establishes a relationship between the structural component demands and the chosen ground motion intensity measure, which can be used to develop component level fragility functions.

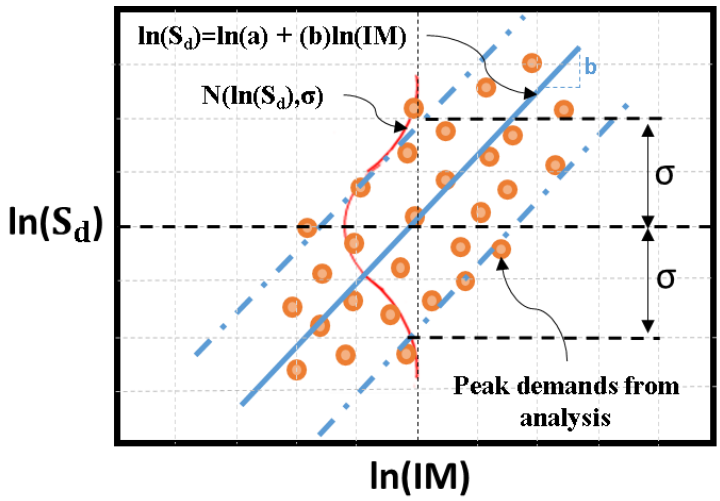

Figure 5.1: Illustration of a Typical PSDM (adopted from Ramanathan, 2012)

5.2 Capacity Limit States:

As previously mentioned (Eq. 5.1), seismic fragility analysis compares the capacity of a structure at a specified limit state to the seismic demand placed on that structure during an earthquake event. An important part of fragility analysis is developing capacity models representing various structural limit states, also known as damage states. The first step in developing the capacity models requires establishing a qualitative definition for each damage state. In past bridge fragility studies, it is common to adopt the damage states used in the FEMA loss assessment package HAZUS-MH, given as slight, moderate, extensive, and complete damage states (Tavares, 2013; Padgett, 2007; Nielson, 2005; Choi, 2002). This adaptation ensures the developed fragility functions are compatible with the existing and widely used HAZUS framework. Using the HAZUS-defined damage states as a basis, these damage states can be refined using engineering judgment based on the condition, age, and typical design and detailing practices of the structural portfolio of interest (Choi et al., 2004). The qualitative definitions for the slight, moderate, extensive, and complete damage

states as given in HAZUS were previously given in Table 1.1. These qualitative descriptions are given in terms of visual damage indicators for various components and, in some cases, indications of potential component failures and loss of load-carrying capacity.

Because fragilities are often used to assess losses or consequences following an event, post-earthquake functionality of the system and required level of repair plays a major role in defining damage states. These damage states are often paired with stepwise restoration functions (an example of which is shown in Figure 5.2) to indicate the length of time required to repair damage and restore a bridge to its full capacity. In this example, damage that is classified as slight damage, results in a 50% reduction in capacity immediately, but should be able to be restored back to full capacity within one day of minor repairs. Moderate damage results in 100% capacity loss initially, but it can be restored to 50% capacity within one day and can be restored to 100% capacity within seven days. Extensive damage results in 100% capacity loss initially, can be restored to 50% capacity within seven days, but repairs required to return to 100% capacity may take longer than a month. Finally, complete damage results in 100% capacity loss for a month or longer.

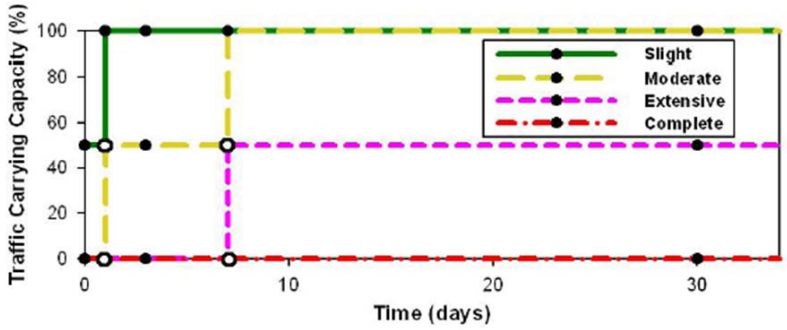

Figure 5.2: Stepwise restoration functions for slight through complete damage (Padgett, 2007)

The qualitative descriptions of damage given in the damage state definitions provides visual damage indicators to assist in performing quick and effective post-earthquake inspections. Thus, it is important to include component damage indicators relevant to the structures of interest and using terminology consistent with regional inspection guidelines. The qualitative damage state definitions adopted in this study (given in Table 5.1) follow the HAZUS framework with slight modifications to be more consistent with the TxDOT Bridge Inspection Manual (TxDOT, 2013) and the TxDOT "Elements" Field Inspection and Coding Manual (TxDOT, 2001).

Table 5.1: Qualitative Damage State Descriptions considering Texas specific details

Damage State	Description
Slight	Minor cracking and spalling of the abutments, appearance of minor cracking at bridge seat, minor inelastic deformation of elastomeric bearing, minor spalling and cracking of columns (damage requires no more than cosmetic repair, and no exposed reinforcing), or minor cracking of the deck (distressed area less than 2% of deck area).
Moderate	Any column experiencing moderate (shear cracks) cracking and spalling (column still sound structurally), moderate movement of the abutment (<2"), prying of masonary plate (e.g., moderate cracking or spalling of bearing area) or severaly bent anchor bolts, rocker bearing instability, or moderate approach settlement.
Extensive	Any column degrading without collapse-shear failure, (column structurally unsafe), significant inelastic bearing displacement, anchor bolt failure, bearing instability iminent (e.g., overturned bearing), extensive elastomeric pad damage, major approach settlement, vertical offset of the abutment
Complete	Any column collapsing, any bearing no longer supported which may lead to imminent deck collapse, tilting of substructure caused by foundation failure.

5.3 Component Capacity Models:

After defining qualitative limit states, the next step in developing capacity models is determining quantitative metrics to evaluate the occurrence of the described limit states. Quantification of these damage metrics is often based on individual component capacities or limit states, and then these limit state capacities are mapped to the corresponding damage states and functionalities of the system. Limit state capacity models must be defined using

a metric consistent with the engineering demand parameters that can be evaluated in a computational model (e.g., ductility demands or deformations) and should be probabilistically characterized by median, S_c, and dispersion, β_c, values. To be consistent with the demand models, which are assumed to follow lognormal distributions, the component capacity models are also assumed to have a lognormal distribution. There are three general methods used to create the capacity models: the prescriptive (physics-based) approach, the descriptive (judgmental) approach, or a combination of both using a Bayesian approach (Nielson and DesRoches, 2007).

The prescriptive method, also known as the physics-based method, is an approach that considers the mechanics of the structure to assess the level of damage and post-event functionality. A component's internal force or deformation is determined from a computational analysis and is used to evaluate the occurrence of damage that corresponds to a certain functionality level. For example, one can assume that at a column curvature ductility of 1.0 the longitudinal steel begins to yield. Bridge officials may use this damage state as a threshold at which the traffic capacity must be reduced until the bridge is inspected.

The descriptive, or judgmental, approach subjectively correlate levels of component deformation or observed damage to post-event functionality and repair requirements based on expert opinion of bridge inspectors and/or officials. This data is typically gathered through surveys. Initial efforts were made through the FEMA-funded Applied Technology Council (ATC)-13 project to gather expert-opinion data for lifeline facilities in California to be used in developing the fragility curves found in HAZUS (Padgett, 2007); however, the scope of the questionnaire was extremely broad (e.g., covering building, bridges, and utility system damage states) and the number of respondents with particular expertise in bridge engineering was low. Padgett and

DesRoches (2007) designed and conducted a survey to gather more extensive data focusing on bridges in the Central and Southeastern United States (CSUS). In this survey, respondents were shown images of damaged bridge components (e.g., abutment settlement, expansion joint offsets, and column damage) from previous earthquakes, and they were asked to identify the level of functionality, repair procedures, and repair time associated with various levels of component deformation (e.g., abutment settlement or expansion joint offset displacements) or observed damage (e.g., column cracking, spalling, bar buckling, etc.). Survey data was collected from twenty-eight bridge engineers from nine different CSUS state departments of transportation. This approach can be very subjective, and it can be difficult to relate observed damage and post-earthquake residual deformations with peak structural demands during the earthquake event; however, expert-based opinion is thought to more accurately represent post-earthquake action decisions made by bridge officials.

The Bayesian approach recognizes that both the prescriptive (physics-based) and descriptive (survey-based) approaches offer valuable information, and thus combine data from both. This combination is done using Bayesian theory, which provides a method to update probability distributions when additional information is acquired (Nielson, 2005). This process is carried out by following Bayes' Theorem as shown in Eq. 5.4.

$$P[B_i|A] = \frac{P[A|B_i]P[B]}{\sum_{j=1}^{n} P[A|B_i]} \tag{5.4}$$

where A is the new information that has been acquired, and B_i is the updated information. Figure 5.3 shows an example of the results for the updated moderate damage state for columns based on a combination of physics-based and survey-based capacity models. A full description of this method can be found in Nielson (2005).

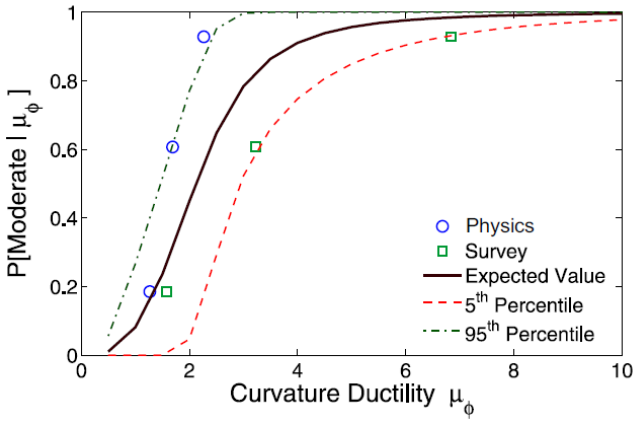

Figure 5.3: Bayesian Updating of Distribution of Moderate Damage State for Columns (Nielson, 2005).

Each of these three techniques were used in determining the component capacities used in this study. The individual component limit state values are discussed in the following sections.

5.3.1 COMPONENT LIMIT STATE MEDIAN VALUES:

In early seismic fragility studies, it was common practice to use column capacity to represent the capacity of the entire bridge system (Karim and Yamazaki, 2003; Mackie and Stojadinovic, 2004; Shinozuka et al., 2000). More recent research, however, has shown that all major vulnerable bridge components should be considered when determining system-level damage (Nielson and DesRoches, 2007; Ramanthan, 2012; Tavares, 2013). Major bridge components considered in this study are listed below:

- Columns
- Bearings – steel (fixed and expansion/rockers) and elastomeric (fixed and expansion)
- Abutments

Details regarding the damage state models that have been used for each of these components in this study are given in the sections below. Details on the behavior and nonlinear modeling of each of these components can be found in Prakhov (2016).

5.3.1.1 Columns

In previous bridge fragility studies (Ramanathan, 2012; Tavares, 2013; Nielson, 2005), the qualitative description of reinforced concrete column damage states remain consistent. These damage states and their descriptions are given as:

- Slight – yielding of outermost reinforcement steel and minor cracking
- Moderate – minor cracking and spalling
- Extensive – major cracking and spalling with exposed core concrete
- Complete – loss of confinement, buckling of reinforcing steel, and core crushing

The engineering demand parameters and values of the parameters used to evaluate the occurrence of these limit states, however, have varied from study to study. Drift, displacement ductility (μ_{Δ}), and curvature ductility (μ_{ϕ}) are all metrics that have been used to define the performance of reinforced concrete columns. In the more recent fragility studies, researchers tend to use curvature ductility as the performance metric of choice for columns as this value can be obtained from computational models employing fiber cross-section-based beam-column elements. Curvature ductility is defined as the maximum curvature demand from the response-history analysis divided by the curvature at yielding of the outer most reinforcing steel. Table 5.2 shows the comparison of performance metrics and limit state median values used in these previous studies.

Table 5.2: Column limit state comparison

Study	Damage State	Description	Performance Metric	Limit State Value
Hwang (2000)	Slight	Yielding	Displacement Ductility (μΔ)	1.00
	Moderate	Cracking		1.20
	Extensive	Spalling		1.76
	Complete	Reinforcement Buckling		4.76
Nielson (2005)	Slight	Yielding	Curvature Ductility (μϕ)	1.00
	Moderate	Cracking		1.58
	Extensive	Spalling		3.22
	Complete	Reinforcement Buckling		6.84
Ramanathan (2012) Pre 1971	Aesthetic damage	Cracking	Curvature Ductility (μϕ)	0.80
	Repairable minor damage	Minor Spalling		0.90
	Repairable major damage	Shear cracks, major spalling, exposed core		1.00
	Component replacement	Loss of confinement, reinforcement buckling		1.20
Ramanathan (2012) 1971 - 1990	Aesthetic damage	Cracking	Curvature Ductility (μϕ)	1.00
	Repairable minor damage	Minor Spalling		2.00
	Repairable major damage	Shear cracks, major spalling, exposed core		3.50
	Component replacement	Loss of confinement, reinforcement buckling		5.00
Ramanathan (2012) post 1990	Aesthetic damage	Cracking	Curvature Ductility (μϕ)	1.00
	Repairable minor damage	Minor Spalling		4.00
	Repairable major damage	Shear cracks, major spalling, exposed core		8.00
	Component replacement	Loss of confinement, reinforcement buckling		12.00

A major reason for the differences in column limit state values in the various studies is due to the regional column design and detailing practices or the design era of the columns in question. Ramanathan (2012) focused on columns in California bridges, but recognized the evolution in column design as brittle columns (pre-1971), strength-degrading columns (1971-1990), and ductile columns (post 1990). Figure 5.4 shows the expected behavior of

columns from these three design eras, indicating the component damage thresholds (CDTs) along with photographic examples of these damage states. Note that as ductile detailing requirements improved in California over the decades, the curvature ductility values corresponding to the damage states increased. The Nielson (2005) study focused on bridge columns in the CSUS that were non-seismically detailed and had little to no confinement in the plastic hinge regions. In this particular study, limit state values were based on displacement ductility values from the Hwang (2000) seismic fragility study of Memphis, Tennessee bridges, but values were converted into curvature ductilities based on guidance from the *Seismic Retrofitting Manual for Highway Bridges* (FHWA 1995). The displacement ductility values selected in the Hwang (2000) study corresponded to key points in the cross-section flexural behavior (i.e., full yielding of the tension steel for the slight damage state, concrete reaching an assumed crushing strain of 0.002 for the moderate damage state, etc.). Note that the curvature ductility values for these damage states had magnitudes similar to those from the 1971-1990 "strength-degrading" California columns from the Ramanathan (2012) study.

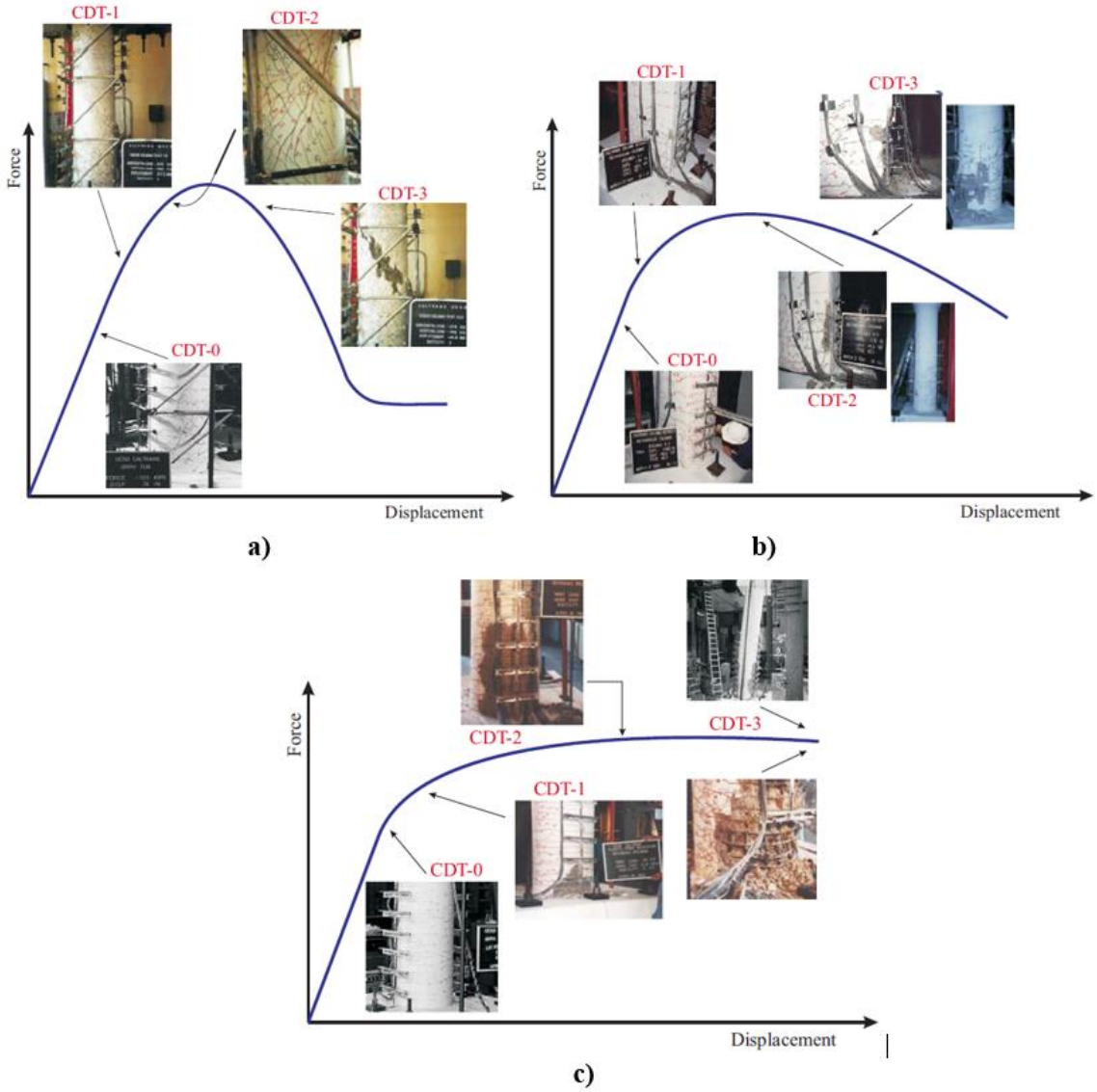

Figure 5.4: Depiction of column performance by design era a) Pre 1971; b) 1971-1990; c) Post 1990 (Ramanathan, 2012)

The reinforced concrete columns found in Texas have similar details as the strength-degrading columns (ca. 1971-1990) found in the Ramanathan (2012) study, and for the purposes of this study are believed to have similar behaviors. For example, it is common for both Texas columns and the 1971-1990 California columns to have transverse

reinforcing spaced at 6 inches and to have inadequate development length of the longitudinal bars into the footings and bent caps with no standard hooks (see Section 4.2.1 for column details). Although these details are an improvement from the brittle columns seen prior to 1971 in California (e.g., with 12 inch spacing of transverse reinforcing), Texas columns have limited ductility and may be susceptible to seismic damage. Thus, the curvature ductility median values used in this study for column limit states correspond to those from the strength-degrading columns in the Ramanathan (2012) study.

It should be noted that the limit state values discussed above were developed only considering flexural behavior of columns; however, reinforced concrete columns that have not been seismically designed and do not provide adequate transverse reinforcing are also susceptible to a more brittle shear failure. To determine which failure mode (i.e., flexural or shear) governs a columns behavior, one must compare the shear and flexural strengths of the column. If the column reaches its nominal flexural capacity prior to reaching its nominal shear capacity, the column is considered flexure-controlled. Using the process described below, all of the bridge columns in this study were found to be flexure-controlled; however, for completeness, the text below outlines the process for determining shear-controlled behaviors and limit state median values for reference.

If the nominal shear capacity of a column is less than the shear demand at its nominal flexural capacity, then the column is deemed as shear-controlled (i.e., column will fail in shear before reaching its flexural capacity), resulting in decreased displacement capacities (ASCE, 2013). More restrictive limit state median values, therefore, should be developed and used to capture the vulnerability of shear-controlled columns. Prakhov (2016) provides details on determining column capacities and the process used to determine the governing behavior of columns used in this study.

Lacking recommendations from past bridge fragility analyses, limit state median values for columns exhibiting shear failure can be developed following the guidance of ASCE-41 (ASCE, 2013), which provides guidance on the behavior and performance of reinforced columns used in building applications. Figure 5.5 shows the generalized backbone behavior of a reinforced concrete column for both flexural and shear controlled failure. For a flexural failure (Figure 5.5a), line A-B represents initial elastic behavior, line B-C delineates a reduced stiffness or post-yield response, line C-D represents a sudden loss of strength, and finally D-E represents the column behavior at a residual capacity prior to complete loss of load-carrying capacity at point E. For columns experiencing shear failure, the strength following the drop of line C-D is essentially zero, resulting in a significant and sudden loss of load-carrying capacity, after which the column continues to deform with negligible resistance up to point E. The parameters *a* and *b* shown in the ASCE-41 backbone behavior (Figure 5.5) give the column inelastic rotation capacities to the points that limit the hardening region and reduced capacity region, respectively, whereas *c* represents the normalized residual capacity ratio. The equations used to define these parameters for flexure- and shear-controlled reinforced concrete columns can be found in ACI (2016) or Prahkov (2016).

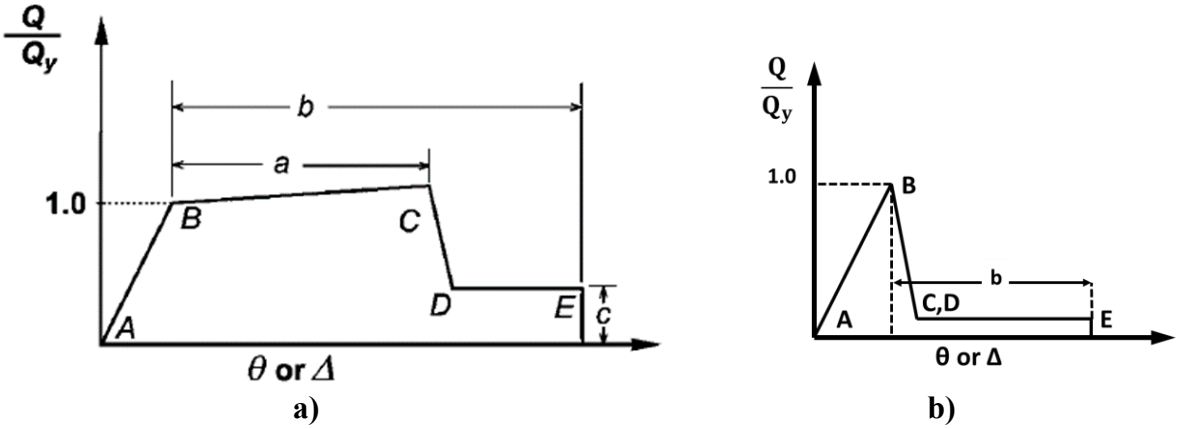

Figure 5.5: Column backbone behavior for a) flexure (ASCE, 2013) and b) shear-controlled columns

In addition to the generalize ductile and brittle behaviors previously described, ASCE (2016) also provides numerical values for deformations associated with specific performance levels or acceptance criteria (e.g., Immediate Occupancy, Life Safety, and Collapse Prevention). For example, a column that experiences no plastic rotation (i.e., remains on line A-B) would be classified as meeting the Immediate Occupancy performance level, where minor cracking and spalling may be observed but the columns maintain all of their vertical and lateral strength and stiffness. A column is expected to exceed the Life Safety performance level when a rotation of approximately 75% of the ultimate rotation (i.e., θ_u, rotation at point E) is reached. At the Life Safety performance level the column is expected to exhibit significant to severe damage and should be shored before re-occupancy. Finally, when a column reaches its ultimate rotation capacity, Θ_u, it is expected to exhibit severe damage and be on the verge of partial or total collapse, which is considered Collapse Prevention.

The performance levels mentioned previously (i.e., Immediate Occupancy, Life Safety, and Collapse Prevention) can be mapped to the damage states used in this study--

moderate, extensive, and complete limits states, respectively. For shear-controlled columns, acceptance criteria presented for the various performance levels in ASCE-41 can be used for the corresponding limit state median values. Knowing the brittle nature of a shear failure, and recognizing that minor cracking may be present prior to reaching the yield rotation, Θ_y, a rotation smaller than the yield rotation (e.g., 90% of Θ_y) can be assumed for the slight limit state. Table 5.3 shows a summary of all the column limit state values for both shear and flexural failures considered in this study; however, it should be noted again that all of the columns in this study exhibited flexural failure.

5.3.1.2 Bearings

Mander et al. (1996) conducted extensive experimental research on the response of steel bearings subjected to cyclic loading, which has been the foundation for estimating limit state median values throughout several past bridge fragility studies. This experimental research showed that failure of the anchor bolts connecting the base of the bearing to the concrete support typically controls the behavior and critical limit state values for steel bearings (see Section 4.3.1 for more details on steel bearings). For high-type fixed steel bearings, yielding of the anchor bolts under loading in the longitudinal direction was typically observed at a bearing deformation of approximately 1mm (Choi, 2002). This displacement could be used as the "slight" damage state value; however, such a small amount of deformation can be difficult to visually identify during a post-event inspection. Visual damage that can be easily identified by inspectors is an important aspect that should be considered when defining limit state values, as the bridge's damage state determined by the inspector is used to determine what action must be taken (e.g., reduce traffic speed, close down traffic lanes, close structure completely, etc.). In the past tests, more noticeable damage was observed at a deformation of 0.25 inch (6mm), when cracks tend to form

around the concrete bearing areas (Mander et al., 1996). For this reason, a 0.25 inch bearing deformation is used for the "slight" limit state median value in this study. The limit state median value for the "moderate" damage state is assumed to be at a deformation of 0.75 inches (20mm), where prying action in the bearing is first observed. This behavior results in more significant cracking and spalling of the concrete bearing areas, and significant deformation of the anchor bolts can be observed. Based on observations of anchor bolt fracture in the past tests, a bearing deformation of 1.5 inches (40mm) is assumed for the "extensive" limit state median value, resulting in subsequent sliding or toppling of the bearing. Finally, the "complete" limit state is assumed to take place at a deformation that exceeds the typical width of the bridge seat, resulting in unseating of the girder and ultimately complete or partial collapse of the span.

While visually being able to determine if a bridge span has collapsed during post-earthquake inspection can be straightforward, determining a bearing deformation value that would indicate collapse in a numerical bridge model is not. Nielson (2005), using the prescriptive approach, suggests that unseating will occur at a displacement of 10 inches (255mm) based on the width of the bridge seat for the bridge population in question. Results from a survey of bridge officials in the CSUS, conducted in the Padgett and DesRoches (2007a) study, indicated an expected bearing deformation of greater than or equal to 6 inches to cause girder unseating. Nielson (2005), using Bayesian updating and the survey results to update the prescriptive expected value, suggests that an expected bearing deformation of 7.25 inches would causing girder unseating. More details on the Bayesian updating process can be found in Nielson (2005).

This variation in median values shows that there is some discrepancy in determining displacement consistent bearing deformations associated with girder unseating. Recognizing these challenges and uncertainties in determining the "complete"

limit state median value for bearings, and due to the lack of experimental data of girder-bearing-seat subassemblies, it was determined to use the updated value, which takes into account engineering judgement, as suggested in the Nielson (2005) study. Through the investigation of TxDOT as-built drawings, it was determined that this value of 7.25 inches is also consistent with the typical distance between the centerline of bearing and the edge of the bridge seat.

Typical details for fixed steel bearings provide the same number of anchor bolts providing restraint in either direction (see Section 4.3.1 for steel bearing details), indicating that fixed type steel bearings have similar behaviors in both the longitudinal and transverse directions (Nielson, 2005). Also, while expansion type steel bearings are expected to accommodate more deformation in the longitudinal direction, the transverse behavior of a steel expansion bearing is expected to be similar to that of the fixed type bearing. Thus, the limit states for the longitudinal and transverse fixed steel bearings, as well as the steel expansion bearings in the transverse direction are assumed to follow the same limit state values as discussed above and are summarized in Table 5.3.

For expansion bearings (e.g., rockers and sliding bearings) in the longitudinal direction, the damage of concern is instability of the bearing, which would result in significant movement in the superstructure, and in the worst cases unseating of the span (Pan et al., 2007). The dimensions of the bearings and ultimately the width of the bridge seat generally govern this damage and instability. The experimental bearing tests conducted by Mander et al. (1996) showed that instability of expansion bearings was first observed at a deformation of half the width of the masonry plate (100mm). Using these test results Choi (2002) proposed a displacement of 4 inches (100mm) as the "moderate" limit state for expansion bearings. Investigation of as-built drawings indicated that the size of the masonry plates used in older steel girder bridges in Texas varies with span length,

ranging from a width of 6-inches up to 14-inches. For example, longer span lengths result in larger bearing forces, which requires a larger masonry plate. However, typical span lengths for steel girder bridges used in this study (e.g., spans less than 120 feet) correspond to bearings with masonry plates ranging in width from 6 to 9-inches. Therefore, a "moderate" limit state median value of 3.75 inches is used in this study. Considering unseating of a span as the "complete" damage state, a displacement of 7.25 inches, as previously discussed, is used as the median value for the "complete" limit state. Following the work of Choi (2002), the "slight" and "extensive" limit state median values were picked between the "moderate" and "complete" values, and do not necessarily correspond to any designated observed damage. These values are 1.5 inches of displacement for "slight" damage and 5 inches for "extensive" damage.

As previously mentioned in Section 4.3.2, elastomeric bearings are common bearing types used with concrete superstructures (i.e., PC girder bridge class). The behavior of these type of bearings is typically characterized by sliding; however, unimpeded sliding can only occur after complete fracture of the retention dowels, if present (Nielson, 2005). As depicted in Figure 4.11, the only difference between expansion and fixed elastomeric bearings are the slotted holes in the elastomeric pad and girder allowing the longitudinal movement of the superstructure at the expansion bearing locations. Because dowels, which are embedded in the bridge seat and extend through the elastomeric pad into the bottom of the concrete girder, cannot be observed after construction, it is difficult for an inspector to visually differentiate between expansion and fixed elastomeric bearings. For this reason, it is common to use the same limit state values for the fixed and expansion elastomeric bearings, in both the longitudinal and transverse directions (Nielson, 2005). This detailing, which causes the dowels to be hidden from external inspection, also makes it difficult to visually inspect and identify damage in the retention dowels (e.g.,

yielding or fracture of the dowel). Thus, limit state expected values related to dowel fracture must be related to observable displacements that can be associated with capacity implications and possible repair efforts, rather than observed dowel damage. For example, Nielson (2005) stated that a peak transient displacement of 1 inch is expected to result in permanent deformations in the bearing that can be easily observed by an inspector and may have caused minor dowel yielding, but this displacement is expected to have little effect on bearing capacity. A peak bearing displacement of 3 inches would imply possible dowel fracture and may require minor deck realignment. At 5 inches of peak bearing displacement, the dowels are expected to be fully fractured, resulting in not only deck realignment, but also requiring installation of a new retention mechanism for the concrete girders. At a bearing deformation of 7.25 inches, unseating of the span is expected to occur, as stated previously for other bearing unseating limit states. Therefore, the values for the slight, moderate, extensive, and complete limit states used in this study are displacements of 1 inch, 3 inches, 5 inches, and 7.25 inches, respectively.

Other reinforced concrete superstructures (e.g., RC slab and girders) do not utilize elastomeric pads as the bearing between the superstructure and the substructure, as discussed in Section 4.3.3. These older details, which typically consist of ¾ inch dowels and roofing felt, do rely on the same type of restraint system (i.e., steel dowels connecting the superstructure and substructure) and are expected to have similar "sliding" type of behavior. For this reason the limit state values for the elastomeric bearings, discussed above, will be used for the alternative concrete bearings typically used in the RC slab and girder bridge classes.

5.3.1.3 Abutments

Abutments primarily resist vertical loads and act as a retaining wall to the backfill supporting the approach slab; however, they do provide resistance against deformation and earthquake induced inertial forces from the bridge superstructure (Saini and Saiidi, 2013). Deformation of the abutment in the longitudinal direction can be resisted passively or actively. Passive resistance is developed as the abutment pushes into the soil backfill (compression), and active resistance is when the abutment is pulled away from the backfill (tension). The passive soil pressure and the foundation (e.g., piles or drilled shafts) provide resistance in passive action, while active action is resisted solely by the foundation (i.e., the soil is assumed to have no tensile resistance), as described in Section 3.2.2.8. Abutments also provide transverse stiffness, which can be attributed to the foundation or the wing walls, if present.

Typically, abutment limit states are defined in terms of the first yield point and ultimate displacement of the abutment foundation and backwall (Tavares et al., 2013; Choi, 2002). Martin and Yan (1995) provide guidelines for estimating ultimate displacement in the passive direction, as they suggest a multi-linear behavior of abutments in the passive action, and their tests show that the ultimate passive earth pressure becomes mobilized at a displacement of 6% to 10% of abutment height, depending on the type of soil (e.g., cohesive vs. cohesionless). Their tests also suggest abutments in the passive action see first yielding and second yielding at displacements of 0.6% and 1.5% of abutment height, respectively. Tavares et al. (2013) and Choi (2002) proposed passive limit state median values to be half the deformation at first yield for "slight" damage, deformation at first yield for "moderate", deformation at second yield (i.e., the deformation at which the multi-linear backbone stiffness reduces further) for "extensive", and the ultimate deformation as "complete" damage. Nielson (2005) proposed that an inspector would not be able to

identify noticeable (i.e., "slight") damage until cracking of the abutment and backwall occurred at or around second yielding, and "moderate" damage would occur at a longitudinal displacement of about 6 inches. Nielson (2005) also proposed, based on survey results of practicing CSUS bridge engineers, that abutment deformation was highly unlikely to reach an "extensive" or "complete" limit state. The current study adopts the limit state values proposed by Nielson (2005) for passive action in the abutments, as will be discussed in further detail later.

Limit states for abutments in the active or transverse directions are again typically defined in terms of first yield and ultimate deformations. When considering pile bent abutments, which are typical in the CSUS and Texas, Caltrans (1999) proposes that ultimate displacement occurs around a displacement of 1 inch, and first yield will occur at 30% of the ultimate displacement. Using these Caltrans recommendations, coupled with relevant engineering judgment (i.e., survey results from practicing bridge engineers) through Bayesian updating, Nielson (2005) proposed that an abutment deformation of 0.375 inches should be considered as "slight" damage, 1.5 inches as "moderate" damage, and 3 inches as "extensive" damage in the active action and transverse direction. Similar to the behavior in the passive action, Nielson (2005) suggested that, based on engineering judgement and the lack of "complete" damage observed in abutments in past earthquakes, abutment displacement in the active or transverse direction during a seismic event would not cause "complete" damage to a bridge structure.

Due to the similar design and details of CSUS and Texas bridge abutments (e.g., seat type pile/shaft abutments), the limit states proposed by Nielson (2005) for abutments were used in this study. Assuming an average abutment height of 7 feet, based on review of as-built drawings and TxDOT Standards, the second yielding point of an abutment in the passive direction is expected to occur at a deformation of about 1.25 inches, which was

considered as the “slight” limit state median value. An abutment deformation of 6 inches in the passive direction was used as the “moderate” limit state value in this study. For both the active and transverse abutment deformations, median values of 0.375 inches, 1.5 inches, and 3 inches are used as the “slight”, “moderate”, and “extensive” limit states, respectively.

5.3.1.4 Foundations and Expansion Joints

Foundations and expansion joints are two other bridge components that are potentially susceptible to damage during an earthquake event. These components are often considered as secondary components (Ramanathan, 2012), as their damage does not necessarily compromise the overall stability of the system (i.e., in the case of expansion joints), or their fragility is far lower than other major components (e.g., damage in columns or bearings is much likelier to occur before damage in the foundation). For some bridge classes in this particular study that are assumed to have drilled shaft foundations, the capacity of the foundation and columns are assumed to be related due to the typical integral drilled shaft/column foundation detail assumed, as discussed in Section 4.2.2. Depending on the design and detailing of this type of substructure component, the foundation and column can act as one component (e.g., with the same diameter column and shaft), or the column can be designed with a smaller diameter than the shaft, causing damage to occur in the smaller column section. In this study, foundation capacity, therefore, is not considered explicitly and is instead implicitly included in the column capacity and median limit state values.

Expansion joints are an important component of a bridge structure and are expected to experience damage during an earthquake event (e.g., due to pounding and crushing of the concrete deck). Although this type of damage may affect the functionality or the

required repair of the structure (e.g., resulting in reduced traffic speed due to rough joints, or required patching of joints that may increase repair costs), it is not expected to affect the overall stability of the structure. The capacity or damage of expansion joints is not typically considered explicitly in a fragility analysis; instead, it is common to map expansion joint damage to the limit states of other components. For example, if an expansion bearing experiences a displacement of 3 inches (which is considered "moderate" damage), it is expected that there will be moderate cracking and spalling at the expansion bearings, which will increase the time and costs of structural repairs. For this reason, expansion joint behavior was considered when developing the qualitative structural level limit states but are not considered explicitly at the component level.

Table 5.3: Limit State Median Values for Bridge Components

Component	Slight		Moderate		Extensive		Complete	
	Median	Disp.	Median	Disp.	Median	Disp.	Median	Disp.
Column - Flexural (μφ)	1	0.25	2	0.25	3.5	0.46	5	0.46
Column - Shear (θ, radians)	0.9θy	0.25	θy	0.25	0.75θu	0.46	θu	0.46
Steel Fixed Bearing - Long. (in)	0.25	0.25	0.75	0.25	1.5	0.46	7.25	0.46
Steel Fixed Bearing - Trans. (in)	0.25	0.25	0.75	0.25	1.5	0.46	7.25	0.46
Steel Expansion Bearing - Long. (in)	1.5	0.25	3.75	0.25	5	0.46	7.25	0.46
Steel Expansion Bearing - Trans. (in)	0.25	0.25	0.75	0.25	1.5	0.46	7.25	0.46
Elastomeric Fixed Bearing - Long. (in)	1	0.25	3	0.25	5	0.46	7.25	0.46
Elastomeric Fixed Bearing - Trans. (in)	1	0.25	3	0.25	5	0.46	7.25	0.46
Elastomeric Expansion Bearing - Long. (in)	1	0.25	3	0.25	5	0.46	7.25	0.46
Elastomeric Expansion Bearing - Trans. (in)	1	0.25	3	0.25	5	0.46	7.25	0.46
Abutment - Passive (in)	1.25	0.25	6	0.25	NA	NA	NA	NA
Abutment - Active (in)	0.375	0.25	1.5	0.25	3	0.46	NA	NA
Abutment - Transverse (in)	0.375	0.25	1.5	0.25	3	0.46	NA	NA

5.3.2 UNCERTAINTY IN COMPONENT CAPACITY MODELS

To be consistent with the probabilistic seismic demand models, the capacity models are represented by median values (described in the previous section) and are assumed to follow a lognormal distribution to capture the uncertainty and variability associated each limit state (Nielson, 2005). Uncertainty is defined in terms of a lognormal standard

deviation or dispersion value. When there is not enough empirical data to determine a dispersion value for a specific limit state, these values must be determined in a subjective manner. One method proposed by Ramanathan (2012) is to assign a constant dispersion to all components. In the study by Ramanathan (2012), the component dispersion values for all components were estimated based on experimental data in the PEER column structural database (Berry and Eberhard, 2004). In that study, a dispersion value of 0.35 was found to be a good estimate for column limit states, and thus was adopted for all component dispersion values. Another method proposed by Nielson (2005) is to adopt the assumption that the variance is less in the lower limit states verses the higher limit states, resulting in a COV of 0.25 for both the slight and moderate limit states and a COV of 0.5 for the extensive and complete limit states. Using Eq. 5.5, the COV can be transformed into dispersions (β) for a lognormal distribution.

$$\beta = \sqrt{ln(1 + COV^2)} \tag{5.5}$$

For this study on Texas bridge fragility, following the guidance of Nielson (2005), a dispersion value of 0.25 was calculated and assigned to the slight and moderate damage states, and 0.47 was calculated and assigned to the extensive and complete limit states.

5.4 Fragility Curve Development:

Once the seismic demand and capacity models for each major bridge component have been established, component and system level fragility curves can be developed. System level fragility curves provide an estimation of the vulnerability of the system, in this case the bridge, and are useful tools in developing post-event action plans or loss estimations. Component level fragility curves highlight the most vulnerable components of the bridge, which provide a very useful tool for refining post-event inspection techniques or developing appropriate retrofit strategies. Development of fragility curves for Texas

bridges is outside of the scope of this thesis; however, an overview of the process of developing component and system fragility curves is provided below for reference.

The mathematical representation of fragility is expressed as the probability of the demand exceeding some capacity, as given in Eq. 5.1. Adopting the common assumption that the demand and capacity models take on a lognormal distribution, the fragility equation can be rewritten as shown in Eq. 5.6:

$$P[D>C|\mathrm{IM}] = \Phi\left[\frac{\ln(S_\mathrm{d}/S_\mathrm{c})}{\sqrt{\beta_{\mathrm{D|IM}}^2 + \beta_\mathrm{c}^2}}\right] \tag{5.6}$$

Where Φ is the standard normal cumulative distribution function, S_c and β_c are the median and dispersion values, respectively, for the limit state in question, and S_d and $\beta_{D|IM}$ are the median demand and dispersion values, respectively, at a given ground motion intensity (IM). Component fragility curves can be generated by plotting the cumulative distribution function (CDF) of the lognormal curves described by Eq. 5.6 (Nielson and DesRoches, 2007b). Examples of component fragility curves from a previous bridge fragility study are shown in Figure 5.6.

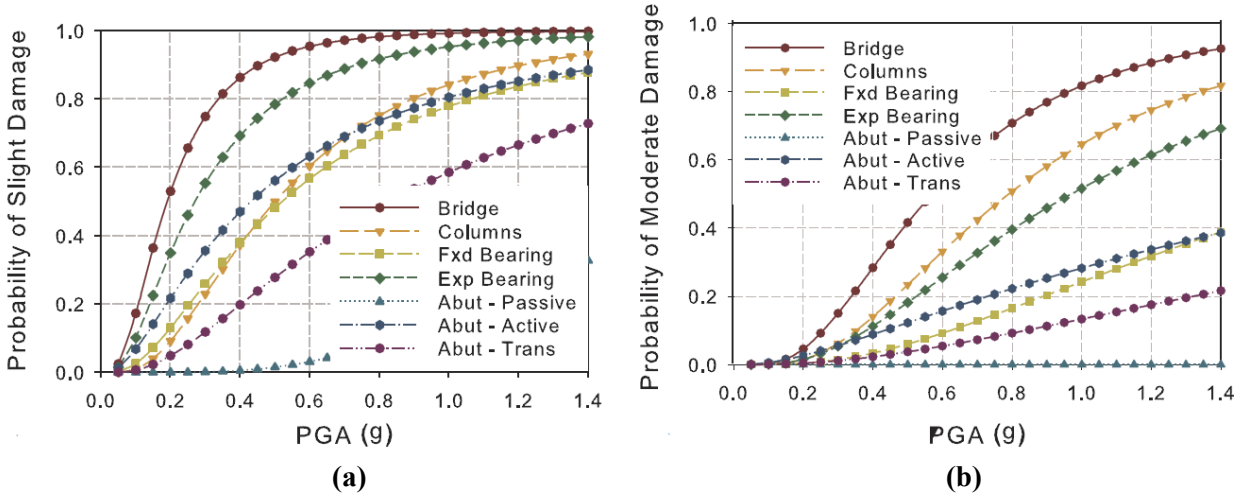

Figure 5.6: Bridge and component fragility curves for: (a) slight and (b) moderate damage (Nielson and DesRoches, 2007b)

The fragility of an entire bridge system is related to the fragility of its individual components. For example, one could assume that the columns are most vulnerable part of the bridge, and thus the column fragility can be assumed to represent the fragility of the entire bridge system, as was done in early bridge fragility studies (Karim and Yamazaki, 2003; Mackie and Stojadinovic, 2004; Shinozuka et al., 2000). More recent fragility studies, powered by advancements in computing capabilities, however, consider the vulnerability of multiple components to more accurately represent the fragility of the bridge system. The combination of multiple component fragilities cannot be done with a closed-form integration, which significantly increases the complexity of fragility analysis.

Researchers have explored several methods for developing system level fragility curves from a combination of component fragilities. One method that has been used in several different studies is the use of first-order reliability bounds (Pan, 2007; Nielson and DesRoches, 2007b). First-order reliability can be expressed as:

$$\max_{i=1}^{m}\left[P(F_i)\right] \le P_{sys} \le 1-\prod_{i=1}^{m}\left[1-P(F_i)\right] \tag{7.4}$$

where $P(F_i)$ is the probability of failure of the ith component. The lower bound assumes complete component correlation and is controlled by the most vulnerable component, while the upper bound is represented by the product of the component survival probabilities and assumes no correlation between components. Nielson and DesRoches (2007b) found that the upper bound provides a good estimate of the system fragility; however, they concluded that direct estimation using numerical integration is a more accurate approach, showing a reduction of vulnerabilities up to 10 percent.

The direct estimation approach recognizes that there is some sort of correlation of damage between the components, as the component PSDMs are compiled into a joint seismic probability density model (JPSDM) for the system. The JPSDM is assumed to take on a multivariate normal distribution, and therefore can be fully described by a vector of mean demands and a covariance matrix. Both the mean vector and covariance matrix can be obtained through a multivariate correlation analysis on the component PSDMs. In order to develop fragility curves, the JPSDM must be integrated over all possible failure domains. This is most commonly done using a numerical integration technique, such as Monte Carlo simulation. Monte Carlo simulation is a process where N number of realizations are randomly sampled from both the demand and capacity, which are paired and evaluated for failure. This sampling is carried out over a reasonable range of IM values, and the data can be used to directly compute the probability of failure for the given IM. It is common to assume the bridge is a system of components in series, where if one component fails the limit state, then the system is assumed to fail that limit state. This direct estimation approach can be computationally demanding (e.g., requiring on the order of 10^6 number of realizations), but has been used in several studies and has been found to

be very effective with advancements in computational resources (Nielson and DesRoches, 2007b; Ramanathan, 2012; Tavares et al., 2013).

Zhang and Huo (2009) proposed a "weighted" approach for the combining of component fragility curves. In other words, a weighting ratio (e.g., 0.75 for columns and 0.25 for bearings) is assigned to the components in order to generate the system level damage probabilities. This approach recognizes that not all components contribute equally to system failure; however, as the number of components considered increases, determining the weighting ratios becomes increasingly difficult. Another approach that was introduced by Duenas-Osorio and Padgett (2011) is the use of augmented system failure events. With this approach the general system of components in series assumption is used, where failure of one component means failure of the system; however, they also suggest that failure of multiple "important" components at a less severe limit state would constitute failure of the system at the current more severe damage state. For example, if columns and expansion bearings both experienced damage that exceeded the slight damage state, then the system would be considered to be at the moderate damage state. A challenge with this approach is properly identifying the "important" components. Duenas-Osorio and Padgett (2007) addressed this challenge by calculating conditional probability importance measures (CIM) for each component, following the work of Kang et al. (2008). The CIMs attempt to quantify the importance of each component to the system reliability.

In summary, combining component fragility curves into system fragility curves is not a trivial task. Research does show that multiple component fragilities should be considered; however, the challenge is in quantifying the correlation between component and system fragilities. Whether creating JPSDMs, assigning weighting ratios, or using augmented failure events, there are assumptions that have to be made, and inevitably introduction of errors associated with these assumptions.

6 CONCLUSIONS

The objective of this project, as outlined in this thesis, was to develop representative bridge samples and capacity models to be used for seismic fragility analysis of Texas bridges. This chapter presents a summary of the thesis and recommended work for later phases of the project.

6.1 Summary

- A thorough analysis of the Texas highway bridge inventory was conducted using the NBI database. It was determined that approximately 85% of TxDOT on-system bridges could be assigned to one of seven different bridge classes:
    - Multi-span simply supported reinforced concrete slab (MS RC slab)
    - Multi-span continuously supported reinforced concrete slab (MC RC slab)
    - Multi-span simply supported reinforced concrete girder (MS RC girder)
    - Multi-span simply supported pre-stressed concrete girder (MS PC girder)
    - Single span simply supported pre-stress concrete girder (SS PC girder)
    - Multi-span simply supported steel girder (MS Steel girder)
    - Multi-span continuously supported steel girder (MC Steel girder).

  The largest of the bridge classes was found to be the MS PC girder bridge class, which accounts for approximately 34% of all on-system bridges.
- Common statistical analyis techniques (e.g., average, standard deviation, cumulative distribution functions, etc.) were used to investigate bridge class characteristics and develop parameter distributions of major geometric bridge descriptors (e.g., number of spans, maximum span length, deck width, column height, skew angle, etc.).
- Past literature and TxDOT standard and as-built drawings were used to develop distributions of material properties (e.g., concrete compressive strength, steel reinforcing strength, damping ratio, etc.) and bridge component behaviors (e.g.,

bearing stiffness, foundation stiffness, abutment stiffness, superstructure mass factors, etc.).

- The Latin Hypercube sampling technique was used to select sixty-four representative bridge samples (i.e., eight geometrically representative samples, paired with eight parametric samples, e.g., variations in material properties and component behavior) for each of the seven bridge classes.
- Generalized design and detailing trends for various bridge components (e.g., column dimensions and reinforcing details, column spacing, bent cap and abutment dimensions, girder types and spacing, foundation type, etc.) were determined through a thorough review of TxDOT standard and as-built drawings pertinent to bridges in the scope of this study.
- Qualitative damage state definitions were developed representing Texas specific damage descriptors and bridge component behaviors.
- Component level capacity statistical models were developed using a combination of structural mechanics and analysis (i.e., the prescriptive approach) and engineering judgment (i.e., the descriptive approach).

6.2 Future Work

There are several potential areas in which the present research can be extended. A few of these are described below:

- Behaviors and capacities of components specific to Texas bridges can be investigated experimentally, including consideration of how behavior is correlated to structural damage states and structural losses and repairs. For example, there has been limited research conducted on steel bearings specific to those found in Texas bridges.
- Column height is a parameter that can have a significant effect on the dynamic response of a structure. Limited column height data is reported in the NBI database only for bridges passing over other roadways or railways, resulting in a range of

approximately 10 to 20 feet column heights considered in this study. In metropolitan areas, where elevated highway interchanges or flyovers are common, columns heights are expected to be well beyond the 10 to 20 foot range. Similarly, over shallow water crossings, bridge columns may be short and may even exhibit different failure modes under lateral loading. The effects of these significantly longer and shorter column heights should be investigated and considered when determining seismic vulnerability.

- A large portion of the Texas bridge inventory has been in service for over 50 years. Effects of the aging infrastructure should be considered in the vulnerability assessment. For example, deterioration of component behaviors and capacities due to factors such as fatigue, cracking and spalling of concrete, corrosion of steel reinforcing, corrosion of steel bearings, limit functionality of expansion joints due to debris build-up, should be considered.
- There are other bridge types outside of the seven bridge classes considered in the study. Additional research on these other bridge types should be conducted to more fully capture the seismic vulnerability of the Texas highway bridge inventory. A few examples of other bridge types include, but are not limited to, reinforced concrete box girders and reinforced concrete Tee-girders.
- This particular study only captures the behavior of circular concrete columns; however, there are a significant number of bridges in the Texas inventory that utilize steel H-piles and square concrete piles as the main column element. The behavior and capacity of pile bents should be investigated and incorporated into the fragility analysis.

APPENDICES

Appendix A: Girder Properties

Steel Girder Selection

A.1 Simply Supported Steel Girders

Simply supported steel girder bridges are typically designed and constructed using rolled wide flange girder sections. As mentioned in Section 4.1.1, TxDOT standard drawings (TxDOT, 2006) provide a variety of different girder sections that can be used for varying roadway widths and span lengths (typically span length ranges in increments of 5 feet). This list of rolled shape options provides flexibility for the designer and contractor make a more economical structure. One method to minimize cost would be selecting the lightest girder section (e.g., the girder that weighs the least has the least amount of steel, which in turn should be the lowest cost). However, depending on the particular situation this may not always improve economy. For example, a designer or builder may pick a heavier section due to section availability or to meet geometric constraints. Therefore, determining a specific steel girder section for a particular bridge geometry is not a trivial task.

To accurately represent the varying girder sections in a fragility assessment, the selection of girder sizes should be treated as a random variable. In this study, the available girder sections were determined from the TxDOT standards based on span length, and then a single girder section was randomly selected for each geometric bridge sample. Table A.1 shows the girders and the section properties used for each MS Steel bridge sample.

Table A-1: MS Steel girder section properties

Bridge Sample	Girder Member	Girder Depth (in)	Girder Area (in^2)	Girder Ix (in^4)	Girder Iy (in^4)
1	W24 x 104	24.06	30.7	3100	259
2	W18 x 130	19.25	38.3	2460	278
3	W30 X 191	30.68	56.1	9200	673
4	W21 x 122	21.68	35.9	2960	305
5	W30 X 173	30.44	50.9	8230	598
6	W27 x 146	27.38	43.2	5660	443
7	W30 X 173	30.44	50.9	8230	598
8	W36 X 135	35.55	39.9	7800	225

A.2 Continuously Supported Steel Girders

Continuous span construction is often used to achieve longer span lengths than are practical with simply supported construction. This trend is depicted in the span length distributions shown in Section 2.2.2, where the average span length for the MS Steel girder bridge class is 48 feet, while the average for the MC steel girder class is 102 feet. These longer span lengths (e.g., greater than 100 to 110 feet span lengths) often require girder depths well beyond the available rolled wide-flange sections. Therefore, design engineers typically use built-up I-girder sections for the longer span continuous girders. The design of built-up girders is specific to the details of each individual bridge, making it difficult to develop standard sections. However, design engineers often follow several "rules of thumb" to develop a preliminary section that can then be refined to fit to the design requirements. These "rules of thumb" assumed in this study are listed below:

- Span length (L)/girder depth (D) ≈ 32
- Girder depth (D)/web thickness (t_w) ≈ 137
- Flange width (b_f)/girder depth (D) ≈ 0.33

- Flange width (b_f)/(2*flange thickness (t_f)) ≈ 9.2

In the design process, span length is often governed by predetermined site constraints. For example, the bridge needs to span a four lane highway, a 120 foot waterway, or needs to avoid existing utility lines. Thus, span length can be used as the starting point in determining the girder depth. Once the girder depth is selected the remaining guidelines help the designer determine the remaining properties of the girder section. Since these "rules of thumb" or guidelines are only intended to provide a preliminary girder section, it is expected that these particular parameters (e.g., L/D, D/t_w, b_f/D, and $b_f/(2*t_f)$) for the final girder design will have some variation. To gain understanding of how much variation is expected, several as-built drawings for long span continuous steel girder bridges (span lengths ranging from 115 to 240 feet; TxDOT, 2007; TxDOT, 1975; TxDOT, 1971a; TxDOT, 1971b; TxDOT, 1965) were used to compare preliminary and final design parameters. Table A-2 shows this comparison.

Table A-2: MC Steel girder parameter comparison

	Span Length (ft)	L/D	D/tw	bf/D	bf/2tf
Final Design	115	30	123	0.26	8
	140	28	160	0.23	9.33
	150	30	137	0.3	12
	150	33.33	123	0.26	9.33
	240	30	170	0.21	10
Preliminary Design		32	137	0.33	9.2

Span Length (L), girder depth (D), web thickness (tw), flange width (bf), flange thickness (tf)

This table verifies the variance in the final design, which should be considered in selecting accurate built-up girder sections. In this study girder sections are selected using the linear regressions shown in Figures A-1 through A-4.

Continuous girder spans can also be used for shorter span lengths (e.g., less than 100 feet). After a thorough review of as-built drawings it was determined that shorter

continuous span girders, similar to their simply supported counterparts, are built using rolled wide flange sections. Therefore, the girder sections for continuous bridge samples with spans less 100 feet were selected using the same method as discussed in Section A-1.

The section properties used for the MC Steel girder bridge samples in this study are show in Table A-3. It should be noted that continuous steel girders often utilize flange cover plates or web stiffeners to increase section capacity at certain places along the length of the span (e.g., cover plates at the mid span and at interior supports, and web stiffeners at bearing locations). The section properties for MC Steel girders used in this study neglect these additional components (e.g., cover plates, bearing stiffeners, and web stiffeners).

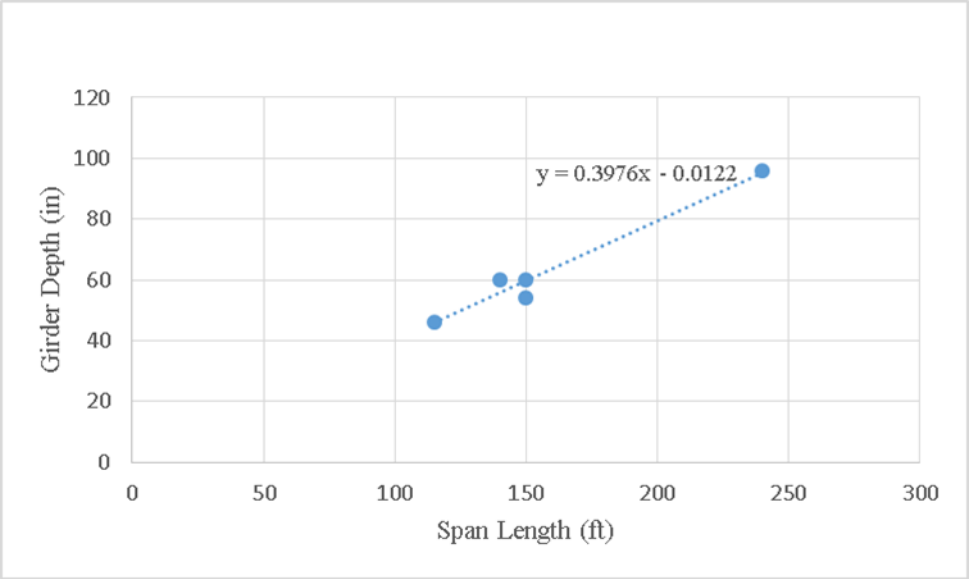

Figure A-1: MC Steel girder - Span Length vs. Girder Depth

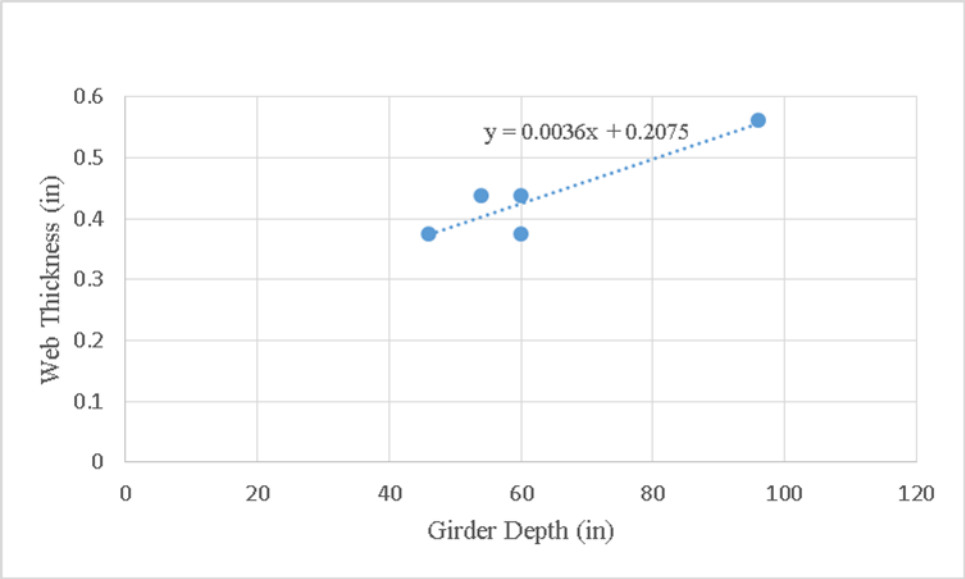

Figure A-2: MC Steel girder – Girder Depth vs. Web Thickness

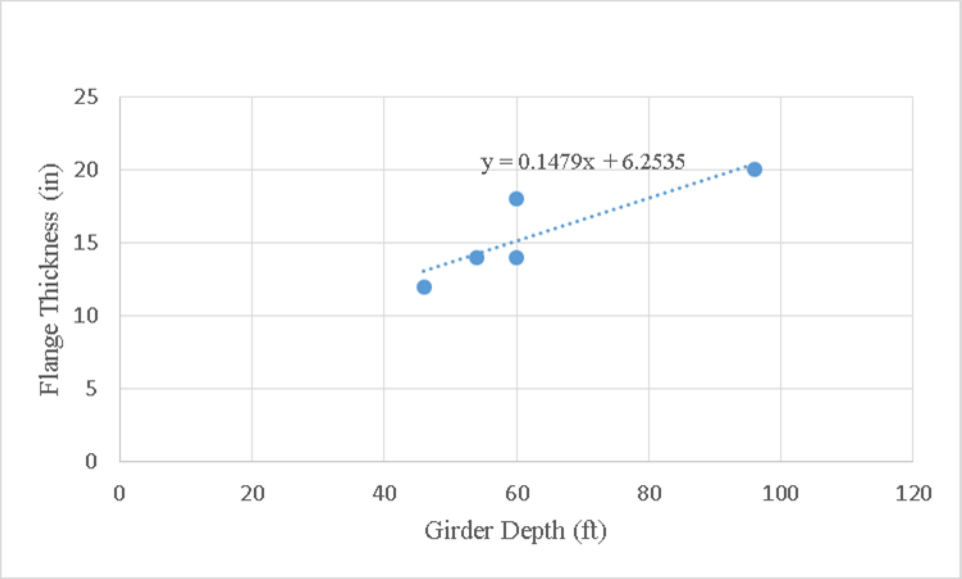

Figure A-3: MC Steel girder – Girder Depth vs. Flange Width

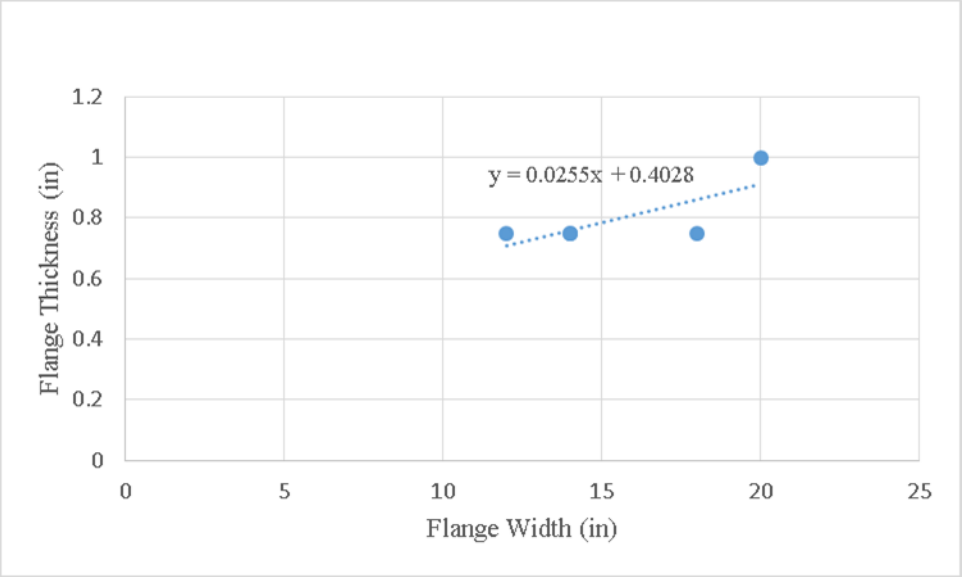

Figure A-4: MC Steel girder – Girder Depth vs. Flange Thickness

Table A-3: MC Steel girder section properties

Bridge Sample	Girder Depth (in)	Girder Area (in2)	Girder Ix (in4)	Girder Iy (in4)
1	35.55	39.9	7800	225
2	38.7	58.8	14900	695
3	31.6	77	13100	959
4	46	36.2	12736	225
5	38.2	43.98	9800	229
6	58	50.9	27906	493
7	35.9	44.3	9040	270
8	96	92.9	129187	1335

A.3 Girder Spacing and Number of Girders

The number of girders and the girder spacing are important parameters in developing representative bridge models. Tables A-4 through A-8 show the number of girders and the corresponding girder spacings for the relevant bridge classes (i.e., MS PC girder, MS Steel girder, MS RC girder, MC Steel girder, and SS PC girder) used in this study. The reinforced concrete slab type bridges (i.e., MS RC slab, and MC RC slab), due to the slab type superstructure, do not have girders and are not listed in this section. Details for the RC slab superstructure models can be found in Section 4.1.4. The procedure for determining the number of girders and girder spacings are presented in Section 4.1.5. The

Table A-4: MS PC Girder – Girder Spacing

Bridge Sample	# of Girders	Girder Spacing (ft)
1	6	8
2	6	7.33
3	7	6
4	5	8
5	11	6.67
6	8	7.33
7	10	6.33
8	7	6.67

Table A-5: MS Steel Girder – Girder Spacing

Bridge Sample	# of Girders	Girder Spacing (ft)
1	8	6.67
2	4	7.33
3	7	6.33
4	6	7.33
5	6	7.67
6	6	7.67
7	5	8.33
8	5	7.00

Table A-6: MS RC Girder – Girder Spacing

Bridge Sample	# of Girders	Girder Spacing (ft)
1	15	3
2	9	3
3	11	3
4	13	3
5	10	3
6	14	3
7	8	3
8	15	3

Table A-7: MC Steel Girder – Girder Spacing

Bridge Sample	# of Girders	Girder Spacing (ft)
1	11	7
2	5	5.67
3	5	6.67
4	9	6
5	6	7.33
6	7	6.33
7	5	9
8	6	6

Table A-8: SS PC Girder – Girder Spacing

Bridge Sample	# of Girders	Girder Spacing (ft)
1	7	6.33
2	11	5.67
3	10	8.67
4	6	6.33
5	8	6
6	7	6
7	7	6.67
8	8	6

Appendix B: Column Properties

As discussed in Section 4.2, cylindrical concrete columns are assumed for each bridge class in this study. After conducting a thorough review of TxDOT standard and as-built drawings, it was determined that there are four prominent column diameters (e.g., 24-inch, 30-inch, 36-inch, and 42-inch) that are used in the design and construction of multi-column bents throughout the Texas bridge inventory and will be used in this study. Column diameter is typically governed by span length and, in some cases, year of construction. For example, for the PC girder bridge class, bridge samples with span lengths less than 100 feet and constructed prior to 2009 are assumed to have 30-inch diameter columns, while bridge samples constructed in 2009 or later and have spans less than 100 feet are assumed to have 36-inch diameter columns. If a PC girder bridge sample has a span length longer than 100 feet, a 42-inch diameter column is used regardless of when the bridge was constructed. Again this was determined through review of current TxDOT standards and as-built drawings for PC girder bridges built in the 1960s through early 2000s. Column sizes for the MS and MC Steel girder bridge classes are governed solely by span length. If a bridge sample has a span length less than 100 feet, it is assumed to have 30-inch diameter columns, or if the span length is greater than 100 feet, 42-inch diameter columns are used. The RC girder and slab bridge classes on average have much shorter span lengths (e.g., average span lengths of 34 feet and 23 feet, respectively) requiring much lower column demands. For both of these two bridge classes, it assumed that all bridge samples utilize 24-inch diameter columns.

The column properties and reinforcing details for each of these column sizes (i.e., 24-inch, 30-inch, 36-inch, and 42-inch diameter) are listed in Tables B-1 through B-4.

Tables B-5 through B-9 list the number of columns and column spacing for each geometric sample and for each bridge class, following the procedure discussed in Section 4.2.1.

Table B-1: 24 inch Diameter Concrete Column

Column Properties	
Diameter (in)	24
Number of Longitudinal Bars	8
Longitudinal spacing (equal, or inches)	Equal
Longitudinal bar size	#7
Transverse type (spiral, tie)	Spiral
Transverse spacing/pitch (in)	6
Transverse bar size	#3
Cover (to center of trans. Bar) (in)	2.25
Reinforcement coating	None
Embedment length - Cap (ft)	2
Embedment length - drilled shaft (ft)	2.25

Table B-2: 30 inch Diameter Concrete Column

Column Properties	
Diameter (in)	30
Number of Longitudinal Bars	8
Longitudinal spacing (equal, or inches)	Equal
Longitudinal bar size	#9
Transverse type (spiral, tie)	Spiral
Transverse spacing/pitch (in)	6
Transverse bar size	#3
Cover (to center of trans. Bar) (in)	2.25
Reinforcement coating	None
Embedment length - Cap (ft)	2.25
Embedment length - drilled shaft (ft)	3

Table B-3: 36 inch Diameter Concrete Column

Column Properties	
Diameter (in)	36
Number of Longitudinal Bars	10
Longitudinal spacing (equal, or inches)	Equal
Longitudinal bar size	#9
Transverse type (spiral, tie)	Spiral
Transverse spacing/pitch (in)	6
Transverse bar size	#4
Cover (to center of trans. Bar) (in)	3
Reinforcement coating	None
Embedment length - Cap (ft)	2.75
Embedment length - drilled shaft (ft)	4.5

Table B-4: 42 inch Diameter Concrete Column

Column Properties	
Diameter (in)	42
Number of Longitudinal Bars	14
Longitudinal spacing (equal, or inches)	Equal
Longitudinal bar size	#9
Transverse type (spiral, tie)	Spiral
Transverse spacing/pitch (in)	6
Transverse bar size	#4
Cover (to center of trans. Bar) (in)	3
Reinforcement coating	None
Embedment length - Cap (ft)	2.75
Embedment length - drilled shaft (ft)	4.5

Table B-5: MS PC Girder – Column Spacing

Bridge Sample	# of Columns	Column Spacing (ft)
1	4	12
2	3	15.5
3	3	15
4	3	13
5	5	15.5
6	4	15.5
7	5	13
8	4	11.5

Table B-6: MS Steel Girder – Column Spacing

Bridge Sample	# of Columns	Column Spacing (ft)
1	4	14.5
2	3	9.5
3	4	11.5
4	4	11.5
5	4	12
6	4	12
7	3	15
8	3	12.5

Table B-7: MS RC Girder – Column Spacing

Bridge Sample	# of Columns	Column Spacing (ft)
1	4	12
2	3	8
3	3	11
4	3	14.5
5	3	9
6	3	16
7	3	7.5
8	4	11.5

Table B-8: MS RC Slab – Column Spacing

Bridge Sample	# of Columns	Column Spacing (ft)
1	3	9.5
2	4	12.5
3	4	12.5
4	3	11.5
5	3	10.5
6	3	10.5
7	3	10.5
8	4	14

Table B-9: MC Steel Girder – Column Spacing

Bridge Sample	# of Columns	Column Spacing (ft)
1	5	16
2	3	9
3	3	10.5
4	4	14.5
5	3	15.5
6	4	11
7	3	15
8	3	12.5

Table B-10: MC RC Slab – Column Spacing

Bridge Sample	# of Columns	Column Spacing (ft)
1	5	16
2	4	9
3	4	10.5
4	4	14.5
5	3	15.5
6	4	11
7	4	15
8	4	12.5

Table B-11: SS PC Girder – Column Spacing

Bridge Sample	# of Columns	Column Spacing (ft)
1	3	16
2	5	12.5
3	6	14.5
4	3	13
5	4	12
6	3	15
7	4	11.5
8	4	12

Appendix C: Parameter Samples

The parameter samples for each geometric representative bridge sample used in this study are presented in this Appendix. The parameter abbreviations and the units for the values in each of these tables can be found in Section 3.2.2. The parameter samples for the MS PC girder bridge class are presented in Section 3.2.2.9 of this thesis.

Table C-1: MS RC Slab parameter for geometric sample 1

	1	2	3	4	5	6	7	8
Conc Str	4528	5820	4225	4333	3847	3172	4849	5213
Reinf Str	60568	45085	57684	53239	49924	56127	53439	66973
COF MF	0.98	1.02	1.18	0.93	1.05	0.97	0.86	1.10
Dowel Str	7.20	7.86	7.09	6.86	6.33	6.80	7.46	6.46
Abt-Pas Stf	36.0	48.9	42.2	31.9	26.0	20.8	45.6	30.8
Pile Stf	20.9	67.6	27.0	48.0	57.4	44.5	38.3	70.0
Mass	137	114	120	132	112	126	134	123
Damp Ratio	0.041	0.047	0.045	0.034	0.054	0.066	0.053	0.025
Small Gap	0.49	1.58	1.85	1.20	0.15	0.59	0.86	1.47
Load Dir	273	323	148	237	95	87	210	45

Table C-2: MS RC Slab parameter for geometric sample 2

	Bridge Sample 2							
	1	2	3	4	5	6	7	8
Conc Str	3547	5490	5063	4086	2701	5362	4544	4281
Reinf Str	52335	58206	45535	64328	53743	57475	54803	51441
COF MF	1.03	0.93	0.87	1.01	1.27	0.98	1.10	0.94
Dowel Str	6.62	7.74	7.39	6.34	6.86	7.10	7.23	6.40
Abt-Pas Stf	48.1	31.2	43.7	20.2	24.2	42.1	37.4	34.1
Pile Stf	63.3	33.8	25.8	33.0	55.0	44.2	48.5	69.4
Mass	112	130	134	127	121	138	125	115
Damp Ratio	0.043	0.056	0.026	0.052	0.059	0.040	0.032	0.049
Small Gap	1.28	0.82	0.58	1.21	1.61	0.26	1.85	0.05
Load Dir	207	140	103	34	326	77	303	270

Table C-3: MS RC Slab parameter for geometric sample 3

	Bridge Sample 3							
	1	2	3	4	5	6	7	8
Conc Str	6085	4950	4385	3605	2787	4646	5302	3951
Reinf Str	58724	42885	50579	55665	54468	63982	57947	52657
COF MF	0.94	1.05	1.01	0.99	1.07	0.87	0.93	1.14
Dowel Str	6.15	6.42	7.03	7.63	6.95	7.31	8.10	6.77
Abt-Pas Stf	39.0	21.9	44.2	49.2	34.6	31.0	24.4	35.9
Pile Stf	43.5	26.3	63.6	60.9	50.5	35.7	71.6	29.5
Mass	122	113	119	127	137	134	131	116
Damp Ratio	0.047	0.041	0.075	0.056	0.035	0.026	0.038	0.052
Small Gap	1.29	1.60	1.10	0.52	1.86	0.50	0.05	0.85
Load Dir	65	101	142	217	274	40	326	237

Table C-4: MS RC Slab parameter for geometric sample 4

	Bridge Sample 4							
	1	**2**	**3**	**4**	**5**	**6**	**7**	**8**
Conc Str	4173	5719	2789	4550	4827	5175	4268	3628
Reinf Str	55544	51683	57408	59076	62232	50159	54172	45434
COF MF	1.03	1.04	0.94	0.92	1.23	0.82	0.99	1.11
Dowel Str	7.61	8.01	6.35	6.70	7.02	6.95	6.52	7.34
Abt-Pas Stf	29.3	39.1	46.3	21.6	27.1	35.3	44.0	31.7
Pile Stf	67.5	59.8	45.8	25.3	35.8	49.2	71.2	29.9
Mass	134	113	127	130	122	115	120	138
Damp Ratio	0.029	0.056	0.034	0.044	0.051	0.039	0.048	0.063
Small Gap	1.62	1.16	1.88	0.66	0.06	1.40	0.82	0.38
Load Dir	109	318	276	82	172	214	236	36

Table C-5: MS RC Slab parameter for geometric sample 5

	Bridge Sample 5							
	1	**2**	**3**	**4**	**5**	**6**	**7**	**8**
Conc Str	4494	4551	3865	5397	5014	2998	6142	4144
Reinf Str	49105	51031	54780	56438	55141	58696	53035	63777
COF MF	0.92	1.13	0.96	1.08	0.79	1.01	1.06	0.99
Dowel Str	6.47	6.20	7.41	8.25	6.62	7.01	6.92	7.23
Abt-Pas Stf	21.2	46.1	34.3	42.3	24.2	46.9	30.8	37.2
Pile Stf	68.3	63.8	33.3	58.7	53.2	45.9	26.5	34.4
Mass	116	129	137	123	119	134	114	126
Damp Ratio	0.053	0.022	0.033	0.063	0.039	0.056	0.043	0.049
Small Gap	1.96	1.24	1.56	1.30	0.43	0.22	0.91	0.54
Load Dir	244	118	35	279	218	158	89	352

Table C-6: MS RC Slab parameter for geometric sample 6

	Bridge Sample 6							
	1	**2**	**3**	**4**	**5**	**6**	**7**	**8**
Conc Str	4527	4916	4293	3490	6065	4039	3881	5201
Reinf Str	54110	63060	43998	52908	54963	58129	50949	58663
COF MF	1.03	1.13	1.12	1.02	0.94	0.92	0.99	0.78
Dowel Str	6.70	6.85	7.63	7.89	7.11	6.25	7.24	6.44
Abt-Pas Stf	21.2	38.5	31.1	26.4	34.7	42.9	46.8	41.0
Pile Stf	31.4	24.9	68.9	52.9	46.6	57.7	61.9	37.9
Mass	117	125	111	121	130	138	135	126
Damp Ratio	0.049	0.062	0.014	0.059	0.047	0.041	0.034	0.042
Small Gap	1.28	0.38	1.05	0.67	1.61	0.90	0.03	1.83
Load Dir	65	307	241	92	201	338	144	41

Table C-7: MS RC Slab parameter for geometric sample 7

	Bridge Sample 7							
	1	**2**	**3**	**4**	**5**	**6**	**7**	**8**
Conc Str	4698	5747	3306	4222	5254	4277	3837	5058
Reinf Str	63370	52091	56488	49499	42456	53414	58448	55088
COF MF	0.93	0.94	0.79	1.12	1.01	1.04	0.99	1.13
Dowel Str	7.63	7.31	6.40	6.19	6.98	7.07	6.65	7.70
Abt-Pas Stf	30.4	36.3	21.6	41.4	47.7	24.8	45.2	33.5
Pile Stf	67.1	22.1	53.5	68.5	55.2	30.2	42.8	33.9
Mass	113	123	136	117	118	134	127	132
Damp Ratio	0.037	0.047	0.024	0.042	0.057	0.034	0.064	0.051
Small Gap	1.21	1.74	0.01	0.83	1.78	1.27	0.33	0.52
Load Dir	329	131	6	228	311	142	49	224

Table C-8: MS RC Slab parameter for geometric sample 8

	Brdge Sample 8							
	1	2	3	4	5	6	7	8
Conc Str	3239	5196	4455	3733	5699	4225	4924	4530
Reinf Str	49767	47536	58693	61042	51875	54584	57794	56106
COF MF	1.26	0.87	1.00	0.96	0.93	1.04	1.03	1.09
Dowel Str	7.13	7.16	6.20	6.70	7.56	6.82	8.34	6.42
Abt-Pas Stf	31.0	33.7	43.2	41.1	35.1	25.2	22.5	46.5
Pile Stf	51.1	68.2	30.4	37.2	21.6	44.8	58.1	67.2
Mass	117	131	119	133	124	128	138	113
Damp Ratio	0.057	0.047	0.070	0.045	0.053	0.020	0.040	0.035
Small Gap	1.72	1.33	0.12	1.86	1.05	0.30	0.87	0.68
Load Dir	314	5	234	120	150	77	318	212

Table C-9: MS RC Girder parameter for geometric sample 1

	Bridge Sample 1							
	1	2	3	4	5	6	7	8
Conc Str	5580	3958	5032	5103	4598	3470	3830	4354
Reinf Str	63265	56497	53575	54845	47029	60568	51862	49629
COF MF	0.96	1.07	0.88	1.13	0.98	1.00	1.07	0.92
Dowel Str	6.30	6.89	6.42	6.74	7.48	7.77	7.32	7.04
Abt-Pas Stf	21.2	44.8	37.4	23.8	31.1	46.7	31.6	39.5
Pile Stf	23.5	42.1	35.7	55.0	62.0	31.5	70.2	53.0
Mass	130	135	117	138	121	125	110	125
Damp Ratio	0.033	0.063	0.029	0.040	0.047	0.058	0.042	0.052
Small Gap	1.62	1.98	1.05	0.80	0.32	0.71	1.34	0.12
Load Dir	203	70	160	346	22	112	278	234

Table C-10: MS RC Girder parameter for geometric sample 2

	Bridge Sample 2							
	1	**2**	**3**	**4**	**5**	**6**	**7**	**8**
Conc Str	4723	5908	5131	3991	4484	3785	3172	4941
Reinf Str	48304	60077	55571	50954	51681	60952	54703	56799
COF MF	1.15	0.89	0.88	1.01	0.96	1.08	1.04	1.00
Dowel Str	7.81	6.38	6.71	7.17	7.56	7.06	5.81	6.94
Abt-Pas Stf	47.1	23.1	39.3	23.8	44.3	27.9	36.5	34.4
Pile Stf	33.0	53.4	42.8	57.8	25.6	64.7	39.6	74.6
Mass	130	137	115	118	113	122	135	128
Damp Ratio	0.053	0.071	0.046	0.030	0.043	0.056	0.032	0.039
Small Gap	0.73	0.84	1.83	1.32	0.28	1.50	1.06	0.10
Load Dir	111	13	66	180	170	265	310	357

Table C-11: MS RC Girder parameter for geometric sample 3

	Bridge Sample 3							
	1	**2**	**3**	**4**	**5**	**6**	**7**	**8**
Conc Str	4620	3070	4220	4335	3799	5453	5813	5010
Reinf Str	61825	57218	50552	48025	56154	52469	53481	58431
COF MF	0.93	0.92	1.10	1.07	0.87	1.00	1.17	1.01
Dowel Str	7.62	6.97	7.13	6.49	6.64	7.30	8.17	6.34
Abt-Pas Stf	21.7	45.1	49.4	36.4	27.5	41.9	26.5	33.5
Pile Stf	39.5	28.5	55.3	52.0	42.8	66.1	23.2	69.3
Mass	137	125	115	128	121	111	135	130
Damp Ratio	0.043	0.038	0.036	0.049	0.058	0.068	0.046	0.026
Small Gap	1.83	0.88	0.45	1.48	1.54	0.71	0.21	1.08
Load Dir	10	130	257	169	291	356	72	220

Table C-12: MS RC Girder parameter for geometric sample 4

	Bridge Sample 4							
	1	**2**	**3**	**4**	**5**	**6**	**7**	**8**
Conc Str	3989	5160	3457	3736	4681	5765	4393	4941
Reinf Str	58601	55434	54113	52846	46407	51170	67862	56748
COF MF	1.12	0.83	1.10	1.01	0.99	1.06	0.91	0.95
Dowel Str	7.65	7.32	6.89	6.47	6.33	6.78	7.10	8.38
Abt-Pas Stf	42.2	31.3	25.1	22.9	29.7	49.5	37.7	45.3
Pile Stf	33.4	72.6	35.6	21.4	64.4	42.8	48.2	60.9
Mass	125	132	121	127	136	110	117	140
Damp Ratio	0.032	0.051	0.047	0.038	0.060	0.044	0.054	0.022
Small Gap	0.88	0.16	1.55	1.05	1.83	1.47	0.49	0.61
Load Dir	75	228	354	192	106	278	27	146

Table C-13: MS RC Girder parameter for geometric sample 5

	Bridge Sample 5							
	1	**2**	**3**	**4**	**5**	**6**	**7**	**8**
Conc Str	2413	4620	4848	4061	4493	5275	5690	3738
Reinf Str	58882	52927	62009	49260	50820	56921	53356	55072
COF MF	1.01	1.08	1.04	0.79	0.99	0.92	0.94	1.16
Dowel Str	6.21	7.57	6.85	6.65	6.53	7.10	7.90	7.30
Abt-Pas Stf	23.9	43.4	31.2	39.9	47.4	21.3	36.7	34.2
Pile Stf	34.4	48.1	57.2	45.2	62.3	23.8	68.8	33.5
Mass	119	112	117	123	136	130	127	140
Damp Ratio	0.058	0.047	0.050	0.043	0.041	0.034	0.067	0.027
Small Gap	1.34	0.61	1.64	1.93	1.12	0.81	0.31	0.11
Load Dir	326	131	195	247	82	273	153	25

Table C-14: MS RC Girder parameter for geometric sample 6

	Bridge Sample 6							
	1	**2**	**3**	**4**	**5**	**6**	**7**	**8**
Conc Str	4032	5282	3666	6073	4497	4625	3361	4786
Reinf Str	47417	56887	58767	52203	61690	54214	55427	51382
COF MF	0.96	0.99	1.11	1.04	0.91	1.22	1.03	0.86
Dowel Str	6.23	7.14	7.31	7.65	6.39	7.41	6.78	6.88
Abt-Pas Stf	41.7	36.7	28.4	26.2	48.3	43.9	20.3	34.4
Pile Stf	24.6	55.7	47.5	27.0	67.3	45.9	40.5	70.8
Mass	126	130	117	123	138	110	133	118
Damp Ratio	0.039	0.054	0.033	0.044	0.049	0.061	0.026	0.046
Small Gap	0.96	1.05	1.34	0.32	0.05	0.73	1.76	1.63
Load Dir	279	84	23	123	253	195	172	347

Table C-15: MS RC Girder parameter for geometric sample 7

	Bridge Sample 7							
	1	**2**	**3**	**4**	**5**	**6**	**7**	**8**
Conc Str	3961	3713	4611	4812	5460	5539	4391	3503
Reinf Str	55734	57021	65656	60106	51421	48480	52000	54427
COF MF	1.04	0.85	0.90	0.99	1.21	1.10	0.95	1.01
Dowel Str	6.32	7.52	7.33	7.72	7.02	6.59	6.83	6.76
Abt-Pas Stf	48.1	41.8	29.6	26.9	32.2	37.4	20.2	46.2
Pile Stf	24.9	53.1	34.3	60.8	43.5	63.7	29.3	69.1
Mass	119	124	131	126	113	139	134	116
Damp Ratio	0.034	0.041	0.041	0.052	0.069	0.030	0.057	0.048
Small Gap	0.71	1.29	1.55	1.93	0.19	0.42	0.79	1.04
Load Dir	274	135	106	265	88	332	19	182

Table C-16: MS RC Girder parameter for geometric sample 8

	Bridge Sample 8							
	1	**2**	**3**	**4**	**5**	**6**	**7**	**8**
Conc Str	4694	3018	3958	3568	4299	5354	4859	6313
Reinf Str	54033	56942	51790	59186	51066	60762	56297	48469
COF MF	0.76	1.03	1.25	1.10	0.96	0.99	0.92	1.04
Dowel Str	6.93	7.02	5.84	6.76	7.22	7.41	6.38	7.70
Abt-Pas Stf	24.6	29.4	22.2	47.7	35.5	32.5	40.5	45.1
Pile Stf	61.2	33.7	40.0	52.6	68.0	72.1	45.2	23.2
Mass	129	139	128	111	115	136	118	123
Damp Ratio	0.050	0.034	0.045	0.039	0.027	0.064	0.044	0.054
Small Gap	1.13	1.38	1.88	0.44	0.23	0.73	0.78	1.69
Load Dir	121	5	259	76	342	283	219	141

Table C-17: MS Steel Girder parameter for geometric sample 1

	Bridge Sample 1							
	1	**2**	**3**	**4**	**5**	**6**	**7**	**8**
Conc Str	4528	5820	4225	4333	3847	3172	4849	5213
Reinf Str	60568	45085	57684	53239	49924	56127	53439	66973
Steel Fix-Long	455	703	492	948	959	1144	781	589
Steel Fix-Trans	156	124	62	93	100	132	77	167
Steel Rocker	0.044	0.116	0.079	0.060	0.105	0.097	0.087	0.067
Steel Sliding	0.390	0.419	0.587	0.272	0.503	0.214	0.316	0.452
Abt-Pas Stf	36.0	48.9	42.2	31.9	26.0	20.8	45.6	30.8
Pile Stf	20.9	67.6	27.0	48.0	57.4	44.5	38.3	70.0
Mass	137	114	120	132	112	126	134	123
Damp Ratio	0.041	0.047	0.045	0.034	0.054	0.066	0.053	0.025
Large Gap	5.26	4.11	2.26	1.16	3.43	5.09	0.61	1.63
Load Dir	273	323	148	237	95	87	210	45

Table C-18: MS Steel Girder parameter for geometric sample 2

	Bridge Sample 2							
	1	**2**	**3**	**4**	**5**	**6**	**7**	**8**
Conc Str	3547	5490	5063	4086	2701	5362	4544	4281
Reinf Str	52335	58206	45535	64328	53743	57475	54803	51441
Steel Fix-Long	1018	815	1091	751	870	608	558	424
Steel Fix-Trans	158	130	74	115	69	92	105	144
Steel Rocker	0.106	0.067	0.051	0.082	0.045	0.119	0.074	0.098
Steel Sliding	0.297	0.360	0.216	0.403	0.595	0.455	0.325	0.519
Abt-Pas Stf	48.1	31.2	43.7	20.2	24.2	42.1	37.4	34.1
Pile Stf	63.3	33.8	25.8	33.0	55.0	44.2	48.5	69.4
Mass	112	130	134	127	121	138	125	115
Damp Ratio	0.043	0.056	0.026	0.052	0.059	0.040	0.032	0.049
Large Gap	3.37	0.50	2.87	1.78	4.82	5.44	4.38	1.23
Load Dir	207	140	103	34	326	77	303	270

Table C-19: MS Steel Girder parameter for geometric sample 3

	Bridge Sample 3							
	1	**2**	**3**	**4**	**5**	**6**	**7**	**8**
Conc Str	6085	4950	4385	3605	2787	4646	5302	3951
Reinf Str	58724	42885	50579	55665	54468	63982	57947	52657
Steel Fix-Long	827	446	1093	491	746	892	966	650
Steel Fix-Trans	100	132	164	109	85	123	68	154
Steel Rocker	0.115	0.098	0.042	0.083	0.102	0.062	0.075	0.057
Steel Sliding	0.557	0.347	0.402	0.245	0.273	0.380	0.545	0.464
Abt-Pas Stf	39.0	21.9	44.2	49.2	34.6	31.0	24.4	35.9
Pile Stf	43.5	26.3	63.6	60.9	50.5	35.7	71.6	29.5
Mass	122	113	119	127	137	134	131	116
Damp Ratio	0.047	0.041	0.075	0.056	0.035	0.026	0.038	0.052
Large Gap	4.11	4.94	2.84	5.36	1.60	3.54	1.04	0.17
Load Dir	65	101	142	217	274	40	326	237

Table C-20: MS Steel Girder parameter for geometric sample 4

	Bridge Sample 4							
	1	2	3	4	5	6	7	8
Conc Str	4173	5719	2789	4550	4827	5175	4268	3628
Reinf Str	55544	51683	57408	59076	62232	50159	54172	45434
Steel Fix-Long	824	695	871	1047	1134	491	438	630
Steel Fix-Trans	86	64	137	114	167	76	100	147
Steel Rocker	0.071	0.054	0.083	0.063	0.046	0.097	0.120	0.105
Steel Sliding	0.390	0.430	0.306	0.487	0.252	0.519	0.242	0.559
Abt-Pas Stf	29.3	39.1	46.3	21.6	27.1	35.3	44.0	31.7
Pile Stf	67.5	59.8	45.8	25.3	35.8	49.2	71.2	29.9
Mass	134	113	127	130	122	115	120	138
Damp Ratio	0.029	0.056	0.034	0.044	0.051	0.039	0.048	0.063
Large Gap	4.92	1.80	5.46	0.99	0.59	3.69	4.29	2.35
Load Dir	109	318	276	82	172	214	236	36

Table C-21: MS Steel Girder parameter for geometric sample 5

	Bridge Sample 5							
	1	2	3	4	5	6	7	8
Conc Str	4494	4551	3865	5397	5014	2998	6142	4144
Reinf Str	49105	51031	54780	56438	55141	58696	53035	63777
Steel Fix-Long	896	748	423	654	1061	1044	828	518
Steel Fix-Trans	68	154	97	112	168	115	142	72
Steel Rocker	0.063	0.059	0.045	0.098	0.102	0.081	0.078	0.111
Steel Sliding	0.491	0.338	0.218	0.410	0.507	0.380	0.294	0.596
Abt-Pas Stf	21.2	46.1	34.3	42.3	24.2	46.9	30.8	37.2
Pile Stf	68.3	63.8	33.3	58.7	53.2	45.9	26.5	34.4
Mass	116	129	137	123	119	134	114	126
Damp Ratio	0.053	0.022	0.033	0.063	0.039	0.056	0.043	0.049
Large Gap	2.74	1.09	5.65	4.77	3.36	0.14	2.18	4.15
Load Dir	244	118	35	279	218	158	89	352

Table C-22: MS Steel Girder parameter for geometric sample 6

	Bridge Sample 6							
	1	**2**	**3**	**4**	**5**	**6**	**7**	**8**
Conc Str	4527	4916	4293	3490	6065	4039	3881	5201
Reinf Str	54110	63060	43998	52908	54963	58129	50949	58663
Steel Fix-Long	431	985	871	568	756	1085	596	766
Steel Fix-Trans	97	73	103	151	71	169	124	130
Steel Rocker	0.112	0.065	0.095	0.079	0.081	0.103	0.052	0.043
Steel Sliding	0.394	0.350	0.592	0.273	0.424	0.231	0.484	0.550
Abt-Pas Stf	21.2	38.5	31.1	26.4	34.7	42.9	46.8	41.0
Pile Stf	31.4	24.9	68.9	52.9	46.6	57.7	61.9	37.9
Mass	117	125	111	121	130	138	135	126
Damp Ratio	0.049	0.062	0.014	0.059	0.047	0.041	0.034	0.042
Large Gap	3.23	5.10	3.78	0.22	1.37	1.92	5.53	2.30
Load Dir	65	307	241	92	201	338	144	41

Table C-23: MS Steel Girder parameter for geometric sample 7

	Bridge Sample 7							
	1	**2**	**3**	**4**	**5**	**6**	**7**	**8**
Conc Str	4698	5747	3306	4222	5254	4277	3837	5058
Reinf Str	63370	52091	56488	49499	42456	53414	58448	55088
Steel Fix-Long	442	1122	655	513	830	673	909	981
Steel Fix-Trans	140	145	113	165	95	75	127	60
Steel Rocker	0.057	0.065	0.046	0.093	0.114	0.103	0.085	0.076
Steel Sliding	0.508	0.361	0.301	0.494	0.580	0.425	0.287	0.248
Abt-Pas Stf	30.4	36.3	21.6	41.4	47.7	24.8	45.2	33.5
Pile Stf	67.1	22.1	53.5	68.5	55.2	30.2	42.8	33.9
Mass	113	123	136	117	118	134	127	132
Damp Ratio	0.037	0.047	0.024	0.042	0.057	0.034	0.064	0.051
Large Gap	2.15	4.16	3.32	5.41	0.44	2.60	4.56	0.83
Load Dir	329	131	6	228	311	142	49	224

Table C-24: MS Steel Girder parameter for geometric sample 8

	Brdge Sample 8							
	1	**2**	**3**	**4**	**5**	**6**	**7**	**8**
Conc Str	3239	5196	4455	3733	5699	4225	4924	4530
Reinf Str	49767	47536	58693	61042	51875	54584	57794	56106
Steel Fix-Long	549	982	849	1076	401	694	637	900
Steel Fix-Trans	94	168	83	132	154	121	110	65
Steel Rocker	0.043	0.073	0.083	0.051	0.115	0.106	0.063	0.096
Steel Sliding	0.496	0.287	0.428	0.518	0.365	0.550	0.203	0.345
Abt-Pas Stf	31.0	33.7	43.2	41.1	35.1	25.2	22.5	46.5
Pile Stf	51.1	68.2	30.4	37.2	21.6	44.8	58.1	67.2
Mass	117	131	119	133	124	128	138	113
Damp Ratio	0.057	0.047	0.070	0.045	0.053	0.020	0.040	0.035
Large Gap	5.46	4.25	3.55	0.62	1.00	1.85	4.63	2.80
Load Dir	314	5	234	120	150	77	318	212

Table C-25: MC Steel Girder parameter for geometric sample 1

	Bridge Sample 1							
	1	**2**	**3**	**4**	**5**	**6**	**7**	**8**
Conc Str	4528	5820	4225	4333	3847	3172	4849	5213
Reinf Str	60568	45085	57684	53239	49924	56127	53439	66973
Steel Fix-Long	455	703	492	948	959	1144	781	589
Steel Fix-Trans	156	124	62	93	100	132	77	167
Steel Rocker	0.044	0.116	0.079	0.060	0.105	0.097	0.087	0.067
Steel Sliding	0.390	0.419	0.587	0.272	0.503	0.214	0.316	0.452
Abt-Pas Stf	36.0	48.9	42.2	31.9	26.0	20.8	45.6	30.8
Pile Stf	20.9	67.6	27.0	48.0	57.4	44.5	38.3	70.0
Mass	137	114	120	132	112	126	134	123
Damp Ratio	0.041	0.047	0.045	0.034	0.054	0.066	0.053	0.025
Large Gap	5.26	4.11	2.26	1.16	3.43	5.09	0.61	1.63
Load Dir	273	323	148	237	95	87	210	45

Table C-26: MC Steel Girder parameter for geometric sample 2

	Bridge Sample 2							
	1	**2**	**3**	**4**	**5**	**6**	**7**	**8**
Conc Str	3547	5490	5063	4086	2701	5362	4544	4281
Reinf Str	52335	58206	45535	64328	53743	57475	54803	51441
Steel Fix-Long	1018	815	1091	751	870	608	558	424
Steel Fix-Trans	158	130	74	115	69	92	105	144
Steel Rocker	0.106	0.067	0.051	0.082	0.045	0.119	0.074	0.098
Steel Sliding	0.297	0.360	0.216	0.403	0.595	0.455	0.325	0.519
Abt-Pas Stf	48.1	31.2	43.7	20.2	24.2	42.1	37.4	34.1
Pile Stf	63.3	33.8	25.8	33.0	55.0	44.2	48.5	69.4
Mass	112	130	134	127	121	138	125	115
Damp Ratio	0.043	0.056	0.026	0.052	0.059	0.040	0.032	0.049
Large Gap	3.37	0.50	2.87	1.78	4.82	5.44	4.38	1.23
Load Dir	207	140	103	34	326	77	303	270

Table C-27: MC Steel Girder parameter for geometric sample 3

	Bridge Sample 3							
	1	**2**	**3**	**4**	**5**	**6**	**7**	**8**
Conc Str	6085	4950	4385	3605	2787	4646	5302	3951
Reinf Str	58724	42885	50579	55665	54468	63982	57947	52657
Steel Fix-Long	827	446	1093	491	746	892	966	650
Steel Fix-Trans	100	132	164	109	85	123	68	154
Steel Rocker	0.115	0.098	0.042	0.083	0.102	0.062	0.075	0.057
Steel Sliding	0.557	0.347	0.402	0.245	0.273	0.380	0.545	0.464
Abt-Pas Stf	39.0	21.9	44.2	49.2	34.6	31.0	24.4	35.9
Pile Stf	43.5	26.3	63.6	60.9	50.5	35.7	71.6	29.5
Mass	122	113	119	127	137	134	131	116
Damp Ratio	0.047	0.041	0.075	0.056	0.035	0.026	0.038	0.052
Large Gap	4.11	4.94	2.84	5.36	1.60	3.54	1.04	0.17
Load Dir	65	101	142	217	274	40	326	237

Table C-28: MC Steel Girder parameter for geometric sample 4

	Bridge Sample 4							
	1	2	3	4	5	6	7	8
Conc Str	4173	5719	2789	4550	4827	5175	4268	3628
Reinf Str	55544	51683	57408	59076	62232	50159	54172	45434
Steel Fix-Long	824	695	871	1047	1134	491	438	630
Steel Fix-Trans	86	64	137	114	167	76	100	147
Steel Rocker	0.071	0.054	0.083	0.063	0.046	0.097	0.120	0.105
Steel Sliding	0.390	0.430	0.306	0.487	0.252	0.519	0.242	0.559
Abt-Pas Stf	29.3	39.1	46.3	21.6	27.1	35.3	44.0	31.7
Pile Stf	67.5	59.8	45.8	25.3	35.8	49.2	71.2	29.9
Mass	134	113	127	130	122	115	120	138
Damp Ratio	0.029	0.056	0.034	0.044	0.051	0.039	0.048	0.063
Large Gap	4.92	1.80	5.46	0.99	0.59	3.69	4.29	2.35
Load Dir	109	318	276	82	172	214	236	36

Table C-29: MC Steel Girder parameter for geometric sample 5

	Bridge Sample 5							
	1	2	3	4	5	6	7	8
Conc Str	4494	4551	3865	5397	5014	2998	6142	4144
Reinf Str	49105	51031	54780	56438	55141	58696	53035	63777
Steel Fix-Long	896	748	423	654	1061	1044	828	518
Steel Fix-Trans	68	154	97	112	168	115	142	72
Steel Rocker	0.063	0.059	0.045	0.098	0.102	0.081	0.078	0.111
Steel Sliding	0.491	0.338	0.218	0.410	0.507	0.380	0.294	0.596
Abt-Pas Stf	21.2	46.1	34.3	42.3	24.2	46.9	30.8	37.2
Pile Stf	68.3	63.8	33.3	58.7	53.2	45.9	26.5	34.4
Mass	116	129	137	123	119	134	114	126
Damp Ratio	0.053	0.022	0.033	0.063	0.039	0.056	0.043	0.049
Large Gap	2.74	1.09	5.65	4.77	3.36	0.14	2.18	4.15
Load Dir	244	118	35	279	218	158	89	352

Table C-30: MC Steel Girder parameter for geometric sample 6

	Bridge Sample 6							
	1	**2**	**3**	**4**	**5**	**6**	**7**	**8**
Conc Str	4527	4916	4293	3490	6065	4039	3881	5201
Reinf Str	54110	63060	43998	52908	54963	58129	50949	58663
Steel Fix-Long	431	985	871	568	756	1085	596	766
Steel Fix-Trans	97	73	103	151	71	169	124	130
Steel Rocker	0.112	0.065	0.095	0.079	0.081	0.103	0.052	0.043
Steel Sliding	0.394	0.350	0.592	0.273	0.424	0.231	0.484	0.550
Abt-Pas Stf	21.2	38.5	31.1	26.4	34.7	42.9	46.8	41.0
Pile Stf	31.4	24.9	68.9	52.9	46.6	57.7	61.9	37.9
Mass	117	125	111	121	130	138	135	126
Damp Ratio	0.049	0.062	0.014	0.059	0.047	0.041	0.034	0.042
Large Gap	3.23	5.10	3.78	0.22	1.37	1.92	5.53	2.30
Load Dir	65	307	241	92	201	338	144	41

Table C-31: MC Steel Girder parameter for geometric sample 7

	Bridge Sample 7							
	1	**2**	**3**	**4**	**5**	**6**	**7**	**8**
Conc Str	4698	5747	3306	4222	5254	4277	3837	5058
Reinf Str	63370	52091	56488	49499	42456	53414	58448	55088
Steel Fix-Long	442	1122	655	513	830	673	909	981
Steel Fix-Trans	140	145	113	165	95	75	127	60
Steel Rocker	0.057	0.065	0.046	0.093	0.114	0.103	0.085	0.076
Steel Sliding	0.508	0.361	0.301	0.494	0.580	0.425	0.287	0.248
Abt-Pas Stf	30.4	36.3	21.6	41.4	47.7	24.8	45.2	33.5
Pile Stf	67.1	22.1	53.5	68.5	55.2	30.2	42.8	33.9
Mass	113	123	136	117	118	134	127	132
Damp Ratio	0.037	0.047	0.024	0.042	0.057	0.034	0.064	0.051
Large Gap	2.15	4.16	3.32	5.41	0.44	2.60	4.56	0.83
Load Dir	329	131	6	228	311	142	49	224

Table C-32: MC Steel Girder parameter for geometric sample 8

	Bridge Sample 8							
	1	**2**	**3**	**4**	**5**	**6**	**7**	**8**
Conc Str	3239	5196	4455	3733	5699	4225	4924	4530
Reinf Str	49767	47536	58693	61042	51875	54584	57794	56106
Steel Fix-Long	549	982	849	1076	401	694	637	900
Steel Fix-Trans	94	168	83	132	154	121	110	65
Steel Rocker	0.043	0.073	0.083	0.051	0.115	0.106	0.063	0.096
Steel Sliding	0.496	0.287	0.428	0.518	0.365	0.550	0.203	0.345
Abt-Pas Stf	31.0	33.7	43.2	41.1	35.1	25.2	22.5	46.5
Pile Stf	51.1	68.2	30.4	37.2	21.6	44.8	58.1	67.2
Mass	117	131	119	133	124	128	138	113
Damp Ratio	0.057	0.047	0.070	0.045	0.053	0.020	0.040	0.035
Large Gap	5.46	4.25	3.55	0.62	1.00	1.85	4.63	2.80
Load Dir	314	5	234	120	150	77	318	212

Table C-33: MC RC Slab parameter for geometric sample 1

	Bridge Sample 1							
	1	**2**	**3**	**4**	**5**	**6**	**7**	**8**
Conc Str	5533	4871	3382	3846	4353	4663	5158	4116
Reinf Str	52786	50560	54011	55556	44698	56812	61025	58578
COF MF	1.01	0.97	1.04	1.00	1.29	1.11	0.92	0.89
Dowel Str	6.80	7.30	7.06	6.83	7.63	7.69	6.32	6.41
Abt-Pas Stf	23.5	44.8	31.2	47.8	32.9	42.5	36.5	26.1
Pile Stf	44.5	35.4	68.1	52.6	20.8	33.4	65.8	56.2
Mass	112	137	133	119	129	125	123	116
Damp Ratio	0.045	0.032	0.057	0.053	0.047	0.024	0.038	0.062
Small Gap	0.48	1.45	1.10	0.93	1.81	1.67	0.06	0.69
Load Dir	308	192	122	165	90	245	340	38

Table C-34: MC RC Slab parameter for geometric sample 2

	Bridge Sample 2							
	1	**2**	**3**	**4**	**5**	**6**	**7**	**8**
Conc Str	5444	2633	3568	5600	4093	4829	4533	4320
Reinf Str	56470	50435	62754	52909	54856	59628	47971	53515
COF MF	1.03	1.00	0.94	0.91	1.07	0.88	1.21	1.10
Dowel Str	6.63	7.43	6.88	6.98	5.94	7.17	7.80	6.53
Abt-Pas Stf	44.6	39.3	32.5	36.9	29.9	24.9	49.6	23.6
Pile Stf	39.6	71.4	33.7	24.0	66.6	56.7	50.9	43.4
Mass	132	135	122	111	120	140	127	117
Damp Ratio	0.049	0.045	0.034	0.067	0.019	0.037	0.046	0.055
Small Gap	0.53	1.79	1.53	1.48	0.82	0.46	0.04	1.07
Load Dir	103	285	219	36	49	140	253	349

Table C-35: MC RC Slab parameter for geometric sample 3

	Bridge Sample 3							
	1	**2**	**3**	**4**	**5**	**6**	**7**	**8**
Conc Str	5493	5223	4780	3913	4450	3179	4596	4132
Reinf Str	61067	50070	55086	54111	60443	53010	57683	49239
COF MF	1.10	0.93	0.84	0.94	1.02	1.13	1.03	0.99
Dowel Str	6.96	7.61	7.16	6.17	6.80	6.60	8.26	7.00
Abt-Pas Stf	47.3	40.7	35.6	45.9	23.7	26.2	29.4	34.2
Pile Stf	71.9	20.2	37.4	44.1	33.6	53.1	62.0	58.6
Mass	121	111	120	140	134	116	127	129
Damp Ratio	0.051	0.036	0.070	0.040	0.028	0.057	0.049	0.043
Small Gap	1.51	0.01	1.49	0.68	0.98	1.04	1.90	0.35
Load Dir	282	62	11	347	171	106	183	234

Table C-36: MC RC Slab parameter for geometric sample 4

	Bridge Sample 4							
	1	**2**	**3**	**4**	**5**	**6**	**7**	**8**
Conc Str	4581	2751	3674	5178	4800	4343	4136	5480
Reinf Str	59270	47888	52311	56391	54252	51107	62313	55173
COF MF	1.07	1.18	0.96	0.86	0.99	1.09	1.01	0.91
Dowel Str	7.62	7.03	8.11	6.91	7.30	6.65	5.38	6.46
Abt-Pas Stf	49.9	34.6	46.1	30.6	39.4	21.7	38.1	24.0
Pile Stf	53.3	55.9	23.3	44.6	39.9	29.4	74.1	64.1
Mass	120	129	121	114	133	112	137	129
Damp Ratio	0.055	0.060	0.041	0.019	0.042	0.051	0.047	0.033
Small Gap	0.85	0.64	1.49	1.15	1.61	0.23	0.45	1.81
Load Dir	14	299	345	105	199	169	73	261

Table C-37: MC RC Slab parameter for geometric sample 5

	Bridge Sample 5							
	1	**2**	**3**	**4**	**5**	**6**	**7**	**8**
Conc Str	4567	2484	3736	4356	4034	5548	5390	4857
Reinf Str	52463	59204	51536	46420	53627	55424	57453	62835
COF MF	0.90	1.04	0.94	1.21	0.88	1.09	1.00	1.02
Dowel Str	7.98	6.50	7.02	7.63	6.03	7.22	6.72	6.88
Abt-Pas Stf	43.1	26.6	28.4	22.7	33.7	41.3	38.5	49.7
Pile Stf	63.3	43.5	68.9	34.0	21.0	52.2	56.7	27.5
Mass	136	118	131	110	138	117	124	128
Damp Ratio	0.037	0.022	0.038	0.048	0.062	0.053	0.042	0.057
Small Gap	0.16	1.13	1.39	0.44	0.96	1.93	1.66	0.69
Load Dir	276	85	140	342	32	191	258	111

Table C-38: MC RC Slab parameter for geometric sample 6

	Bridge Sample 6							
	1	**2**	**3**	**4**	**5**	**6**	**7**	**8**
Conc Str	3608	2451	4718	4359	4149	4943	6099	5312
Reinf Str	57201	50981	47986	52783	58849	60937	54339	55592
COF MF	1.12	0.89	0.99	0.91	1.00	0.95	1.09	1.04
Dowel Str	6.66	7.21	6.90	6.35	6.59	7.01	7.45	8.62
Abt-Pas Stf	22.2	47.5	31.1	36.0	38.8	33.6	44.3	24.6
Pile Stf	57.5	32.6	68.8	64.2	21.1	47.7	35.1	43.7
Mass	129	114	112	120	129	134	138	124
Damp Ratio	0.052	0.059	0.042	0.032	0.049	0.068	0.037	0.030
Small Gap	1.99	0.15	1.03	0.65	0.81	0.31	1.69	1.27
Load Dir	244	23	324	70	313	136	191	109

Table C-39: MC RC Slab parameter for geometric sample 7

	Bridge Sample 7							
	1	**2**	**3**	**4**	**5**	**6**	**7**	**8**
Conc Str	4317	5024	3781	3151	4620	5606	4011	5105
Reinf Str	50702	45183	61666	53886	53095	56321	58000	59390
COF MF	0.89	1.03	1.07	0.99	1.18	0.92	1.11	0.95
Dowel Str	7.24	6.79	7.62	7.13	7.67	6.84	6.45	5.63
Abt-Pas Stf	34.2	38.1	39.0	42.9	22.3	27.0	30.7	50.0
Pile Stf	22.7	48.0	54.9	61.3	45.7	34.1	74.2	27.8
Mass	139	123	131	114	121	127	136	113
Damp Ratio	0.030	0.056	0.044	0.049	0.051	0.040	0.033	0.077
Small Gap	1.28	1.22	1.79	1.54	0.39	0.72	0.23	0.96
Load Dir	70	157	259	25	219	111	297	358

Table C-40: MC RC Slab parameter for geometric sample 8

	Bridge Sample 8							
	1	2	3	4	5	6	7	8
Conc Str	4437	3831	4190	6211	3297	4775	5121	4571
Reinf Str	46036	62741	57933	49775	54470	59815	55885	51816
COF MF	0.84	0.97	0.93	1.03	0.94	1.14	1.07	1.11
Dowel Str	7.64	6.22	6.76	7.07	7.18	8.06	6.87	6.61
Abt-Pas Stf	25.1	33.0	40.6	36.1	29.8	21.4	48.8	45.9
Pile Stf	22.0	38.1	30.0	51.9	41.0	65.1	60.5	69.1
Mass	133	121	132	124	117	112	125	138
Damp Ratio	0.054	0.039	0.030	0.032	0.052	0.046	0.065	0.043
Small Gap	0.70	0.91	0.20	1.75	1.95	1.39	0.33	1.13
Load Dir	274	195	115	7	72	249	340	165

Table C-41: SS PC Girder parameter for geometric sample 1

	Bridge Sample 1							
	1	2	3	4	5	6	7	8
Conc Str	3894	3937	4334	5401	3278	4531	4904	5767
Reinf Str	59779	55321	51054	57668	48356	51937	62575	53885
Elasto Shear Mod	187	258	237	145	105	148	288	208
Elasto MF	1.12	0.85	1.16	1.02	0.92	1.00	1.06	0.94
Dowel Str	19.64	22.76	19.98	18.19	19.19	21.46	20.75	18.38
Dowel Gap	0.180	1.936	1.150	2.427	1.505	0.934	2.336	0.537
Abt-Pas Stf	42.5	49.2	20.7	26.1	33.3	30.8	39.6	37.0
Pile Stf	58.1	21.5	28.1	43.2	38.1	48.3	66.4	74.5
Mass	115	112	124	129	128	133	120	137
Damp Ratio	0.060	0.044	0.045	0.017	0.036	0.038	0.053	0.059
Large Gap	4.11	3.12	0.83	5.30	4.91	1.68	0.05	2.39
Load Dir	278	30	69	105	333	219	269	174

Table C-42: SS PC Girder parameter for geometric sample 2

	Bridge Sample 2							
	1	**2**	**3**	**4**	**5**	**6**	**7**	**8**
Conc Str	4560	4055	4351	3347	4901	3526	5819	5184
Reinf Str	52046	54624	55522	49848	61229	48284	57636	60290
Elasto Shear Mod	142	117	183	157	257	292	239	215
Elasto MF	1.00	1.12	0.87	0.92	1.04	1.03	1.13	0.96
Dowel Str	22.88	19.79	21.21	21.03	20.42	18.45	17.48	19.16
Dowel Gap	1.248	1.901	0.171	1.406	2.679	2.290	0.490	0.864
Abt-Pas Stf	26.9	38.0	21.1	42.7	32.6	46.7	30.4	39.9
Pile Stf	52.7	70.5	24.4	64.8	58.5	45.2	38.8	28.5
Mass	137	116	129	125	112	124	136	118
Damp Ratio	0.045	0.033	0.041	0.027	0.037	0.050	0.066	0.054
Large Gap	5.68	3.88	0.29	2.10	3.14	0.76	2.89	4.61
Load Dir	315	183	290	139	61	235	19	126

Table C-43: SS PC Girder parameter for geometric sample 3

	Bridge Sample 3							
	1	**2**	**3**	**4**	**5**	**6**	**7**	**8**
Conc Str	3752	4483	5015	4678	5542	4217	3309	5200
Reinf Str	52450	46517	57945	61079	55508	54775	60179	51105
Elasto Shear Mod	111	141	160	232	202	174	297	257
Elasto MF	0.90	0.97	0.86	1.02	1.15	1.05	1.11	0.96
Dowel Str	21.23	18.19	17.83	18.91	20.82	19.49	20.21	22.71
Dowel Gap	0.511	2.464	1.064	2.158	1.587	0.929	1.825	0.041
Abt-Pas Stf	29.4	47.3	35.9	45.2	41.8	27.3	33.4	21.1
Pile Stf	65.5	28.5	41.2	49.6	54.6	39.8	70.6	24.2
Mass	138	123	134	119	115	128	111	130
Damp Ratio	0.055	0.039	0.066	0.041	0.027	0.031	0.049	0.051
Large Gap	1.64	3.49	0.38	1.41	4.07	4.86	2.73	5.35
Load Dir	13	300	254	198	319	168	92	57

Table C-44: SS PC Girder parameter for geometric sample 4

	Bridge Sample 4							
	1	**2**	**3**	**4**	**5**	**6**	**7**	**8**
Conc Str	5413	4295	3084	3786	5565	4760	5042	3944
Reinf Str	63053	52270	55486	50589	54348	56559	58299	45967
Elasto Shear Mod	232	250	293	133	200	194	101	170
Elasto MF	1.09	1.25	0.95	0.84	1.03	0.93	0.99	1.03
Dowel Str	20.13	21.25	18.41	20.82	17.61	19.66	23.51	19.14
Dowel Gap	1.714	0.902	2.349	1.189	0.309	2.049	0.367	2.416
Abt-Pas Stf	22.0	48.7	45.0	38.4	41.0	26.6	33.2	28.6
Pile Stf	26.6	68.6	47.2	37.4	31.1	50.7	54.4	61.9
Mass	128	113	137	130	123	114	134	120
Damp Ratio	0.053	0.056	0.028	0.046	0.032	0.043	0.070	0.040
Large Gap	4.60	1.27	1.94	5.39	4.22	0.43	2.93	3.25
Load Dir	111	233	156	78	344	307	29	216

Table C-45: SS PC Girder parameter for geometric sample 5

	Bridge Sample 5							
	1	**2**	**3**	**4**	**5**	**6**	**7**	**8**
Conc Str	4146	3825	5338	5065	4252	5662	4706	3198
Reinf Str	47748	52731	75355	55429	54521	51234	57870	59266
Elasto Shear Mod	251	138	105	277	160	207	237	195
Elasto MF	1.13	0.98	0.82	1.10	1.06	1.01	0.94	0.92
Dowel Str	21.51	19.67	19.06	18.30	17.86	20.11	21.88	20.99
Dowel Gap	2.119	2.749	1.842	0.755	0.603	1.697	0.253	1.340
Abt-Pas Stf	22.9	33.8	44.9	37.9	40.0	28.5	27.5	48.7
Pile Stf	42.1	64.4	60.6	68.9	52.6	23.7	31.5	35.4
Mass	121	127	134	137	130	117	114	125
Damp Ratio	0.044	0.048	0.020	0.041	0.035	0.051	0.055	0.065
Large Gap	1.24	0.59	5.80	3.68	5.14	2.76	4.05	2.13
Load Dir	321	15	212	240	61	140	95	300

Table C-46: SS PC Girder parameter for geometric sample 6

	Bridge Sample 6							
	1	**2**	**3**	**4**	**5**	**6**	**7**	**8**
Conc Str	3475	5266	3825	4659	4937	3969	5648	4496
Reinf Str	56827	61464	54872	60530	51947	47938	54358	51513
Elasto Shear Mod	279	232	188	154	264	120	132	216
Elasto MF	0.93	0.97	1.09	0.87	1.21	1.04	0.98	1.02
Dowel Str	17.95	21.42	22.74	18.50	19.01	19.88	20.03	20.54
Dowel Gap	1.891	0.707	2.650	0.558	2.367	0.012	1.226	1.690
Abt-Pas Stf	21.5	49.7	30.5	24.6	41.2	35.6	45.7	32.4
Pile Stf	67.7	56.6	36.9	23.3	73.2	48.5	41.8	33.6
Mass	123	136	139	132	112	126	119	114
Damp Ratio	0.024	0.042	0.034	0.052	0.054	0.046	0.037	0.083
Large Gap	2.34	3.82	5.04	0.65	6.00	2.01	1.10	3.13
Load Dir	89	247	103	284	140	193	3	360

Table C-47: SS PC Girder parameter for geometric sample 7

	Bridge Sample 7							
	1	**2**	**3**	**4**	**5**	**6**	**7**	**8**
Conc Str	5752	4419	4841	3023	4516	5260	3739	3995
Reinf Str	46900	70603	54438	58345	56746	52398	51470	56032
Elasto Shear Mod	151	276	186	132	198	111	269	227
Elasto MF	1.08	1.00	0.92	0.96	1.06	1.16	0.82	1.02
Dowel Str	19.43	20.86	20.16	19.50	21.81	21.96	18.07	18.33
Dowel Gap	2.000	0.665	2.196	1.478	0.993	2.717	0.138	1.096
Abt-Pas Stf	21.3	45.4	31.3	49.7	41.0	35.1	29.4	25.2
Pile Stf	51.0	57.7	34.9	44.7	72.2	20.3	65.8	32.8
Mass	115	132	111	121	138	133	126	124
Damp Ratio	0.034	0.040	0.057	0.030	0.048	0.042	0.064	0.050
Large Gap	0.16	5.37	3.23	5.19	1.65	2.90	4.07	1.07
Load Dir	338	170	233	292	40	119	53	219

Table C-48: SS PC Girder parameter for geometric sample 8

	Bridge Sample 8							
	1	**2**	**3**	**4**	**5**	**6**	**7**	**8**
Conc Str	4635	3916	4122	4405	5348	4988	2925	6313
Reinf Str	67937	56886	52075	55018	53940	45614	60526	50057
Elasto Shear Mod	222	132	235	284	259	161	194	102
Elasto MF	1.08	0.90	1.26	0.87	0.94	1.00	0.97	1.05
Dowel Str	18.93	21.22	19.65	19.95	16.97	20.47	22.29	18.65
Dowel Gap	1.622	0.942	0.156	1.189	2.479	1.764	2.136	0.354
Abt-Pas Stf	23.1	46.7	33.0	35.1	26.4	42.7	40.2	28.3
Pile Stf	64.3	28.6	44.0	60.4	52.5	34.3	22.8	71.3
Mass	123	120	129	126	115	136	110	138
Damp Ratio	0.010	0.067	0.037	0.053	0.037	0.045	0.054	0.044
Large Gap	1.18	5.94	2.17	0.02	3.32	4.89	2.52	4.34
Load Dir	216	347	167	296	68	93	7	257

Appendix D: As-Built Drawings

Table D-1: As-built drawing inventory

Bridge Class	NBI Structure #	Year Built	# of Spans	Max Span Length (ft)	Deck width (ft)
MS PC	1092004518125	1970	3	80	42
	21200013405027	1993	3	80	45
	61869914991318	1983	4	83	40
	161780032603016	1964	2	80	50
	180710017204204	2003	3	80	40
MS Steel	41070003005030	1939	3	40	45
	90500018401019	1950	3	40	45
	102120024506026	1939	4	48	60
	141500015004027	1942	4	40	50
MC Steel	30390135001006	1964	3	75	25
	41800009003052	1969	4	75	28
	121020050201008	1952	3	75	82
	1813300049501150	1964	4	86	25
	230470103902014	1959	3	90	25
	161290112201002	1949	3	90	25
	120200017902050	1958	3	240	46
	120200017902098	2007	3	240	40
	151310007205174	1971	34	150	42
	180570035304135	1975	17	150	44
	180570009214192	1971	4	115	26
	180570044202067	1965	3	115	48
MS RC Girder	32430221502001	1956	4	30	25
	52190078904002	1970	4	30	28
	102340049502017	1963	3	30	25
	30390082403007	1966	3	40	42
	141440033403048	1986	4	40	36
MS RC Slab	10920051001007	1955	3	25	25
	130760033408021	1947	2	25	25
	112030263701002	1963	4	25	25
	15083001706216	1968	3	25	42
	111740181001004	1956	4	25	43

REFERENCES

ACI. (2014). Building Code Requirments for Structural Concrete (ACI 318-14). American Concrete Institute, Committee 318.

ACI. (2016). Code Requirements for Seismic Evaluation and Retrofit of Existing Concrete Buildings. American Concrete Institute, Committee 369.

ASCE, 2013. Seismic Evaluation and Retrofit of Existing Buildings. s.l.:American Society of Civil Engineers.

Arsoy, Samy, et al. (1999). The Behavior of Integral Abutment Bridges. Virginia Transportation Research Council, 38 pgs.

ATC (1985). "Earthquake Damage Evaluation Data for California." Report No. ATC-13, Applied Technology Council.

Bavirisetty, R., Vinayagamoorthy, M., Duan, L. (2003). *Dynamic Analysis*, Bridge Engineering – Seismic Design, Edited by Wai-Fah Chen and Lian Duan, CRC Press LLC, Boca Raton, FL, ISBN: 0-8493-1683-9/02.

Berry, M. P., Eberhard, M. O. (2004). PEER Structural Performance Database User's Manual, Pacific Earthquake Engineering Research Center, University of California, Berkeley, CA.

Bournonville, Matt, Jason Dahnke, and David Darwin. Statistical Analysis of the Mechanical Properties and Weight of Reinforcing Bars. Tech. no. 04-1. N.p.: U of Kansas.

Caltrans (1999). Caltrans Structures Seismic Design References. California Department of Transportation, Sacramento, CA, first edition.

Caltrans (2007). Caltrans Seismic Design Criteria. California Department of Transportation, Sacramento, CA, version 1.7.

Choi, E. (2002). *Seismic Analysis and Retrofit of Mid-America Bridges*. PhD thesis, Georgia Institute of Technology.

Choi E, DesRoches R, Nielson B. (2004). Seismic fragility of typical bridges in moderate seismic zones. *Eng. Struct*., *26*(2):187–99.

Duenas-Osorio, L., Padgett, J. E. (2011). Seismic reliability assessment of bridges with user-defined system failure events, *Journal of Engineering Mechanics*, *137*(10), pp: 680-690.

Erberik, Murat Altug. (2015). "Seismic Fragility Analysis." *Encyclopedia of Earthquake Engineering*, pp. 1–10., doi:10.1007/978-3-642-36197-5_387-1.

Fang, J. Q., Li, Q. S., Jeary, A. P. and Liu, D. K. (1999), Damping of tall buildings: its evaluation and probabilistic characteristics. Struct. Design Tall Build., 8: 145–153. doi:10.1002/(SICI)1099-1794(199906)8:2<145::AID-TAL127>3.0.CO;2-1.

FEMA (2003). *HAZUS-MH MR4: Technical Manual*, Vol. Earthquake Model. Federal Emergency Management Agency, Washington DC.

FHWA (1994). *National Bridge Inspection Standards*. Report No. Sec. 650.301, Federal Highway Administration.

FHWA (1995). *Seismic Retrofitting Manual for Highway Bridges*, Vol. FHWA-RD-94-052. Office of Engineering and Highway Operations R&D, Federal Highway Administration, McLean, VA.

Frohlich, C., DeShon, H., Stump, B., Hayward, C., Hornbach, M., & Walter, J. (2016). A Historical Review of Induced Earthquakes in Texas. *Seismological Research Letters, 87*(4). Retrieved from https://www.jsg.utexas.edu/news/2016/05/humans-have-been-causingearthquakes-in-texas-since-the-1920s/

HAZUS-MH (2011). Multi-Hazard Loss Estimation Methodology: Earthquake Model HAZUS-MH MR5 Technical Manual, Federal Emergency Management Agency, Washington DC.

Huntington, D., & Lyrintzis, C. (1998). Improvements to and limitations of Latin hypercube sampling. Probabilistic Engineering Mechanics, 13(4), 245-253. doi:10.1016/s0266-8920(97)00013-1.

Hwang, H., Jernigan, J. B., and Lin, Y.-W. (2000). Evaluation of Seismic Damage to Memphis Bridges and Highway Systems. Journal of Bridge Engineering, 5(4), p 322–330.

Iman, R.L., Conover, W.J., 1982. A distribution-free approach to inducing rank correlation among input variables. Communications in Statistics B11, 311-334.

Kang, W.-H., Song, J., and Gardoni, P. (2008). Matrix-based system reliability method and applications to bridge networks. *Reliab. Eng. Syst. Saf.*, *93*(11), 1584–1593.

Karim, K. R. and Yamazaki, F (2003). A simplified method of constructing fragility curves for highway bridges, *Earthquake Engineering and Structural Dynamics*, *32*: 1603-1626

Mackie, K. and Stojadinovic, B. (2004). Fragility Curves for Reinforced Concrete Highway Overpass Bridges. *13th World Conference on Eartquake Engineering*, Vancouver, B.C. Canada.

Mander, J. B., Kim, D. K., Chen, S. S., and Premus, G. J. (1996). Response of Steel Bridge Bearings to the Reversed Cyclic Loading. *Report No. NCEER 96-0014*, NCEER.

Martin, G. R. and Yan, L. (1995). Modeling Passive Earth Pressure for Bridge Abutments. Earthquake-Induced Movements and Seismic Remediation of Existing Foundations and Abutments, ASCE 1995 Annual National Convention, Vol. Geotechnical Special Publication 55, San Diego, CA. ASCE.

Mtenga, P. V. (2007). Elastomeric Bearing Pads under Combined Loading, Report to the Florida Department of Transportation, Contract No: BC352-16, Tallahassee, FL.

NBI Coding Guide (1995). Recording and Coding Guide for the Structure Inventory and Appraisal of the Nation's Bridges, Report No. FHWA-PD-96-001, U.S. Department of Transportation, Federal Highway Administration, Office of Engineering Bridge Division, Washington, DC.

Nielson, B. G. (2005). *Analytical fragility curves for highway bridges in moderate seismic zones*. Ph.D. thesis, Dept. of Civil and Environmental Engineering, Georgia Institute of Technology, Atlanta.

Nielson, B. G. and DesRoches, R. (2007a). Analytical Seismic Fragility Curves for Typical Bridges in The Central and Southeastern United States, Earthquake Spectra, 23(3): 615-633

Nielson, B. G. and DesRoches, R. (2007b). Seismic Fragility Methodology for Highway Bridges Using a Component Level Approach, Earthquake Engineering and Structural Dynamics, 36: 823-839.

Olsson, A. and Sandberg, G. (2002). Latin Hypercube Sampling for Stochastic Finite Element Analysis. J. Eng. Mech., 121-125.

Padgett, J. E., DesRoches, R. (2007a). Bridge Functionality Relationships for Improved Seismic Risk Assessment of Transportation Networks, Earthquake Spectra, 23(1), pp: 115-130.

Padgett J.E, DesRoches, R. (2007b) Sensitivity of Seismic Response and Fragility to ParameterUncertainty. Journal of Structural Engineering, 133(12):1710–8

Pan, Y. (2007). Seismic fragility and risk management of highway bridges in New York State, Ph.D. thesis, the City College of New York.

Pan, Y., Agrawal, A. K., and Ghosn, M. (2007). Seismic Fragility of Continuous Steel Highway Bridges in New York State. *J. Bridge Eng.*, *126*, 689–699.

Pottatheere P, Renault P. (2008).Seismic vulnerability assessment of skew bridges. In: Proceedings of the 14th world conference on earthquake engineering (14WCEE), Beijing, China.

Prahkov, V.O. (2016). *Nonlinear Modeling of Texas Highway Bridges for Seismic Response-History Analysis*. Masters. Thesis, Dept. of Civil and Environmental Engineering, The University of Texas at Austin.

Priestley, M. J. N., Seible, F., Calvi, G. (1996). Seismic Design and Retrofit of Bridges, John Wiley & Sons, Inc. New York, NY, ISBN:0-471-57998-X.

Ramanathan, K. N. (2012). *Next Generation Seismic Fragility Curves for California Bridges Incorporating the Evolution in Seismic Design Philosophy,* Ph.D. Dissertation, Georgia Institute of Technology, Atlanta, GA.

Saini, A., & Saiidi, M. (2013). Post-earthquake bridge damage mitigation: post-earthquake damage repair of various reinforced concrete bridge components. Sacramento, CA: California Department of Transportation, Division of Research and Innovation.

Shinozuka, M., Feng, Maria, Q., Kim, H.-K., and Kim, S.-H. (2000). Nonlinear Static Procedurefor Fragility Curve Development. *Journal of Engineering Mechanics*, *126*(12), 1287–1296.

Sullivan I, Nielson BG. (2010). Sensitivity analysis of seismic fragility curves for skewed multi-span simply supported steel girder bridges. In: Proceedings of the structures congress 2010: 19th analysis and computation specialty conference, Orlando, Florida, USA

Tavares, D. S. (2013). Seismic Fragility of a Highway Bridge in Quebec. ASCE Journal of Bridge Engineering, 18(11), 1131-1139.

Torbol, M. and Shinozuka, M. (2012), Effect of the angle of seismic incidence on the fragility curves of bridges. Earthquake Engng Struct. Dyn., 41: 2111–2124. doi:10.1002/eqe.2197.

TxDOT (2017). Bridge Standards – Prestressed Concrete I-Girders, Texas Department of Transportation, Austin, TX. Retrieved from: http://www.txdot.gov/insdtdot/orgchart/cmd/cserve/standard/bridge-e.htm#PRESTRESSEDCONCRETEI-GIRDERS

TxDOT (2015). Bridge Standards – Common Foundation Details (FD), Texas Department of Transportation, Austin, TX. Retrieved from: www.dot.state.tx.us/insdtdot/orgchart/cmd/cserve/standard/bridge-e.htm.

TxDOT (2012). Geotechnical Manual, Texas Department of Transportation, Austin, TX. Retrieved from: http://onlinemanuals.txdot.gov/txdotmanuals/geo/foundation_design.htm#CACJECFJ

TxDOT (2007). As-built Drawing – NBI Bridge No.120200017902098, Texas Department of Transportation, Austin, Tx.

TxDOT (2006). Bridge Standards – Steel Beam Standard Design (SBSD), Texas Department of Transportation, Austin, Tx. Retrieved from: http://www.txdot.gov/insdtdot/orgchart/cmd/cserve/standard/bridge-e.htm#STEELBEAMS

TxDOT (2005). Bridge Standards – 30'-4" Concrete Slab and Girder Span – 24ft Roadway (CG-30-24), Texas Department of Transportation, Austin, TX. Retrieved from: http://www.txdot.gov/insdtdot/orgchart/cmd/cserve/standard/bridge-e.htm#CONCRETESLAB&GIRDER(PANFORM)

TxDOT (2004). Bridge Standards – Steel Beam Spans 24' Roadway (SSB-24), Texas Department of Transportation, Austin, Tx. Retrieved from:

http://www.txdot.gov/insdtdot/orgchart/cmd/cserve/standard/bridge-e.htm#STEELBEAMS

TxDOT. (1975). As-built Drawing – NBI Bridge No. 180570035304135, Texas Department of Transportation, Austin, TX.

TxDOT. (1971a). As-built Drawing – NBI Bridge No. 151310007205174, Texas Department of Transportation, Austin, TX.

TxDOT. (1971b). As-built Drawing – NBI Bridge No. 180570009214192, Texas Department of Transportation, Austin, TX.

TxDOT. (1970). As-built Drawing – NBI Bridge No. 2405500030312, Texas Department of Transportation, Austin, TX.

TxDOT. (1966). As-built Drawing – NBI Bridge No. 03039082403077, Texas Department of Transportation, Austin, TX.

TxDOT. (1965). As-built Drawing – NBI Bridge No. 180570044202067, Texas Department of Transportation, Austin, TX

TxDOT. (1962). As-built Drawing – NBI Bridge No. 161780032603016, Texas Department of Transportation, Austin, TX.

TxDOT. (1955). As-built Drawing – NBI Bridge No. 01092051001007, Texas Department of Transportation, Austin, TX.

TxDOT. (1939). As-built Drawing – NBI Bridge No. 10212024506026, Texas Department of Transportation, Austin, TX.

Unanwa, C. and Mahan, M. (2014). "Statistical Analysis of Concrete Compressive Strengths for California Highway Bridges." J. Perform. Constr. Facil., 10.1061/(ASCE)CF.1943-5509.0000404, 157-167.

Zhang, J., Huo, Y. (2009). Evaluating effectiveness and optimum design of isolation devices for highway bridges using the fragility function method, Engineering Structures, 31, pp: 1648-1660.